BERICHTE
aus dem Fachbereich Geowissenschaften
der Universität Bremen

No. 66

Nyandwi, N.

THE NATURE OF THE SEDIMENT DISTRIBUTION PATTERN IN THE SPIEKEROOG BACKBARRIER AREA, THE EAST FRISIAN ISLANDS

Berichte, Fachbereich Geowissenschaften, Universität Bremen, No. 66
162 pp., 86 figs., 8 tables, Bremen 1995

ISSN 0931-0800

The "Berichte aus dem Fachbereich Geowissenschaften" are produced at irregular intervals by the Department of Geosciences, Bremen University.

They serve for the publication of experimental works, Ph.D.-theses and scientific contributions made by members of the department.

Reports can be ordered from:

Gisela Eggerichs

Sonderforschungsbereich 261

Universität Bremen

Postfach 330 440

D 28334 BREMEN

Phone: (49) 421 218-4124

Fax: (49) 421 218-3116

Citation:

Nyandwi, N.

The Nature of the Sediment Distribution Patterns in the Spiekeroog Backbarrier Area, the East Frisian Islands.

Berichte, Fachbereich Geowissenschaften, Universität Bremen, No. 66, 162 pp., 86 figs., 8 tables,

Bremen 1995.

ISSN 0931-0800

THE NATURE OF THE SEDIMENT DISTRIBUTION PATTERNS IN THE SPIEKEROOG BACKBARRIER AREA, THE EAST FRISIAN ISLANDS.

Ph.D. Thesis

Submitted to
FB5 - Geowissenschaften, Universität Bremen

By

NTAHONDI NYANDWI
1995

Gedruckt mit Unterstützung des Deutschen Akademischen Austauschdienstes

DEDICATION

This work is dedicated to my wife Rose and children, Christina, Rosemary and Moses. The wholehearted encouragement from my wife to concentrate on this study despite having to endure difficult times without me has no example.

ABSTRACT

Wadden seas are coastal water bodies associated with barrier islands like those found along the southern North sea coast. Both sedimentological and hydrological studies indicate presence of a landward energy gradient between the open sea and the waddens. Explanations of the energy gradient through the changing current velocities along the inlets have long been considered. But a closer examination of the sediment distribution in the backbarrier areas reveals the general energy gradient to be oriented normal (N-S direction) to the shore and thus, oblique to perpendicular to the general tidal flow direction (NW-SE in the inlet and E-W in the tidal channels). Therefore, it remains to be explained as to how the flow dynamics leads to the observed sediment distribution. In this study a process-response approach involving the hydrology, sedimentology and geomorphology of the Otzum ebb tidal catchment in the Spiekeroog backbarrier area has been adopted. The primary aim of the study is the understanding of the origin and maintenance mechanism of the energy gradient as represented by the sediment distribution patterns across the backbarrier area of the Spiekeroog island.

The following objectives were realised:
- determination of the morphodynamics of tidal channels and their catchment areas;
- determination of the sediment distribution;
- determination of major and minor energy gradients;
- determination of the sediment transport pathways and processes;
- determination of the interrelationship between the flow, bottom morphology and sediment distribution;
- developing a model for the nature of the shore-normal energy gradient.

The data base included analysis of large scale topographic chart series, a close grid bottom sampling, flow measurements as well as existing literature.

The morphological data from the topographic charts shows that the main physiographic features of the backbarrier area are the NW-SE running tidal inlets separating adjacent islands, the E-W oriented tidal channels dissecting the tidal flats

and the tidal flats themselves. With the exception of the Schillbalje, which appears to have occupied the same position since the 1960s, the inlets and channels are very dynamic both in location and dimension. Their geographic orientations, however, show very little or no change at all.

The relationships between various characteristic morphometric parameters of the channels and their cathment areas, such as those established and widely applied for fluvial systems, appear to be useful in tidal drainage systems as well. In the same way as the size of the tidal channels are proportional to the volumes of tidal discharges, they are also proportional to the size of the catchment areas which they drain. In this respect the length of a channel required to drain a given catchment area has been found to be similar in both fluvial and tidal systems. Empirical relationships also show a geometrical similarity between fluvial and tidal channels in that the sinuosity index grows with the length of the channels, i.e. longer channels tend to become more sinuous. However, since the landward reaches of tidal channels are limited and hence unable to form very long channel meanders (sinuosity index >1.5) are rarely fully developed in tidal environments.

Although there has not been any substantial increase in the overall size of the backbarrier area, an analysis of catchment areas of individual tidal channels shows that there has been an increase in the volume of the channels, at least over the past 30 years. This has been at the expense of the tidal flats as well as through the deepening of the channels as revealed by mass balance estimates. The channels have also generally grown in length. In order that the proportionality between the channel size and its catchment area is maintained, the growth of the large channels leads to the closure of the much smaller ones.

Sediment dynamics in the backbarrier areas is without doubt bi-directional. A mass balance estimate indicates that the Spiekeroog backbarrier area experiences a net accumulation resulting in an average bottom rise of about 16 cm/100 yr. Given this slower basin filling rate as compared to the average local sea level rise of about 24 cm/100 yr., the Wadden Sea appears to be deepening. This is taken to indicate that

sediment influx from the upper island shoreface is not keeping pace with sea level rise at present. This would explain the increase in channel volume outlined above.

The sediment distribution patterns show that the sediment generally becomes finer landwards, irrespective of tidal channel orientations. A closer examination, however, shows two distinct patterns. The first pattern, which has been observed and explained by several workers before, is a general landward fining of the sediments within the inlet from as coarse as 1.0 phi (0.5 mm) in the inlet throat to 3.5 phi (0.09 mm) on the landward reaches of the inlet. This pattern is not difficult to understand since the tidal currents flowing through the inlet decrease in velocity from the inlet throat landwards. The second pattern, however, which is the most conspicuous on the mean grain size map, shows a distinct shore-normal (N-S) landward sediment fining trend even crossing the tidal channels, from about 2.0 phi (0.25 mm) on the islands to 2.5 - 3.0 phi (0.25 - 0.13 mm) on the tidal flats to as fine as 3.5 phi (0.09 mm) along the dyke (mainland coast).

Given that the main tidal flow directions are generally NW-SE in the inlet and main channels (e.g. Schillbalje) and E-W in the minor tidal channels draining the tidal flats, the shore-normal energy gradient does not coincide with the current directions and it is consequently considered not to be directly caused by the flow variations along the current axes. Mathematical modelling of the velocity gradient in some selected E-W oriented tidal channels in the course of the rising tide shows that peak velocities become progressively smaller the closer to the land a channel is situated. Thus peak velocities of up to 1.18 m s^{-1} were estimated for the northernmost (farthest from land) channel (Swinnbalje), reducing to 0.69 m s^{-1} in the southernmost, near-land channel. These estimates were subsequently confirmed by field measurements. From one E-W oriented tidal channel towards its immediate southern neighbour the overbank flow velocity, to which the interchannel grain size responds, thus decreases southwards at all locations along the channel. At some distance beyond the centre line the overbank velocities from the two channels are equal and at their minimum. This process repeats itself between successive channels, ultimately resulting in a pronounced energy gradient. A plot of the mean grain size (or mean settling velocity) of the sand fraction against distance along a N-S transect running across the tidal

channels depicts 1) a general landward energy decrease across the tidal flats and 2) energy level fluctuations in the interchannel regions.

Using this model, the occurrence and areal distribution of the mud pockets along the drainage divides as well as on elevated interchannel regions can be explained. On the one hand the low energy levels enhance supply of finer sediments towards these areas. The higher elevation on the other hand provides for shallow water depths and hence increased mud deposition. Such mud pockets have in the past been interpreted to represent purely biogenic deposits following observations that they were often associated with mussel beds.

The most important empirical relationships between morphological and hydrological parameters observed in the course of this study are summarised below:

1. Basin (catchment) volume: $V = 1.56\ A^{1.1}$ (1)
2. Channel volume: $V = 2.24 \times 10^{4}\ A^{1.68}$ (2)

Channel dimensions:

3. $D = 2.96 \times 10^{-4}\ A^{1.58}$ (3)
4. $W = 1.13 \times 10^{-3}\ A^{2.22}$ (4)
5. $W = 1.16 \times 10^{2}\ D^{1.35}$ (5)
6. Channel length (tidal): $L = 0.81\ A^{0.87}$ (6)
7. Channel length (tidal and fluvial): $L = 1.45\ A^{0.57}$ (7)
8. Dominant flow velocity, $V_{cm/s} = -75.83psi + 24.87$ (8)

Notations:

V: Volume

A: Catchment area (except in equations (3) & (4) where it denotes cross-sectional area)

D: Depth

W: Width

L: Length

psi: $= -\log_2 W$, where W is the grain settling velocity (cm/s)

ACKNOWLEDGEMENTS

This study is a result of the long standing objective of the Senckenberg Institute in Wilhelmshaven to provide answers to many vexing sedimentological, hydrological and geomorphological questions on backbarrier environments using the Wadden Sea as a model. One of the questions that arose was as to why sediment distribution in the area pointed to a clear coast-perpendicular energy gradient, a feature which the hydrology did not seem to support. As I embarked on this study it became clear to me how difficult it was going to be to formulate the right line of research. In this respect I am very grateful to Prof. Dr. B. W. Flemming, head of the Marine Research Division of the Senckenberg Institute in Wilhelmshaven for the interest and consent to take an advisory role in this research.

Special thanks also go to Prof. Dr. G. Wefer, FB 5 - Geowissenschaften, University of Bremen for agreeing to act as academic supervisor. The close co-operation between the two professors and their friendly attitude is the secret behind the successful conclusion of this study. I express my gratitude that not only did I receive academic supervision but also unmeasurable help in social matters.

The entire scientific, technical and supporting staff of the Senckenberg Institute in Wilhelmshaven is acknowledged for the friction-free co-operation I received. Specially acknowledged are Mrs. A. Raschke, Technical Assistant, for her help in handling of the data from the sedimentation column, Mrs. R. Flügel for her assistance with catographical work and Dr. A. Batholomä for his assistance with computer problems.

As no research runs without finances I would like to express my sincere gratitude to the Deutscher Akademischer Austauschdienst (DAAD) for financing this study as well as my stay in Germany. The Senckenberg Institute is acknowledged for providing working space and facilities.

And lastly I thank God for everything.

ZUSAMMENFASSUNG

Das Wattenmeer ist ein Küstengewässer, daß zwischen dem Festland und den küstenparallelen Inseln liegt, wie es an der südlichen Nordsee Küste zu finden ist. Sedimentologische und hydrologische Studien weisen auf eine landwärts gerichtete Energieabnahme durch das Watt hin. Die Ursache dieses Energiegradienten ist bisher noch nicht geklärt aber über einen Zusammenhang zwischen dem Energiegradienten und den Strömungsverhältnissen in Prielen ist schon lange spekuliert worden. Allerdings, genaue Untersuchungen der Sedimentverteilung im Rückseitenwatt zeigen deutlich, daß der Energiegradient generell senkrecht (N-S Richtung) zur Küste gerichtet ist und damit senkrecht zur Richtung der Tideströmung liegt (NW-SE in den Baljen und E-W in den Prielen). Es stellt sich somit die Frage, auf welche Weise die Sedimentverteilung von der Hydrodynamik gesteuert wird. In dieser Arbeit wurden die Wechselbeziehungen zwischen Hydrologie, Morphologie und Sedimentologie im Otzumer Einzugsgebiet (Spiekerooger Rückseitenwatt) analysiert. Das Hauptziel war den Ursprung des Energiegradienten und dessen Instandhaltungsmechanismus zu erklären.

Die folgende Arbeitsschritte wurden durchgeführt:
- Bestimmung der Morphodynamik der Priele und deren Einzugsgebiete;
- Bestimmung der Sedimentverteilung;
- Bestimmung der Haupt- und Sekundärenergiegradienten;
- Bestimmung der Transportwege und -prozesse;
- Bestimmung der Wechselbeziehungen zwischen Abfluß, Sohlformen und Sedimentverteilung;
- Modellierung des senkrecht zur Küste gerichteten Energiegradienten.

Die Analyse der topographischen Karten zeigt die NW-SE orientierten Baljen, die E-W orientierten Priele und das Höhenwatt als die wesentlichsten morphologischen Merkmale. Die Baljen und Priele sind in der Regel sehr dynamisch, ausgenommen von der Schillbalje, die seit 1960 stabil zu sein scheint. Die generelle Orientierung der Priele dagegen zeigt kaum Veränderungen.

Es konnte gezeigt werden, daß die in fluviatilen Systemen ermittelten Beziehungen zwischen den verschiedenen morphometrischen Parametern der Rinnensysteme und deren Einzugsgebiete auch für tidale Systeme gelten. Typisch dafür ist die Beziehung zwischen der Prielenlänge und dem Größe des Einzugsgebietes. Es folgt, daß die Größe der Priele nicht nur proportional zu ihren Einzugsgebieten ist sondern auch zu deren Abflußvolumen. Empirische Gleichungen zeigen außerdem die Ähnlichkeit zwischen der Sinuosität der fluviatilen Rinnen und deren tidaler Gegenstücke; je länger die Priele und Rinnen, desto sinuös werden sie. Voll entwickelte Meander (Sinuosity Index >1.5) sind in den Tidalesystemen jedoch sehr selten. Dies läßt sich dadurch erklären, daß Priele landwärts in ihrer Ausdehnung eingeschränkt sind.

Obwohl im allgemeinen keine wesentliche Zunahme in der Größe des gesamten Einzugsgebietes ermittelt wurde, konnte dennoch eine Zunahme der individuellen Prielenvolumina nachgewiesen werden, zumindest über die letzten 30 Jahre. Dies wurde durch eine Vertiefung der Priele und Erosion der Höhenwattbereiche erreicht, wie die Massenbilanzen bestätigen. Die Priele zeigen auch eine allgemeine Zunahme in ihren Längen. Um die proportionale Beziehung zwischen der Länge und der Größe des Einzugsgebietes aufrecht zu halten, führte die Zunahme zur Verfüllung kleinerer Priele. Dies erklärt auch die Zunahme der Prielenvolumina.

Trotz der E-W Orientierung der Priele, zeigt das Sedimentverteilungsmuster eine generelle landwärts gerichtete Sedimentverfeinerung. Eine nähere Untersuchung dieses Phänomens ließ zwei Muster erkennen. Das erste Muster, das bereits früher dokumentiert worden ist, zeigt eine Sedimentverfeinerung entlang der Baljen von 1.0 phi (0.5 mm) im Seegat bis zu 3.5 phi (0.09 mm) an der Festlandküste. Dieses Muster läßt sich durch die landwärts abnehmende Strömung erklären. Das andere Muster, das sich auf den Sedimentverteilungskarten deutlich abhebt, zeigt eine senkrecht zur Küste (N-S Richtung) verlaufende, landwartige Sediementverfeinerung von 2.0 phi (0.25 mm) auf den Inseln, bis zu 2.5 - 3.0 phi (0.25 - 0.13 mm) auf dem Watt, und 3.5 phi (0.09 mm) im deichnahen Bereich.

Aufgrund der Tatsache, daß die Strömungsrichtung in den Baljen (z.B. Schillbalje) NW-SE bzw. E-W in den Prielen verläuft, ließ zunächst vermuten, daß es keine

Beziehung zwischen der Strömung und dem N-S Energiegradienten gab. Modellberechnungen der maximalen Strömungsgeschwindigkeiten in den E-W orientierten Prielen zeigten allerdings eine von Priel zu Priel nach Süden gerichtete progressive Geschwindigkeitsabnahme. Im nördlichsten Priel (Swinnbalje) wurde eine maximale Strömungsgeschwindigkeit von 1.18 m s^{-1} gerechnet, in der südlichsten dagegen nur 0.69 m s^{-1}. Diese Modellierungsergebnisse wurden durch Strömungsmessungen bestätigt. Es folgt demnach, daß zwischen zwei benachbarten Prielen die Überbankströmungsgeschwindigkeit nach Süden hin abnimmt, wobei die Geschwindigkeit in der Mitte der jeweiligen Plate ihren minimalen Wert erreicht. Dieser Prozess wiederholt sich zwischen allen benachbarten Prielen und erklärt somit den N-S gerichteten Energiegradienten. Wenn man die Beziehung zwischen der mittleren Korngröße der Sandfraktion und der Entfernung graphisch darstellt ergibt sich 1) eine generelle, landwärts gerichtete Energieabnahme durch das Watt und 2) Energieschwankungen zwischen den einzelnen Prielen.

Mit Hilfe dieses Modells konnte auch das Vorkommen und die Verteilung von Schlick auf den Hochwasserscheiden sowie auf dem Höhenwatt erklärt werden. Niedrige Energie bzw. große Höhe in diesen Bereichen begünstigt die Ablagerung feinere Sedimente.

Im Folgenden sind die wichtigsten empirisch ermittelten Beziehungen zwischen morphologischen und hydrologischen Parametern aufgeführt:

1. Beckenvolumen: $V = 1.56\ A^{1.1}$ (1)

2. Prielvolumen: $V = 2.24 \times 10^{4}\ A^{1.68}$ (2)

Prieldimensionen:

3. $D = 2.96 \times 10^{-4}\ A^{1.58}$ (3)

4. $W = 1.13 \times 10^{-3}\ A^{2.22}$ (4)

5. $W = 1.16 \times 10^{2}\ D^{1.35}$ (5)

6. Länge (Priele): $L = 0.81\ A^{0.87}$ (6)

7. Länge (fluviatile Rinne u. Priele): $L = 1.45\ A^{0.57}$ (7)

8. Optimale Strömungsgeschwindigkeit, $V_{cm/s} = -75.83psi + 24.87$ (8)

Kenngrößen:

V: Volumen

A: Größe des Einzugsgebietes (in (3) & (4) ist Querschnittsgröße)

D: Tiefe

W: Breite

psi: = $-\log_2 W$, wobei W die Sinkgeschwindigkeit (cm/s) ist.

TABLE OF CONTENTS

LIST OF FIGURES

LIST OF TABLES

CHAPTER 1

INTRODUCTION

1.1 Research problem

The understanding of the natural environment, whether purely marine or estuarine, requires a multidisciplinary approach, particularly more so when dealing with process - response problems. The backbarrier tidal catchment area investigated in this study constitutes a highly dynamic environment characterised by changing dimensions and geometry of the tidal channels, changing dimensions of the tidal basin (partly due to natural processes and partly due to man's activities such as dyking and dredging), a large tidal range (mesotidal) and variable meteorological conditions associated with frequent storm surges. This dynamic nature of the environment must be reflected in the type and distribution patterns of the fauna, flora and substrate (sediment) in the area. Most of the studies carried out in the German part of the Wadden Sea in the past have been dealing either with processes (hydrodynamics) or with responses (morphodynamics, sediment transport and products) but rarely with both in combination. The few studies which have been of combined process - response character have mainly been undertaken at minor scales, being concentrated in crisis areas such as harbour entrances, island's sea side beaches and inlet areas, especially in relation to coastal protection schemes.

Recognising the complexity of the Wadden Sea environment and the interrelating nature of the various hydrodynamic, geomorphologic and sedimentation processes, the Marine Science Division (Abteilung für Meeresforschung) of the Forschungsinstitut Senckenberg in Wilhelmshaven, has since 1985 embarked on an ambitious study program evolving around the barrier island of Spiekeroog. To date different but interrelated major (Ph.D.) and minor (Diplom, etc.) projects have been carried out on process - response problems covering different environmental settings. Amongst these are barrier island shoreface, the inlet and tidal delta complex, the barrier island and backbarrier area, the latter forming the basis of this dissertation.

Available information on the surficial sediment distribution of the Spiekeroog backbarrier area (GROTJAHN, 1987), the eastern part of the East Frisian Islands (BUNDESANSTALT FÜR BODENFORSCHUNG, 1973), the German bight as a whole (DEUTSCHES HYDROGRAPHISCHES INSTITUT, 1981; RAGUTZKI, 1982) and the Wangerooge backbarrier area (REINECK, et al., 1986) shows a general landward fining of the sediment which is unequivocally understood to indicate existence of a shore-normal energy gradient across the backbarrier region. The character of the implied energy gradient, i.e. how it behaves on the tidal flats and in the vicinity of the islands as well as the mainland coast has recently been addressed (FLEMMING & NYANDWI, 1994). The actual cause of the energy gradient and how it is sustained are not yet fully understood. Tidal currents are widely suspected to be the major cause of the energy gradient, but drift currents and wave action may also be important. Although currents and waves are considered to be the main hydraulic force responsible for the sediment distribution patterns, tidal flat elevations and tidal channel morphology, while themselves being modified by the hydraulic forces, control the avenues and the spatial distribution of these forces, thus in turn contributing to the resulting energy gradient.

This study, therefore, has been carried out with the primary intention of revealing, on the one hand, the geomorphological and hydrological controls on sedimentation in the backbarrier tidal catchment and, on the other hand, establishing the nature and cause of the energy gradient across backbarrier basins. In doing so, it was necessary to identify the characteristic geomorphological, sedimentological and hydrological parameters of this environment and to establish their interrelationships. Since the environment is highly dynamic, the element of time is obviously important and thus the behaviour of the various parameters and their interrelationships at different times were of particular interest. Some preliminary results and related aspects have recently been published by FLEMMING & DAVIS (1994) and FLEMMING & NYANDWI (1994).

Although this study is restricted to the backbarrier region of Spiekeroog, there is ample evidence (e.g., LUCK, 1976a & b; NUMMEDAL & PENLAND, 1981;

FITZGERALD et al., 1984a & b; FITZEGERALD & PENLAND, 1987) that results are applicable to the region as a whole. Most important though, the study makes a significant contribution to the understanding of process - response problems in coastal marine environments.

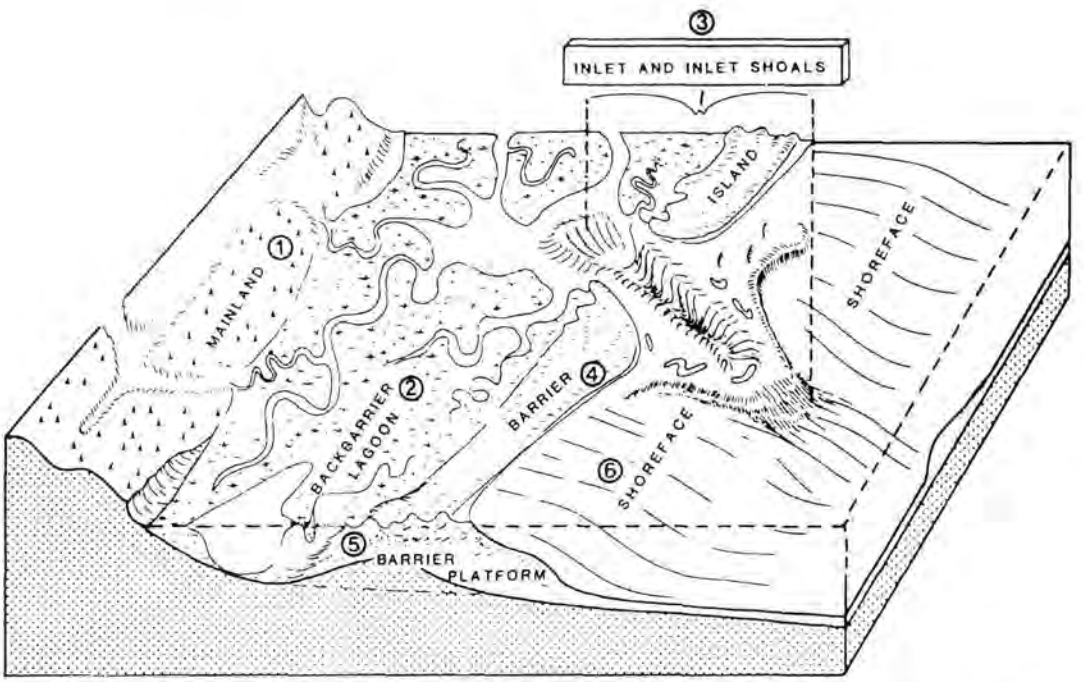

Figure 1-1 Geomorphic elements of a barrier island system (after OERTEL, 1985).

1.2 The barrier island system

The term *barrier island system* implies an association of geomorphic, geological and sedimentological entities around a barrier island. A barrier island may be described as a near-shore, subaerial, coast-parallel clastic deposit detached from the mainland by a body of water which has a connection to the open sea. The barrier island system according to OERTEL (1985) consists of six genetically related elements namely, the barrier island, the shoreface, the barrier platform, the inlets and inlet shoals, the backbarrier lagoon and the mainland shore (Fig. 1-1). However, from the consideration of fluid energy transfer between the open sea and the backbarrier lagoon and associated sediment transport and morphodynamics, three directly interacting subsystems can be recognised. These are: (i) barrier island - shoreface; (ii) barrier

island - backbarrier lagoon - mainland; and (iii) inlet - delta. Whereas the shoreface acts as a hydraulic energy transition zone between the open sea and the backbarrier lagoon, the inlet - delta system acts as filter and energy concentrator.

CHAPTER 2

STUDY AREA

2.1 The Wadden Sea and its barrier islands

The East Frisian islands are part of a barrier island chain lining the North Sea coasts of Holland, Germany and Denmark. The East Frisian Islands comprise 7 inhabited major islands and several minor sand banks (Fig. 2-1). The body of water behind these Northwest European barrier islands is regionally referred to as the Wadden Sea. A *wadden* is technically defined as that part of the coastal area which is intermittently submerged (GRIPP, 1956). The present day usage of the term, however, defines the Wadden Sea as the intermittently submerged part of the backbarrier region, including tidal inlets and islands (EHLERS, 1988). A lesser commonly used technical definition describes the Wadden Sea as the area between the barrier islands and the mainland (BEHRE et al, 1979). Spiekeroog Island is the penultimate of the inhabited islands looking eastwards.

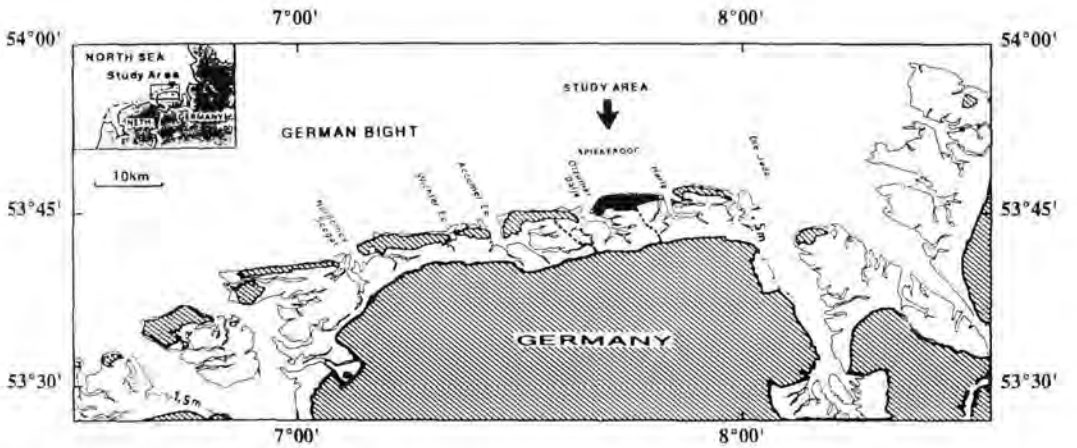

Fig. 2-1 The East Frisian islands chain showing the position of the study area.

Barrier islands world wide have attracted considerable scientific and public interest in attempts to understanding their origin, dynamics and stratigraphy, partly due to their fragile nature and partly due to economic, ecological and social reasons. Many barrier

islands have been urbanised and developed into recreational centres, thereby becoming both economically and socially important. Their importance as potential hydrocarbon host rocks, the nature of their distribution around the world and the fact that in some cases barrier islands have been observed in the process of their formation or destruction are some of the reasons for the growing scientific interest in them. Perhaps most important, the barriers themselves are a basic requirement for the existence of the waddens in micro- to mesotidal environments. Barrier islands world wide have much in common concerning sediment type, environmental setting, size, shape and stratigraphy.

Barrier islands become unstable with increasing energy flux and hence are rare along coastlines with large tidal ranges (GIERLOFF-EMDEN, 1961; HAYES, 1975; 1979; EHLERS, 1988). The tidal range along the East Frisian islands is typically less than 3 m. The size and shape characteristics of the Frisian islands, however, are a result of factors relating to their geological setting, hydrodynamic conditions and human activities. Although most barrier islands are elongated with length-width ratios typically larger than 10 (BERRYHILL et al., 1969), the Frisian islands, with the exception of the islands of Juist and Terschelling, show ratios typically under 10 (Fig. 2-2). Furthermore, the eastward increasing tidal range seems to correlate with a general decrease in island length but without a corresponding trend in the island width. Inlet widths too show no defined coastwise variation. Consequently, as the tidal range increases eastwards and the islands become shorter, but with no corresponding decrease in width, the islands assume a bulged "drum stick" shape. These shape and size characteristics of the Frisian islands clearly attest to the general view that barrier islands along microtidal coasts are long, linear and narrow, whereas their mesotidal counterparts are short and wide with bulges at their updrift ends (HAYES, 1975; 1979), a feature particularly prominent along intermediate wave energy coasts of trailing edge continental margins (DAVIS & HAYES, 1984). The formation of such bulges on the updrift ends of some of the East Frisian islands has been explained by FITZEGERALD et al. (1984b) as a result of the welding of swash bars on to the downdrift inlet shoreline.

The Frisian islands, like other barrier islands world-wide, are mainly composed of sands, with finer-grained sediments characterising the backbarrier tidal flats. Seawards the marine deposits also become essentially finer. Since the region has in its Quaternary geological history experienced substantial sea level fluctuations, both regressive and transgressive stratigraphic sequences may have developed and become superimposed locally.

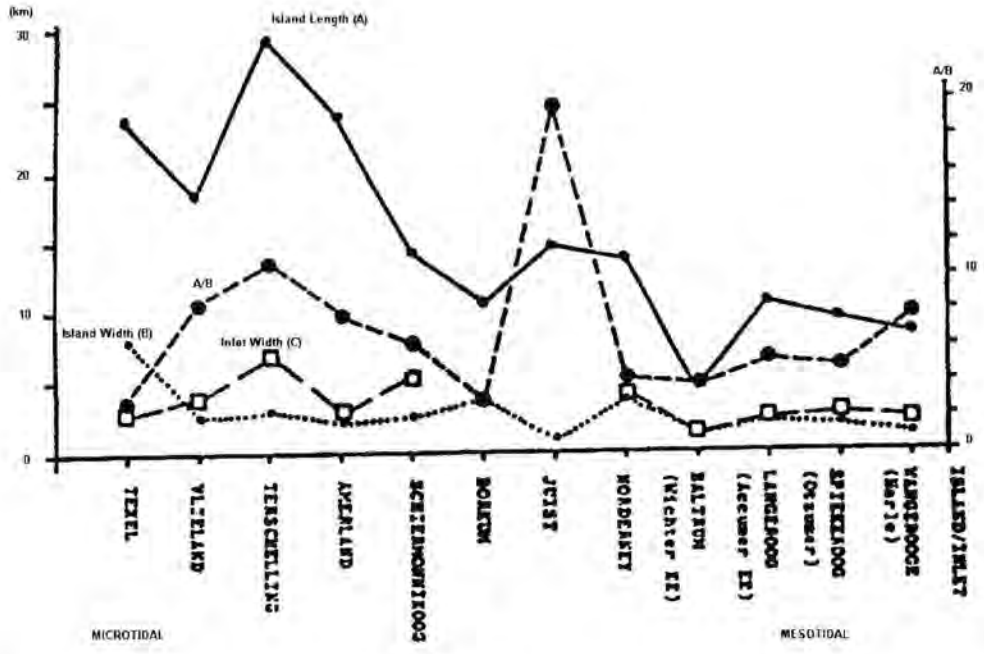

Fig. 2-2 Morphometric relations of the West and East Frisian islands.

2.2 Hydrodynamics

The hydrodynamics of the Spiekeroog backbarrier region and the Wadden Sea at large is directly linked to the North Sea water circulation which is mainly a result of combined effects of tidal currents, atmospheric pressure fields and transmitted energy flux from outside the region.

2.2.1 Tides

The tidal water movement in the North Sea is driven by a system of three amphidromic points, one situated in the north along the Norwegian coast, another in the central North Sea part (north-west of the German Bight) and the third in the south within the English Channel (HUNTLEY, 1980). In the southern North Sea the tidal circulation is controlled by the central amphidromic point, around which the M_2 tide moves in an anti-clockwise direction from west to east (FITZGERALD & PENLAND, 1987). In this way the tidal wave propagates eastwards along the East Frisian islands and, the more east an island is situated the greater the delay in the time of high water. Corange lines are fairly evenly spaced from this amphidromic point towards the East Frisian barrier islands (Fig. 2-3). Coupled with the orientation of the barrier island chain, this leads to an increase in tidal range both from the North Sea towards the islands and from west to east along the island shoreline. The variation pattern of the tidal range within the backbarrier basins, though much more modified by the local physiography, still shows a NW-SE increase between the islands and the mainland (Fig. 2-4). This fact points to an inherent gross inaccuracy when estimating tidal prisms on the basis of tidal observations at a single selected site (bench mark). For this reason FITZGERALD et al. (1984a), unlike WALTHER (1972), were hesitant in calculating tidal prisms for the tidal catchments along the East Frisian islands.

Tidal current measurements in the backbarrier areas of Spiekeroog Island are rather sparse. Nevertheless, the summary by FITZGERALD & PENLAND (1987) of published data from the island of Juist (KOCH & LUCK, 1975), coupled with unpublished data from the island of Norderney may provide some insight into the scale of expected tidal flows. In short: (i) there is a pronounced time-velocity asymmetry with shorter and faster flood currents; (ii) the current velocities are strongest near the inlet mouths and decrease towards the tidal drainage divides; and (iii) whereas the eastern portion of the drainage system is ebb-dominated, the western part is flood-dominated. This time-velocity asymmetry has also been noted by ANTIA (1993) during fair weather conditions on the island shoreface.

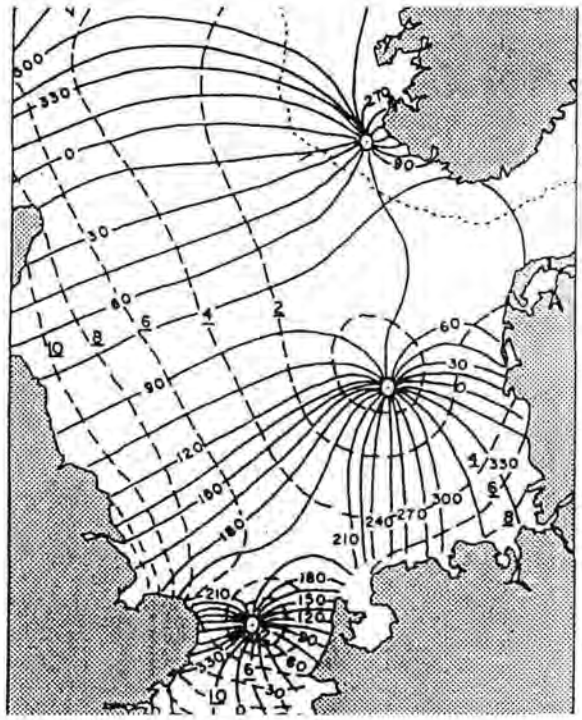

Fig. 2-3 Tidal circulation in the North Sea. Along the German North Sea coast the tidal circulation is driven by the amphidromic point situated to the north-west of the German Bight. The tidal range (shown in cm) increases from West to East and cotidal lines (hours) increase from North to South (after HUNTLEY, 1980).

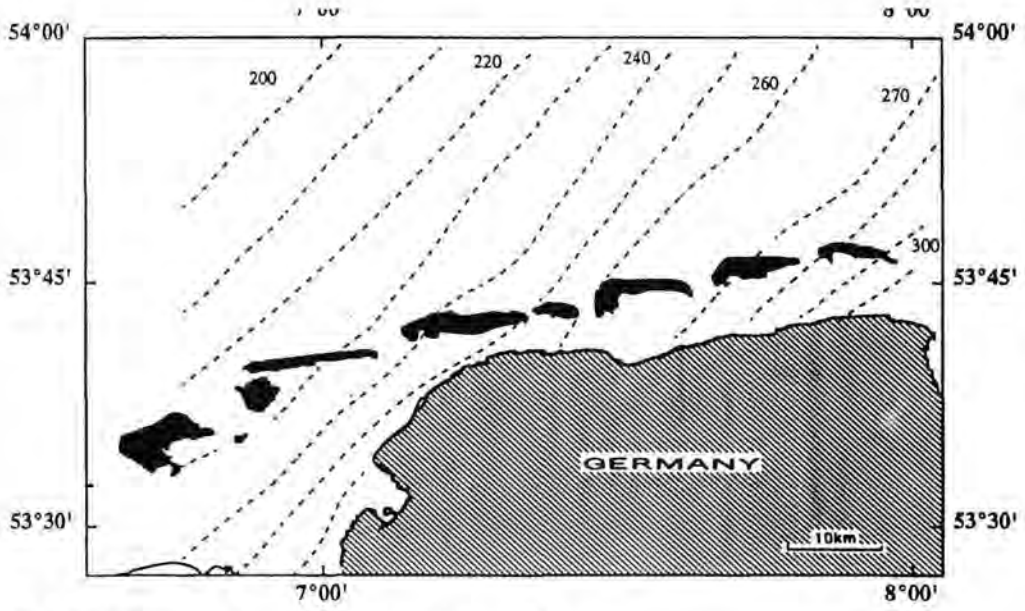

Fig. 2-4 Tidal range (cm) in the backbarrier basins.

2.2.2 Wind driven currents, storms and waves

The summary of the hydraulic character of the backbarrier areas outlined above also mentions the influence of wind on the tidal flow. On the one hand, when the wind blows in the direction of the tidal current the induced drift current enhances the tidal current and vice versa. On the other hand, wind-induced set-up of water levels may also result in flow enhancement. This was demonstrated by the study of KOCH & NIEMEYER (1978). Their current measurements made over periods of stormy weather conditions revealed, among other things, an increase of ebb tidal velocities to ebb-dominated currents and a corresponding reduction of flood velocities, all being contrasted by fair weather observations mentioned previously. Given the prevailing wind direction, it was clear that the ebb current enhancement was a result of a large wind-induced set-up of water levels.

The wind regime of the area can be represented by data collected at Norderney, where monitoring of meteorological conditions has been continuously maintained since 1947 (LUCK, 1976b). During one half of the year (September - March) prevailing winds blow from the south-westerly quadrant with the strongest average velocity of 36 km/hr. Prevailing winds during the rest of the year blow from the Northwest quadrant but are not as strong. Analysis of most recent meteorological data (1965-1986) contained in the annual reports of the Forschungsstelle für Insel- und Küstenschutz, Norderney, shows that 85% of the winds >10 Beaufort Force occur during the winter months, 30% of which are confined to the month of November. For these strong winds too, the NW quadrant contributes 47% followed by the W (30%), SW (19%) and N (4%) (ANTIA, 1993). The occurrence and frequency of storms in coastal waters of the North Sea has received relatively greater attention. There is overwhelming evidence that the frequency of storm events and their severity has been on the increase since the early 1950s (FÜHRBÖTER, 1979; STEPHAN, 1982). Their potential to causing flooding of the coastal areas is well known. The associated increase in current strengths has a potential of moulding the tidal flats.

The predominance of prevailing westerly winds along the East Frisian islands produces a westerly wave climate (NUMMEDAL & PENLAND, 1981;

FITZGERALD et al., 1984b) which is thought to drive the sediment transport to the east and thereby causing eastward island elongation and inlet migration (LUCK, 1976a). Not clearly documented, however, is the wave climate and its propagation behind the islands. Short and long waves of appropriate amplitudes filter through the ebb tidal deltas and inlet mouths to break behind the barriers. Furthermore, the lagoons themselves are large enough to enable generation of local wind waves.

Although the records of the nearshore wave conditions along the coast of the East Frisian islands are too few and mostly short in duration to warrant accurate definition of the wave climate, they are still instructive of some features. Based on two nearshore (10 m depth) wave records reported at different time intervals covering a range of sea states at the islands of Sylt and Norderney (DETTE, 1977; NIEMEYER, 1979), ANTIA (1993) observed that the similarity in the two data sets from such two distantly located sites suggests a similar wave climate along all the islands. His statistical re-evaluation of the Sylt data set (DETTE, 1977) for the period 1971 - 1974 reveals that the wave height distribution has a broad range of 0.5 - 5.0 m and is unimodal with a high wave asymmetry. The most frequent significant wave heights (80% of the time) are greater than 1.5 m and those greater than 3.0 m still occupy 25% of the time. A significant wave height of less than 1 m has a frequency of less than 1%. The significant wave heights for the island of Norderney data set (NIEMEYER, 1979), in the period 1976 - 1978, range from 1.8 m to 4.5 m but may reach higher values during severe storms.

The existing sea states in the area may on the basis of wave data be classified into three regimes: 1) normal (significant wave height 1-2 m); 2) seas (significant wave height 2.5-3.5 m); and 3) swells (significant wave height $>$ 3.5 m), constituting about 90% of the record (ANTIA et al., 1994). Although most of the waves will break and dissipate up to 90% of their energy on the ebb delta shoals, almost all of the wave types are capable of entering the backbarrier area, where their remaining energy is dissipated depending on the variations in tidal flat elevations as well as channel depths.

2.3 Backbarrier sediments

A synthesis of the sediment distribution in the backbarrier tidal flats of the East Frisian islands has been provided by the BUNDESANSTALT FÜR BODENFORSCHUNG (1973); DEUTSCHES HYDROGRAPHISCHES INSTITUT (1981) and RAGUTZKI (1982). The map of the Deutsches Hydrographisches Institut based on the sand classification of coarse-medium-fine sand, shows fine sand to constitute > 60% of the sediment. Mud content increases towards the mainland coast and where the island-mainland separation is large enough, e.g. in the Leybucht embayment and behind the island of Langeoog, pure mud flats (> 50% mud) borders the mainland. Coarser sediments are shown to exist in deeper channels, with extreme cases of gravel beds and hard rock outcrops occurring in the Weser and Ems estuaries. Based on the mud content, the classification of sand flats, mixed flats and mud flats RAGUTZKI (1982), on the other hand, shows large tracts of the flats as sand flats, with mixed flats occupying essentially the interchannel areas (see also BUNDESANSTALT FÜR BODENFORSCHUNG, 1973; NIEDERSÄCHSISCHES LANDESAMT FÜR BODENFORSCHUNG, 1970). Mud flats are confined more or less to the areas in front of the mainland coast but can also occur within the mixed flats. Separate studies done on Wangerooge (REINECK et al, 1986) and Spiekeroog (NIEDERSÄCHSICHES LANDESAMT FÜR BODENFORSCHUNG, 1970; GROTJAHN, 1990) confirm the trend and show further that the mud content in the sediment not only follows the same trend, but also increases along tidal water divides. Of the minor and major sedimentological studies carried out in the backbarrier areas, very few indeed have addressed the problem of sediment dynamics.

The fact that the Wadden Sea sediments are composed of a mixture of sand and mud just as those of the North Sea basin suggests some provenance relationship. A number of authors, based on petrographical and mineralogical analyses, have concluded that sand as well as silt and clay accumulating in the Wadden Sea come from the North Sea (VAN STRAATEN & KUENEN, 1957). There is, however, documented evidence that sediment is also supplied from sources other than the North Sea. In the inner German Bight, for example, fine grained sediments come partly from the Weser

and Elbe rivers and partly from erosion of tidal flats during storm surges (REINECK et al., 1967; 1968; GADOW & REINECK, 1969).

The possible mechanism by which fine sediment accumulates towards the mainland coast has been elaborated by VAN STRAATEN & KUENEN (1957, 1958) in terms of "settling lag and erosion lag" effects assuming the North Sea to be the source. The fact that suspended sediment concentration levels in the inlet mouths have been observed to be much lower than those in the inner areas and close to the mainland coast would seem to suggest a landward source of the fine sediment. Given the high tidal flushing of the Wadden Sea, however, such a gradient is very improbable and POSTMA (1961) concludes that this gradient can only be sustained through the settling lag and erosion lag effects. GROEN (1967), on the other hand, developed a model which suggests that the tidal asymmetry could be responsible for the landward accumulation of mud.

2.4 Geological evolution of the Wadden Sea

The geological evolution of the Wadden Sea and its constituting barrier islands can not be understood well without looking at the North Sea as a whole. The barrier islands and their associated features are actually late stage products of the Quaternary evolution of the North Sea basin. The present day physiography of the basin is a result of variable tectonic processes in space and time, as may be suggested by the variable geology of its flanking boundaries: Precambrian to the Northeast, early Palaeozoic to the Northwest, and late Palaeozoic to the south (LÜDERS, 1968).

The sedimentary succession of the North Sea basin is related to the Quaternary history of structural deformation and climatic changes in the basin. The Quaternary sediments blanketing much of the basin has a maximum thickness of over 1 km in its central southern part, extending linearly in a NNW direction (CASTON, 1979). The Holocene sediments, however, increase in thickness landwards and reach a maximum thickness of 30 m in the barrier islands.

The geologic evolution of the German Bight and hence the East Frisian islands in the Quaternary is discussed in SINDOWSKI (1970; 1973), STREIF & KÖSTER (1978), BEHRE et al. (1979), LUDWIG et al. (1981), EHLERS (1988) and STREIF (1989, 1990). The evolution of the region is marked by a series of transgressions and regressions, governed by glacial and interglacial phases. The following is a summary account of the events during Pleistocene and Holocene times:

The first series of marine transgressions in the area during the Quaternary occurred early in the Pleistocene between about 0.4 and 2.5 ma. These are the Cromean, Waalian and Tiglian transgressions. Thereafter a set of three glacial periods, i.e. the Elsterian (0.33-0.4 ma), Saalian (0.125-0.31 ma.) and Weichselian (0.01-0.115 ma.) as well as two interglacials, the Holsteinian (between the Elsterian and Saalian) and Eemian (between the Saalian and Weichselian) are documented. The early glacial phases of the Pleistocene are believed not to have reached the present coast (STREIF, 1990), but the associated early transgressive deposits, mainly made up of fine- to medium grained-quartz sands, reaching total thicknesses of 20-50 m (SINDOWSKI, 1973), are well documented in the East Frisian coastal region.

The Elsterian glaciation is known to have covered the whole of the North Sea basin and extended far inland (STREIF & KÖSTER, 1978; STREIF, 1990), on retreat depositing morainic material of Scandinavian and English-Scottish origin. The following transgression (Holsteinian) did not cover the whole of the East Frisian coastal region. The Saalian glaciation, in turn, was less extensive than its predecessor. Its subsequent interglacial (Eemian), unlike the Holsteinian, is known to have reached higher level stands than present sea level. The Eemian trangressive deposits are rich in the mollusc Venerupis senescens, being encountered at 7 m below the present mean sea level in the East Frisian region. There is no record of the last glacial phase along the coast of the East Frisian region, the glacial advance terminating at the present Danish North Sea coast.

The course of transgressive events in the North Sea area since the beginning of the Holocene some 10,000 years B.P. is not accurately known. However, there is general agreement of a lower sea level stand at 110 - 130 m below present sea level at about

18,000 years B.P. and during the late Weichselian at about 15,000 - 10,000 years B.P., i.e. at the beginning of the Holocene the southern North Sea coastline was situated about 200 km north of its present position. It is thus believed that the barrier islands and the Wadden Sea have formed during the subsequent sea level rise. Figure 2-5 summarises the sea level curves from different workers.

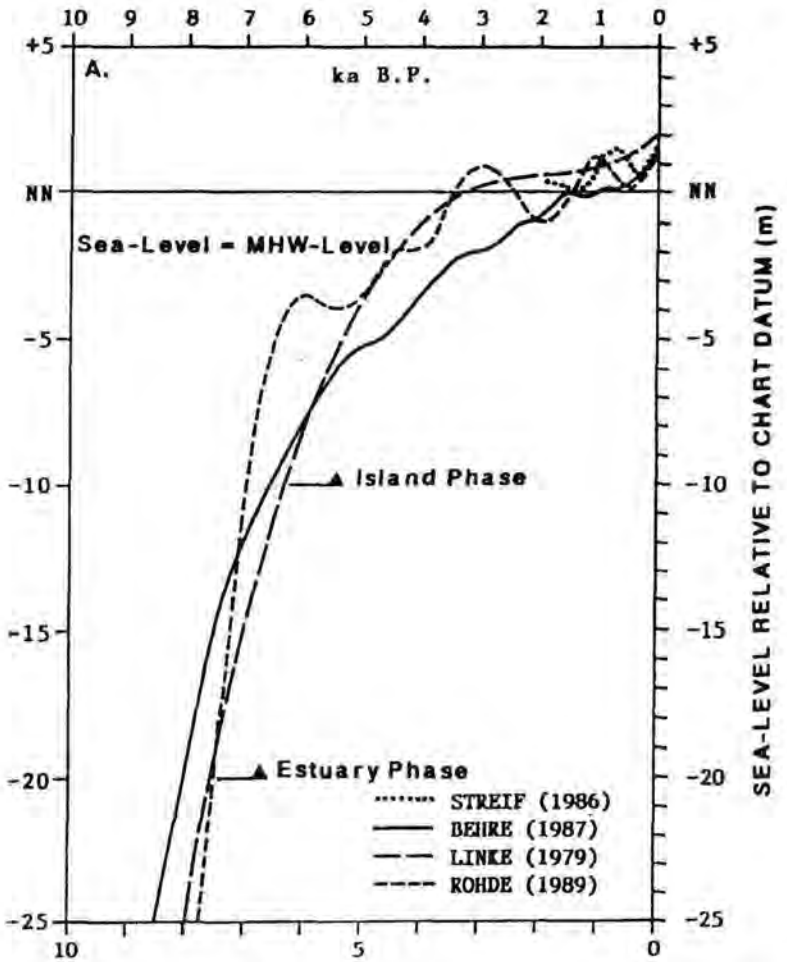

Fig. 2-5 Sea level fluctuations in the North Sea (after FLEMMING, 1991).

2.5 The origin of the East Frisian barrier islands

Barrier islands as found along the North Sea coast are not a rare phenomenon along the world's coastline. The east coast of the United States in particular is quite comparable and has been a subject of intensive investigations leading to various hypotheses regarding the origin of barrier islands (ANTIA, 1993). Research in the North Sea region has nevertheless, developed almost independently, in the main

proposing three mechanisms through which the North Sea barrier islands could have been formed. These are: 1) Drowning of coastal dune ridges, 2) Spit formation followed by breaching by the sea, and 3) Emergent shoals developing into islands. The development of the different views is fairly well documented in EHLERS (1988). FLEMMING (1990; 1991) and FLEMMING & DAVIS (1994) revisit each of the proposed mechanisms and, bearing in mind the many shortcomings of the above mechanisms, provide a more refined explanation to the possible course of events leading to the formation of the North Sea barrier islands.

Prior to the work of FLEMMING (1990) the Frisian barrier islands have been genetically divided into some stable (Borkum, Juist and Langeoog) and unstable (Baltrum, Spiekeroog and Wangerooge) islands. The genesis of the stable islands, as represented by Langeoog, was considered to have begun during the late Holocene. According to BARCKHAUSEN (1969) a shoal was formed on top of early Holocene deposits (conceived to have been formed in former valleys). The overlying tidal flat became enlarged later by younger sedimentary units including the peat layers now found below the islands' dunes. This peat layer has been dated at 1230-1340 AD. The genesis of the unstable islands, on the other hand, was thought to have been different. These barrier islands, having a tendency to migrate south-eastwards, were considered to have their centres of origin to the north-west of their present positions (SINDOWSKI, 1973). Having been initiated as shoals they must have owed their existence to landward directed sand transport from the shoreface. The most widely accepted model of barrier island formation thus involved: 1) sand supply from the foreshore led to nearshore shoal formation; 2) increasing sand supply caused an upward growth of the shoal until it emerged above low water level; 3) with continued accumulation the shoal eventually remained dry even during ordinary floods, and 4) under aeolian deposition parts of the former shoal finally grew above spring tidal level, thereby developing into an island.

The major departure point of FLEMMING & DAVIS (1994) from the above model is the idealised formation of shoals in the nearshore. Although such shoals are known from microtidal, low gradient coasts such as the Gulf coast of Florida, they are yet to be observed along mesotidal coastlines such as the southern North Sea. Furthermore,

the consideration that the island-forming shoals would have formed as permanently emerging, high elevation intertidal sand flats is also not justified by field observations. Such elevated intertidal sand flats, as observed in the North Sea area (mesotidal to lower macrotidal), are known to be ephemeral features that never occur at the seaward margins of open intertidal flats and also lack any inherent regularity in their position to explain the formation of an island chain.

The model of FLEMMING (1990) of the genesis of the barrier island chain on the southern North Sea is illustrated in Fig. 2-6. It suggests that island formation began at about 7,500 yr. B.P. during which time, the sea level standing some -20 m below present level and about 5 to 10 km seawards, might have just started to invade the lower reaches of river valleys incised into the Pleistocene sands, thereby creating restricted estuarine conditions landwards (Fig. 2-6A). Evidence from borehole data suggests a gradual transition from fresh water to brackish and finally marine conditions in identified valley fill deposits to which the islands belong (SINDOWSKI, 1973; STREIF, 1989; 1990). Wave attack on the headlands separating successive estuaries would have resulted in the formation of spit bars at the estuary mouths.

With the rising sea level the system of spit bars (shoals) was pushed landwards while at the same time growing higher due to continued sand supply and coastal dune development. As the sea level rise continued and the tidal amplitude grew, the expanding estuaries flooded ever increasing tracts of land behind the shoals causing neighbouring estuaries to coalesce, eventually leading to the detachment of the elevated spit bars to form barrier islands. This is thought to have occurred some 6,500 yr. B.P., at which time the sea level stood at -10 m below the present and some 3 km or so seawards of today's coastline (Fig. 2-6B). The deepening of the North Sea basin and the expanding backbarrier tidal lagoons resulted in increased tidal ranges from microtidal to lower mesotidal conditions with correspondingly enlarged (wider) inlets at the expense of the islands themselves. Fig. 2-6C shows the last known outline of the natural mainland coastline at about 800 AD. After that time anthropogenic influences on the evolution of the islands played a major role.

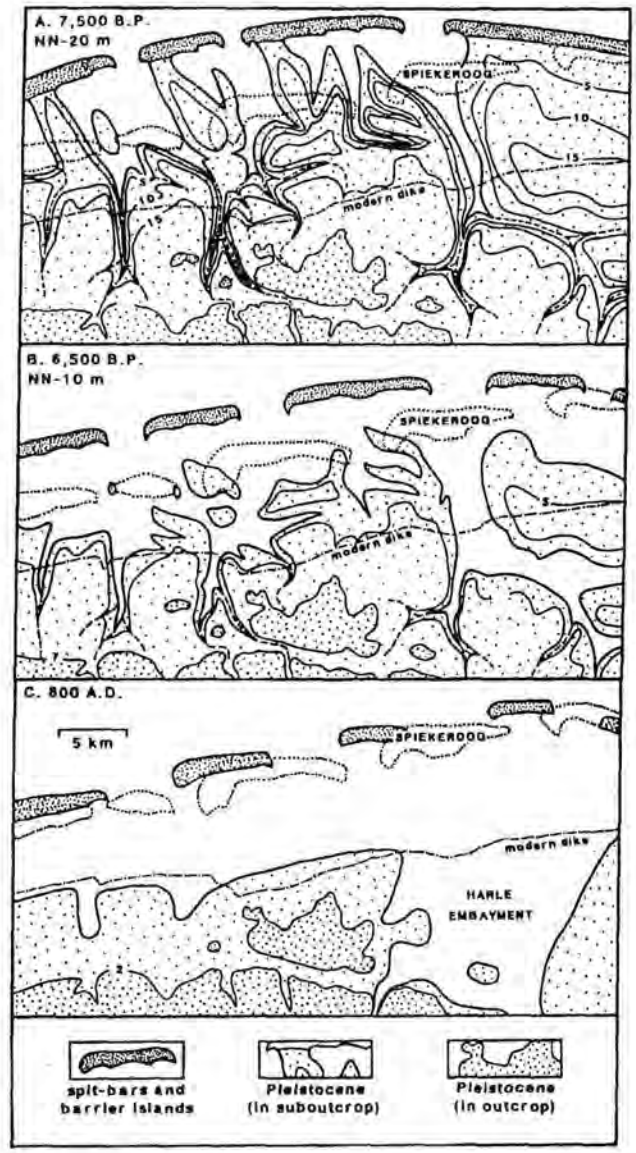

Fig. 2-6 A more plausible model for the origin of the North Sea barrier islands (after FLEMMING & DAVIS, 1994).

2.6 Evolution of the barrier islands in historical times

The morphological evolution of the barrier islands and their backbarrier areas in historical times can be traced to both human activities and natural processes (FITZGERALD et al., 1984a). The human activities are represented by a series of dyking measures on the mainland coast and repeated stabilisation measures of the western heads of the islands. The last known form of the undyked shoreline dates

some 1,200 yr. B.P. (BEHRE, 1987). This period marks the beginning of man-influenced coastal development (FLEMMING, 1990). As early as 1300 AD. a continuous dyke line stretched along the whole of the East Frisland coast (HOMEIR, 1979; EHLERS, 1988). The successive seaward displacement of the coastline and the resulting configuration of the backbarrier area and the islands between 1650 and 1960 can be traced from the maps of HOMEIR & LUCK (1969) (Fig. 2-7). Analysis of the maps (LUCK, 1975; FITZGERALD et al., 1984a) shows that during the 310 years of record the combined inlet width as well as the total drainage area have been decreasing, while the total islands' length has been increasing (Fig. 2-8).

Although the lateral elongation of the islands towards the east coupled with the narrowing down of the inlets would appear to be a response to natural processes, man's influence has played a major role. The island of Spiekeroog demonstrates this point particularly well. With the dyking of the Harle Bay (Fig. 2-9), the catchment area of the Harle was reduced from over 180 km^2 (its size following the major storm surge of 1362) down to only about 60 km^2, i.e. a reduction to about 33% of its original size, in 1960. This led to a reduction in the tidal volume on a similar scale. The filling up of the western part of the inlet was thus accompanied by an eastward growth of the island of Spiekeroog. As the islands migrated or elongated eastwards, the tidal water drainage divides between neighbouring inlets also moved eastwards. The eastward movement of the western margin of Spiekeroog was hampered as the Otzum inlet encountered a resistant pleistocene subsurface, thus preventing further eastward migration. But since the island continued to grow eastwards the water divide between the Otzum and Harle inlets continued to move eastwards with the consquence that: 1) the effective catchment area (and hence the tidal prism) of the Otzum inlet increased unproportionately to the inlet size, contrary to established emperical relationship between the size of tidal catchment areas and inlet widths (FITZGERALD et al., 1984a; FLEMMING, 1990); 2) the eastern arm of the Otzum inlet behind Spiekeroog has increased in length and become more hooked to the east with time. The translational development of the Otzum inlet and water divides are depicted in Fig. 2-7 & 2-9, respectively.

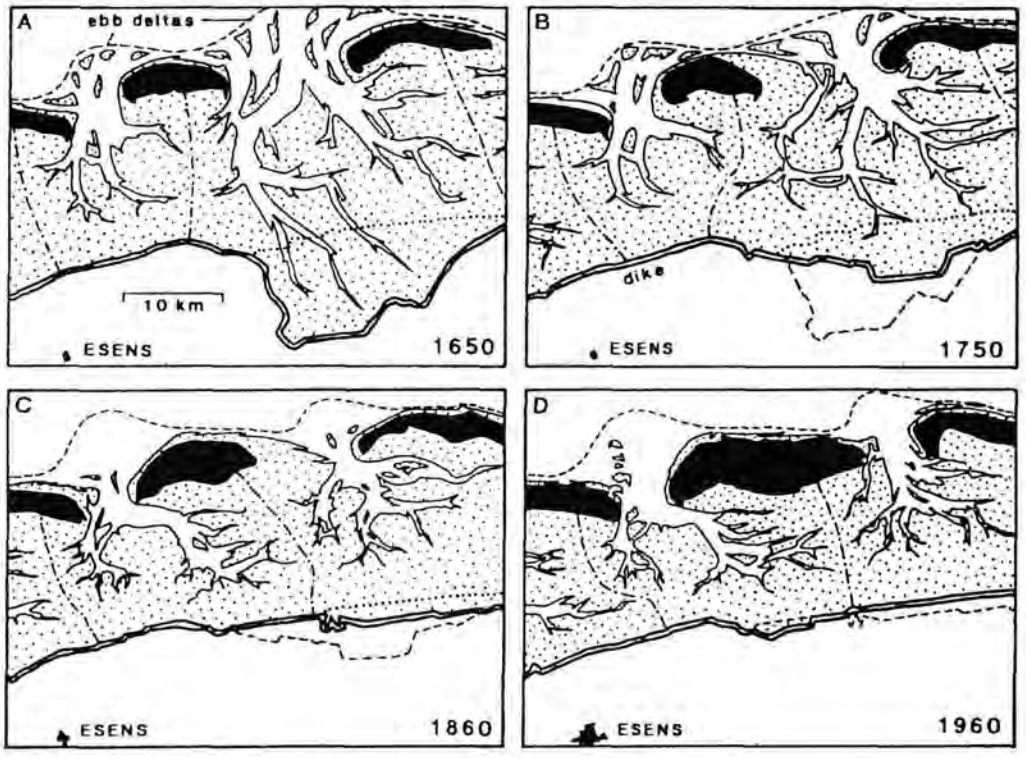

Fig. 2-7 Morphological evolution of the North Sea barrier islands in historical times as exemplified by the Langeoog - Spiekeroog - Wangeroog area (after FLEMMING & DAVIS, 1994).

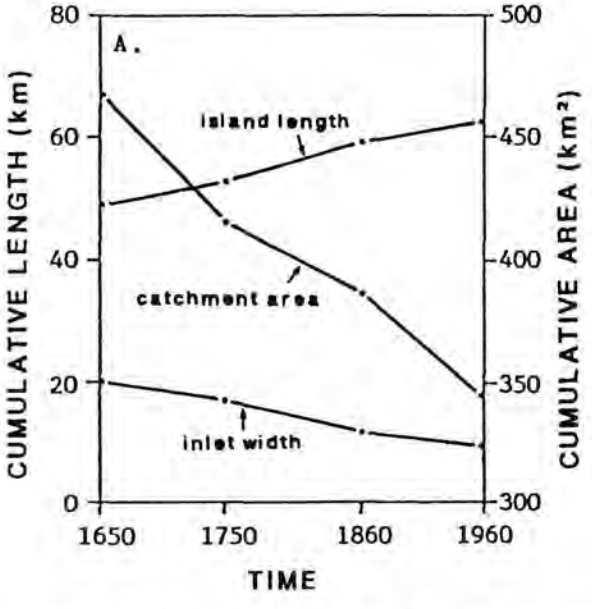

Fig. 2-8 Morphometric changes of the barrier islands between 1650 and 1960 (after FITZGERALD et. al., 1984).

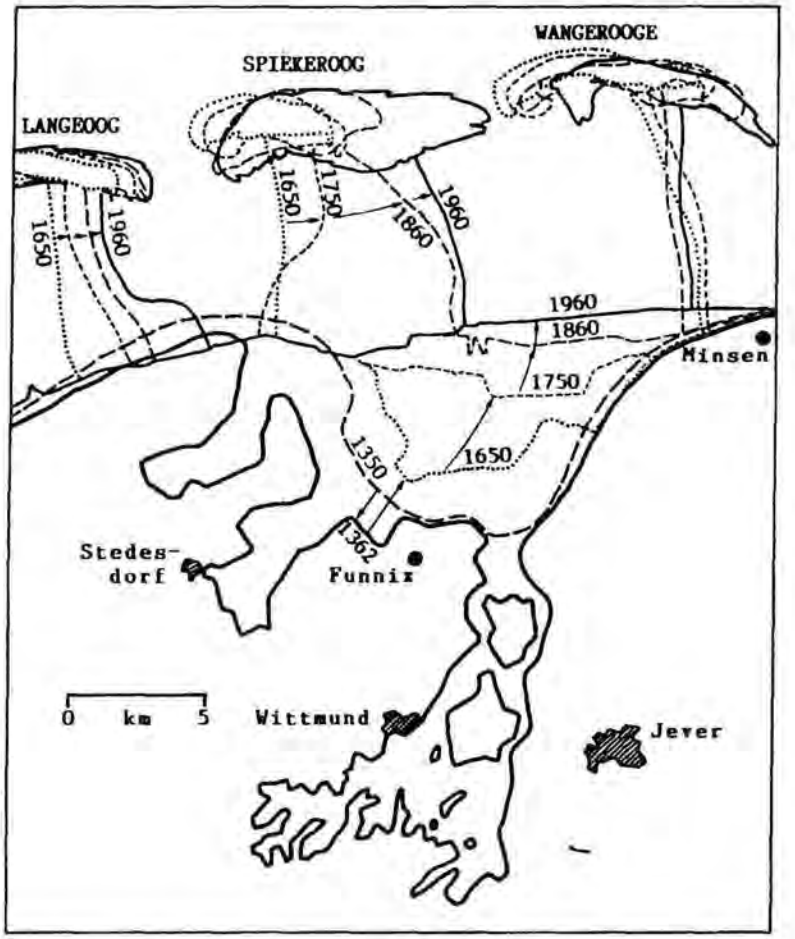

Fig. 2-9 Changes in the size of the Harle tidal catchment area as a result of the dyking of the Harle Bay (after FLEMMING & DAVIS, 1994).

2.7 Geomorphology

As mentioned earlier, the islands have a shape showing a tendency towards drum stick form (very small widths as opposed to large lengths), being generally aligned in an E-W direction. The area of Spiekeroog island is presently about 20 km^2 (10 km long by 2 km wide). The islands are laterally separated from each other by tidal inlets. Thus, Spiekeroog is bounded to the east and west by the Harle and Otzum tidal inlets (15-20 m deep and up to 2 km wide), respectively. From west to east the islands and their sea side shorelines show a successive seaward displacement such that Spiekeroog

island has its seaward-facing shoreline displaced some 2.5 km seaward of Langeoog but 1.3 km landward of Wangerooge.

Spiekeroog island is separated from the mainland coast by a 7 km wide backbarrier area. Generally, the tidal inlets have eastern and western arms, with the eastern arm being more developed and hooked to the right (looking seawards). Thus, the Spiekeroog backbarrier tidal catchment is drained mainly by the eastern arm of the Otzumer Balje. The tidal drainage divide between the Otzum and Harle tidal inlets therefore, is located more than half way the W-E length of Spiekeroog (Fig. 2-10). The main channel is connected to a network of more or less W-E running tidal channels. The geometric characteristics of these channels and their stability over time have thus far not been investigated in any detail but there are observations showing that the channels are not stable (REINECK, 1958), mostly undergoing a cyclic oscillation about a central axis (FLEMMING & DAVIS, 1990).

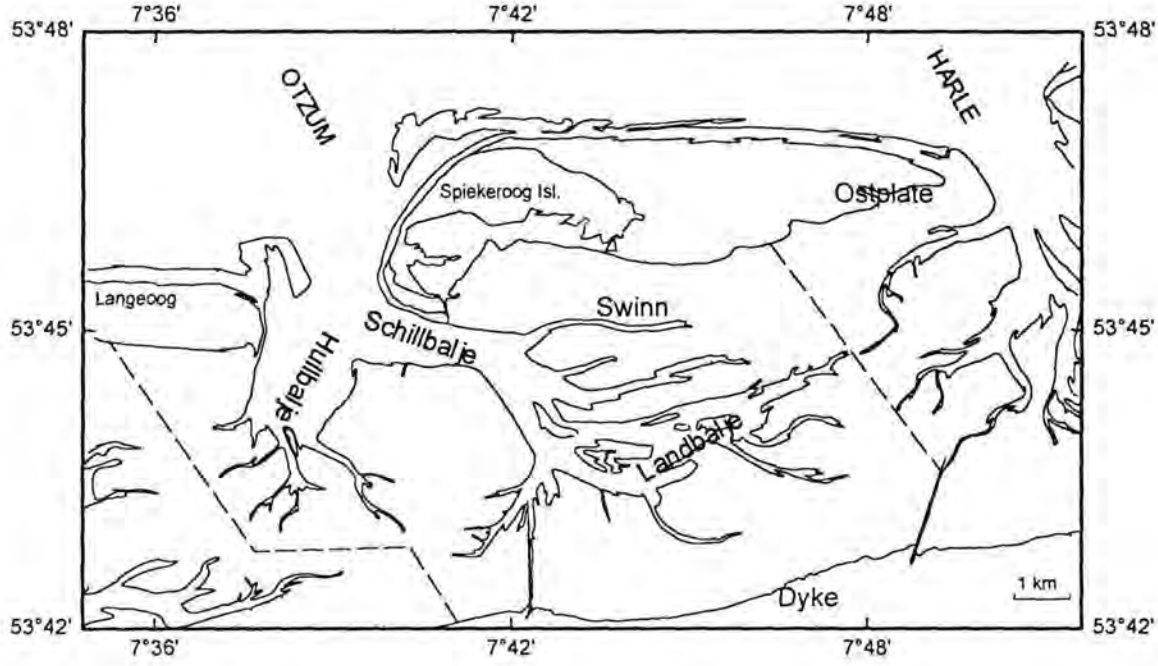

Fig. 2-10 Outline of the Otzum tidal catchment area.

CHAPTER 3

MORPHOLOGY AND MORPHODYNAMICS OF THE OTZUM TIDAL CATCHMENT

3.1 Introduction

The Wadden Sea tidal flats are incised by a network of tidal channels and creeks connected to each other to form what may be called an ebb tidal drainage pattern. There is a close similarity between the drainage patterns of the backbarrier areas and those of fluvial catchments on land. The channel network and the tidal flats are very unstable. Concern over the stability conditions of such environments has a long history, the subject being approached from different angles. A first line of approach has been looking at the stability of the tidal inlets in a given environmental setting in relation to the hydraulic forces, mainly the tidal prism (e.g. WALTHER, 1972). This approach requires accurate measurements of the tidal prism. It is a well established fact that the size of an inlet (cross-sectional area) is dependent on the tidal prism, large tidal prisms requiring large inlets and catchment areas. It is thus possible to predict the course of change in the inlet dimensions following a reduction in the size of a catchment area or tidal prism. A second line of approach has been to quantify the differences in elevation of the tidal flats over a known time interval. This provides an insight into the mass balance as well as the rates of deposition or erosion. A more recent approach is aimed at predicting the topographic response of the tidal flats following changes in basin dimensions (e.g. RENGER & PARTENSCKY, 1974). This approach has been conceived to assess the effects of engineering structures on tidal environments. It has the advantage that it is not only applicable to large areas with several inlets, but also to small catchments with one inlet or even a sub-catchment within a tidal basin. All these approaches have in common that they aim at establishing empirical relationships which may be used for modelling tidal catchment dynamics and as baseline for later monitoring.

In this chapter a series of empirical relationships between various characteristic morphological parameters are established which are then used to describe the morphodynamic character of the Otzum tidal catchment. The temporal and spatial variations in these equations are also examined.

3.2 Characteristic morphological parameters

The tidal flats and tidal channels constitute the basic morphologic units of a tidal catchment. Analysis of a time series of topographic maps of the tidal catchments of the various inlets in the Wadden Sea clearly shows that the tidal flat elevations and the forms and sizes of the tidal channels change over time. The same is true of the dimensions of the catchment areas (FITZGERALD et al., 1984a). In order to establish the stability conditions of such environments the stability character of these dynamic morphologic units must be known. The morphological parameters that can be measured and monitored include:

- the size of the catchment area: area, A (km^2);
- the size of the inlet: cross-sectional area, A (m^2);
- the size and form of the channels: Depth, D (m); Width, W (m); cross-sectional area, A (m^2) and length, L (km);
- the elevation of the tidal flats: height, H (m).

Based on such parameters the morphological character of catchment areas can be established.

The use of morphological parameters in characterising drainage systems on land (morphometrics and hydraulic geometry) has for a long time been a standard routine (DURY, 1969; STRAHLER, 1971; GREGORY & WALLING, 1973). Measurements of the dimensions of stream channels give the morphometric parameters. The relationship between the flow (discharge) and the morphometric parameters gives the hydraulic geometry, which is another important parameter in describing channel characteristics. Since tidal channel networks resemble stream networks on land, it is anticipated that the methods of network analysis (stream ordering and delimitation of

catchment areas), which have been successfully applied on land, should also be applicable, at least in certain limits, to tidal environments with comparable basin forms. KNIGTON et al (1992) for instance, found that tidal creek evolution in the Mary river, northern Australia, despite its tidal character, closely obeyed the law of stream numbers (HORTON, 1945). This observation is further supported by the findings of KIRCHNER (1993) that all networks obey the laws of drainage network composition. KIRCHNER (1994) elaborates further that the laws of drainage network composition must be obeyed as long as the conventional rules of stream ordering are followed. It is therefore surprising that the highly successful methods of stream network analysis have thus far not been systematically applied to tidal environments.

3.3 Delimitation of the tidal catchment area

The tidal catchment area of an inlet is the basin which is filled up with the flood tide waters. During the ebbing tide the basin acts as the catchment area of the inlet, collecting the tidal waters from the flats and channelling it through the tidal creeks, channels, etc. into the inlet. The delimitation of the tidal catchment areas, just like the river catchment area on land, requires accurate and large-scale topographic maps. Areas of sub-catchments are then delimited accordingly and channel orders designated. The designation of stream orders on land has evolved a number of approaches, each with its own merits and shortcomings (GREGORY & WALLING, 1973). However, unless a derivation of some functional relationship of the channel orders is desired, it is immaterial which system of channel ordering is adopted.

The catchment area of an inlet is traditionally delimited by carefully identifying the different creeks and channels draining the tidal flats during ebb tide. The landward and seaward boundaries are determined by the highest high water mark on land and the line joining the islands' high water mark across the inlet, respectively. The water divides (a line of maximum topography) separating neighbouring channels from each other define the sub-catchment areas (Fig. 3-1) (KNOP, 1963; RODLOFF, 1970; RENGER & PARTENSCKY, 1974).

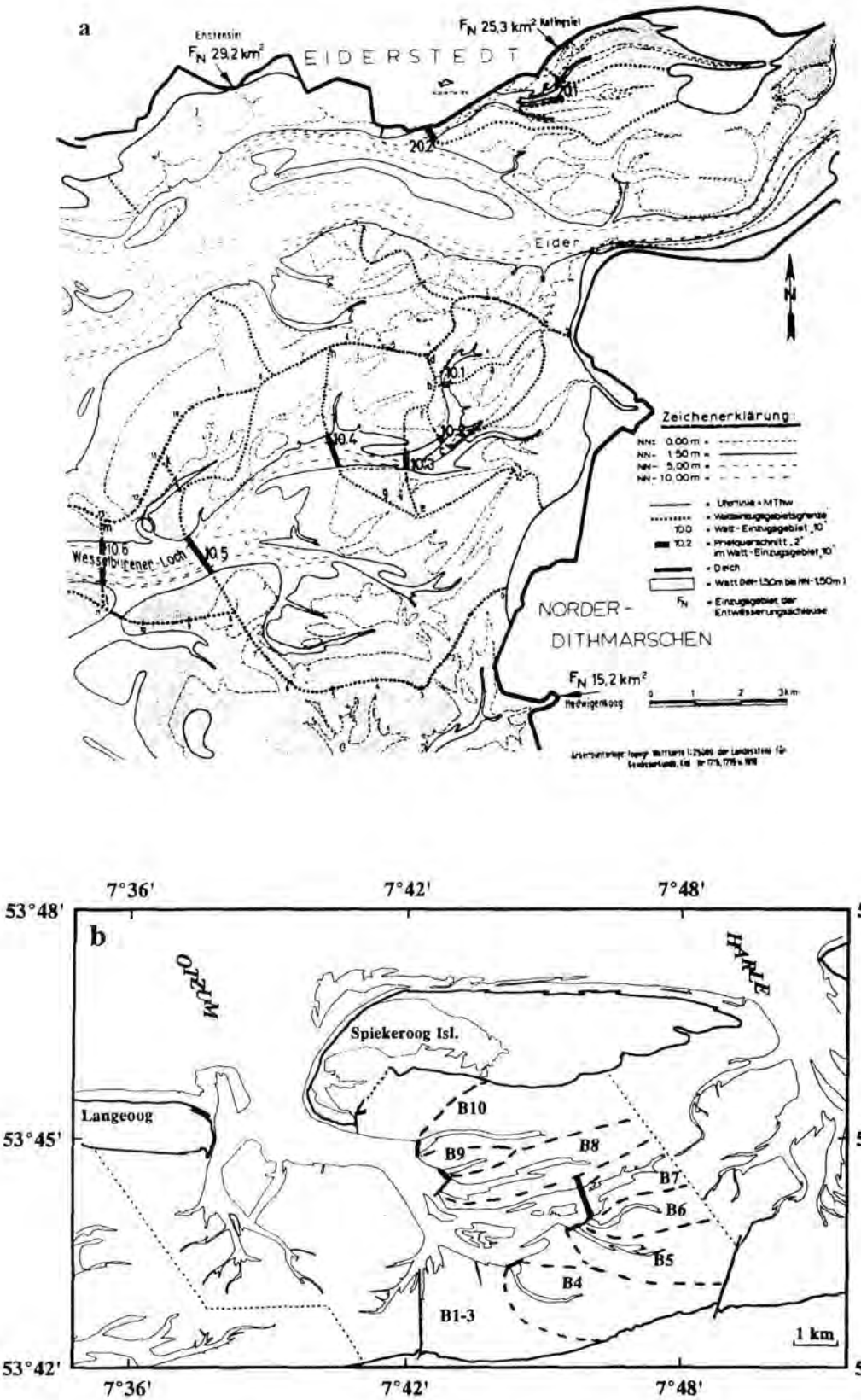

Fig. 3-1 Delimitation of tidal catchment areas. a) Cross-sections are arbitrarilly selected along channels (KNOPP, 1963); b) Cross-sections are drawn at the seaward limits of channels.

3.4 Distribution functions of tidal basin morphology

The structure of the tidal basin, in this case the tidal catchment area or the backbarrier area, plays a major role in determining the course of tidal development in the area. Although a large basin should have a large tidal prism, this depends on the internal structure of the basin, i.e. the distribution of the topographic elevations.

3.4.1 Tidal flat elevations

Traditionally topography was represented by selected cross-sections. However, this method does not give a complete picture of the basin structure in plan. The plan-view of the basin structure is best represented by an area curve (RENGER & PARTENSCKY, 1974). This is essentially an areal distribution of bottom elevations summarised in a curve. The area under a given elevation is normally presented relative to the area below chart datum or the area below the mean high water level. Whether the chart datum or the mean high water level is to be used depends on the intended application of the results. Here, the mean low water or chart datum is considered to be the basis for assessing tidal volumes.

Using a large scale topographic map (1 : 25000), the area under every contour was digitally calculated using the Sigma Scan computer program. This method, unlike the conventional planimetry is very fast and much more accurate. The area values determined in this way were subsequently normalised relative to the area under chart datum and plotted against the elevation to give the area distribution curve. Fig. 3-2a shows the distribution of the bottom elevations (area curve) in the whole of the Otzum tidal catchment. The curve shows a small increase in area for a given rise in elevation below chart datum and large increases above chart datum. The area under the high water line is more than four times as large as the area below chart datum ($A_{1.0}/A_{CD}$ = 4.4, where $A_{1.0}$ and A_{CD} are the areas below NN + 1 m and chart datum, respectively). This corresponds to a ratio of 1:3.4 ($(A_{1.0} - A_{CD})/A_{CD}$) between the water filled channels and the dry tidal flats at low tide. The mean high water mark lies at 1.3 m above the ordinance datum (German NN).

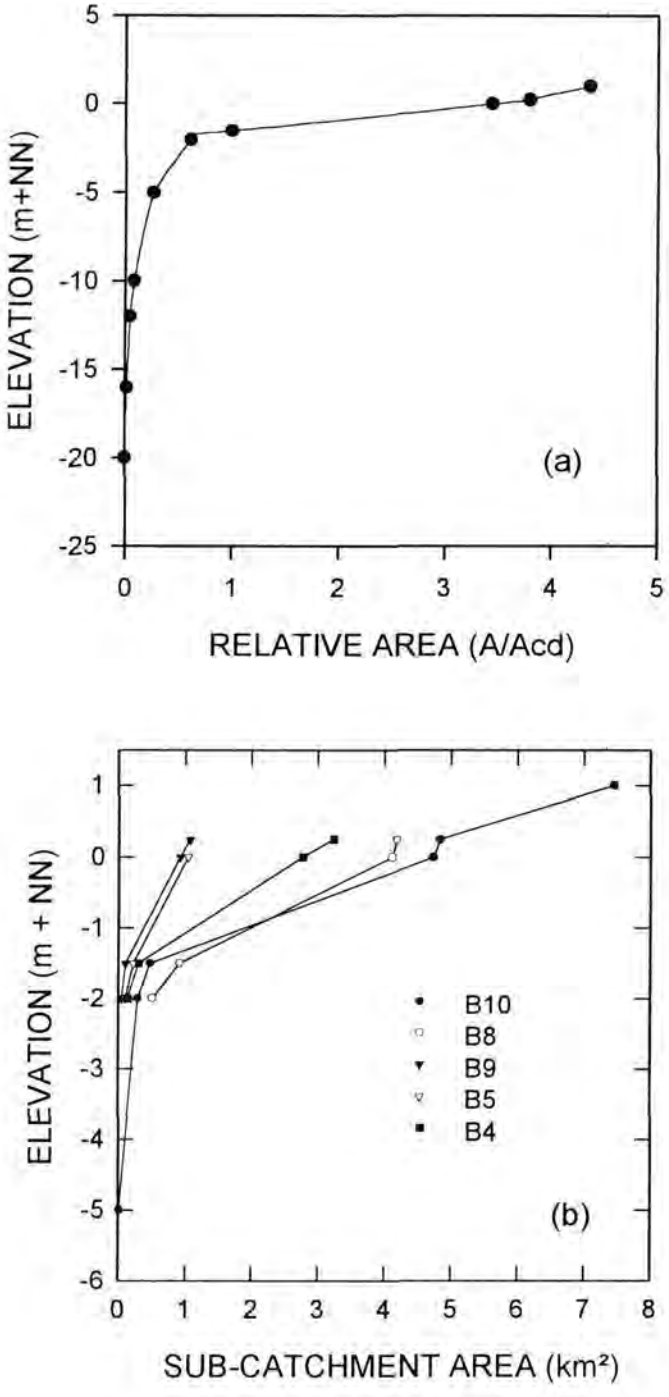

Fig. 3-2 Areal distribution of the topography: a) the whole Otzum catchment; b) various subcatchments.

In effect, the area curve for the whole tidal catchment represents the average for the whole area. Figure 3-2b shows that the area curves of sub-catchments within the basin differ both from one another and from the overall trend. Due to the different topographic distributions in the sub-catchments of the tidal channels and creeks the rate of rise of the tidal stage differs from one area to another. FITZGERALD et al. (1984a) avoided evaluating the tidal prism for the backbarrier areas on the ground that using an average tidal range would lead to inaccurate results. PETHICK (1980) observed velocity surges in tidal creeks which he interpreted as being due to abrupt increases in the discharge as the rising tidal waters began to fill the creeks and areas lying above chart datum. This interrelationship will be dealt with in detail in Chapter 6.

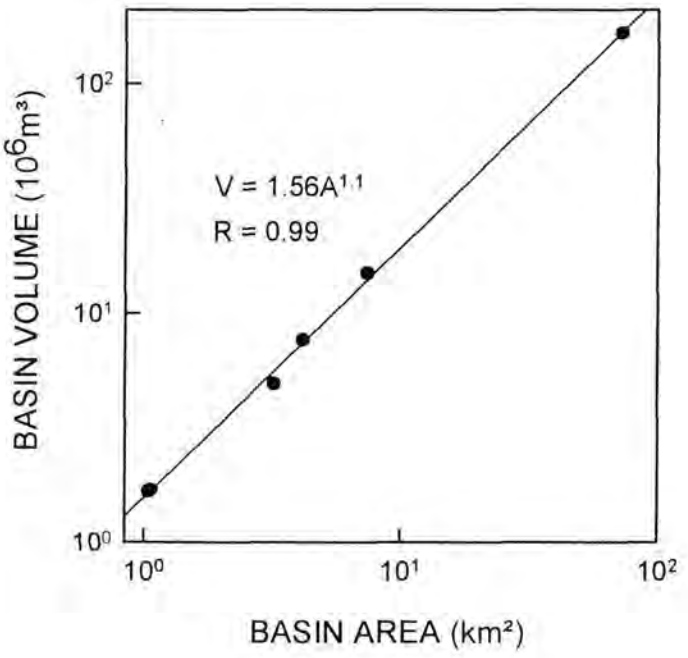

Fig. 3-3 Dependence of discharge volume on the basin (catchment) area.

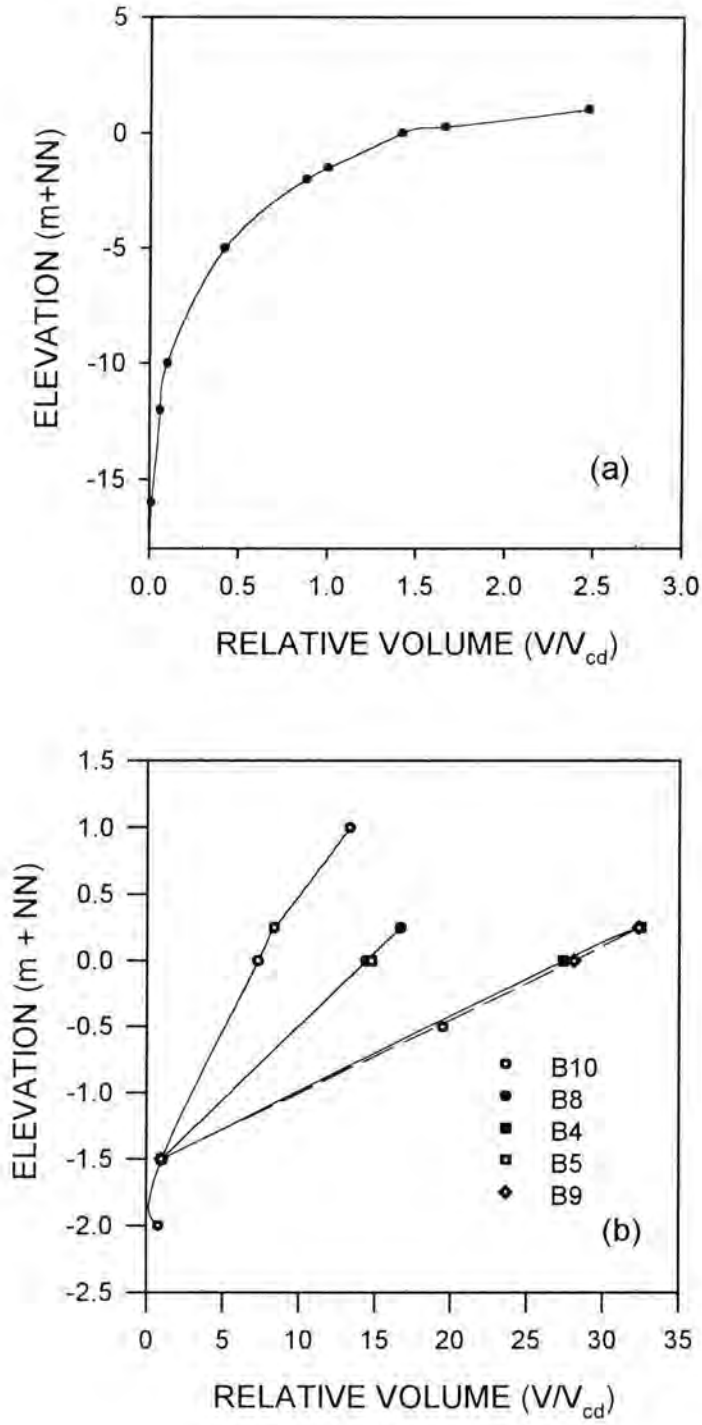

Fig. 3-4 Variation of the basin volume with elevation above bottom: a) the whole Otzum catchment; b) various subcatchments.

3.4.2 Volume of water-filled basin

The volume of water in a basin depends on the size and shape of the basin. By plotting the volumes of different catchment areas against their areas in the eastern Otzum tidal basin, the following empirical power relationship is obtained:

$$V = 1.56\, A^{1.1} \qquad (1)$$

where, V is the basin volume below mean high water level in 10^6 m^3 and A is the catchment area in km^2 (Fig. 3-3). This volume includes both channel and overbank waters.

The volume of a basin varies with its elevation above the bottom. If the bottom is strongly elevated its storage capacity decreases and vice versa. The volume distribution curve or simply the volume or storage curve is obtained from the integral of the area curve and provides a direct method of calculating the volume of the water-filled basin relative to any elevation in that basin. Figure 3-4a shows the volume curve for the Otzum tidal catchment. Like the area curve, the volume curves of subcatchments, owing to differences in their topographies, also differ greatly (Fig. 3-4b). Since the basin storage is a function of both the elevation and the size of the catchment area, which in turn is a function of the elevation, this relationship can also be described by an empirical equation involving both elevation and area (e.g. RENGER & PARTENSCKY, 1974).

3.5 Dimensional relationships between channels and catchment areas

The discharge volumes through the tidal channels are determined by the dimensions and shapes of the tidal channels. The size parameters include the cross-sectional area, depth, width, volume and length. It is well known, both in rivers and tidal channels, that the size of the channel (width, depth, cross-sectional area, etc.) bear fixed relationships with the discharge volumes or catchment areas (RODLOFF, 1970; CARRAGHER et al., 1983).

3.5.1 Channel cross-sectional area

The tidal flat areas which are usually covered by water at high tide are drained during the next low tide. During the ebbing tide a large proportion of the water volume is forced through the available tidal channels. The discharge at any given point along a channel depends on the volume collected from the area landwards of that point. There should thus be a relationship between the channel cross-sectional area and the size of the catchment area.

Although linear relationships between cross-sectional areas and catchment areas have been established in various studies (RODLOFF, 1970; RENGER & PARTENSCKY, 1974), dissatisfaction with the data scatter in smaller channel regions has always been pronounced. The data used in these studies were collected from selected channels along which cross-sections were measured. A catchment area was subsequently delimited for each of the cross-sections (Fig. 3-1 (b)). In this method smaller cross-sections are unnecessarily numerous and, due to map inaccuracies in the areas of smaller channels, the measured cross-sections vary greatly. Assuming the numerous cross-sections and sub-catchment areas to be the cause of the amplified data scatter a different method is proposed in this study. Thus the cross-sections at the seaward boundaries of the catchment areas of each of the selected channels (all channels in a selected area) were measured in order to reduce the number of smaller cross-sections.

In Fig. 3-5 (a - e) the resulting relations (cross-sectional area - catchment area) of the modified method for the western and eastern parts of the Otzum tidal basin are shown together with that of RODLOFF (1970). The similarity in the results is striking. All the correlations are highly linear ($R > 0.95$) and data points tend to form linear clusters. The data scatter in the smaller channel regions is still evident (Fig. 3-5 (b - e)). Three clusters (possibly four in Fig. 3-5 (a)) are identifiable:

a) catchments smaller than 20 km^2
b) catchments between 20 and 50 km^2
c) catchments larger than 50 km^2.

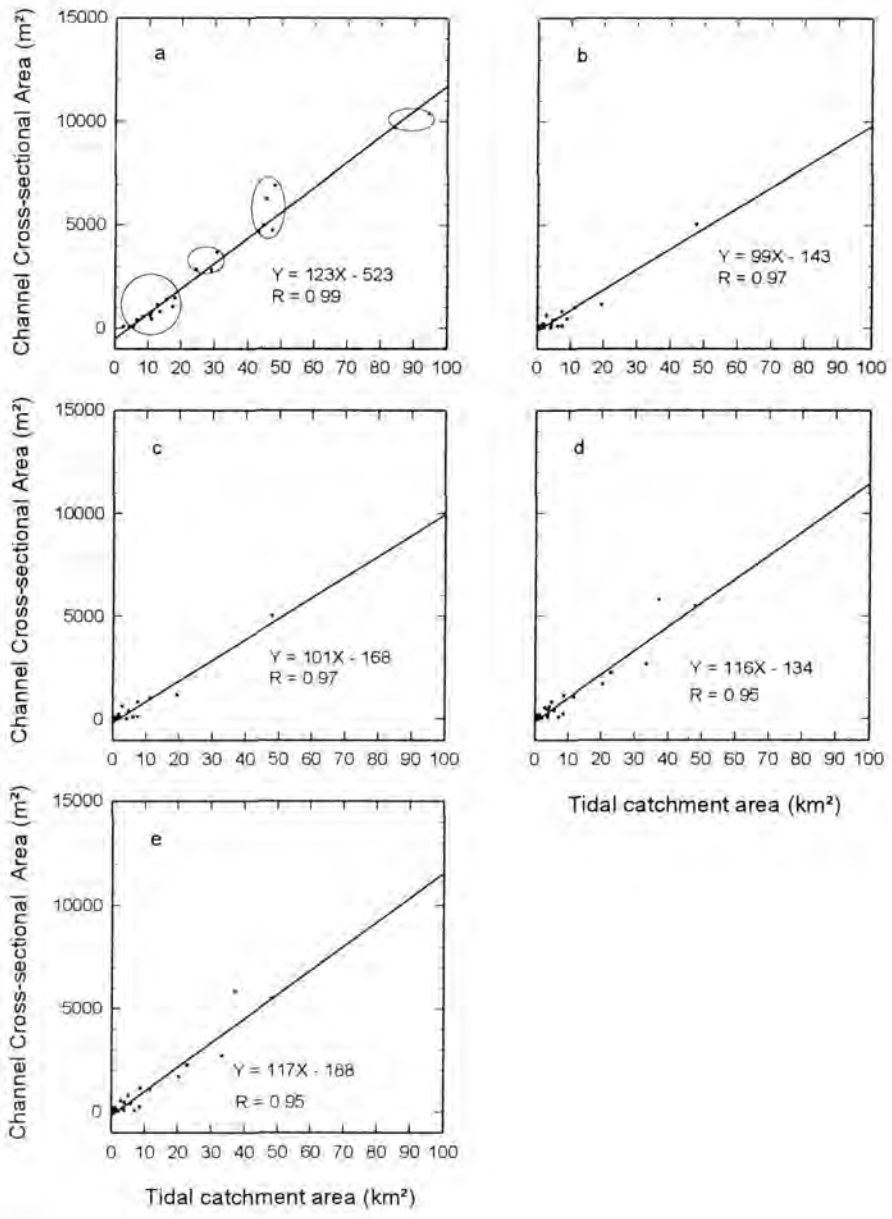

Fig. 3-5 Dependence of channel size (cross-sectional area) on the size of its catchment area: a) data of RODLOFF (1970); b) Otzum catchment, 1960; c) Schillbalje catchment, 1960; d) Otzum catchment, 1975; e) Schillbalje catchment, 1975. Note the data clusters in various catchment size categories (e.g. (a)).

These clusters indicate that the relationships obtained are, in fact, composed of discontinuous linear functions describing each of the individual clusters. The physical meaning of the clusters may lie in either or both of the following:

1) A changing response of the channel dimensions to increasing discharges as the catchment area increases. This channel behaviour has long been known from rivers (e.g. CARRAGHER et al., 1983). In their work dealing with catchment areas less than 3 km^2 CARRAGHER and co-workers pointed out that the breaks in the relation between catchment area and width or depth reflected changes in discharge volumes as well as changes in bed material downstream.

2) A natural occurrence of tidal channels which are skewed towards smaller ones. Channels draining less than 20 km^2 are numerous while the bigger ones draining larger areas diminish almost geometrically.

The persistence of the spread of data points in the smaller catchment areas does not appear to be associated with the methodology adopted (establishment and analysis of cross-sections along channels). Instead, as pointed out above, it seems to follow a natural law of occurrence. Since smaller tidal channels are highly dynamic - some may be in equilibrium, while others may be growing or shrinking - their sizes tend to vary greatly, a situation which would explain the data spread for smaller channels.

3.5.2 Channel volume

The relationship between the volume of a channel and its catchment area is perhaps one of the most widely established characteristics of tidal channels. Bearing in mind that the bigger a channel the larger the area it drains, the whole basin was divided into a western and an eastern region drained by the Hull and Schill channels, respectively. Within each of these regions first and higher order channels were initially separately analysed before combining them at a later stage. This procedure was applied to the topographic charts of 1962 and 1975. Cross-sectional areas at selected intervals along a channel were measured and the volume of the channel calculated by the summation of the products of the multiplication of cross-sectional areas and their effective distances (the distance of constant cross-section) over the whole length of a channel. The catchment area of a given channel as well as the channel cross-sections were digitally measured using the Sigma Scan computer program.

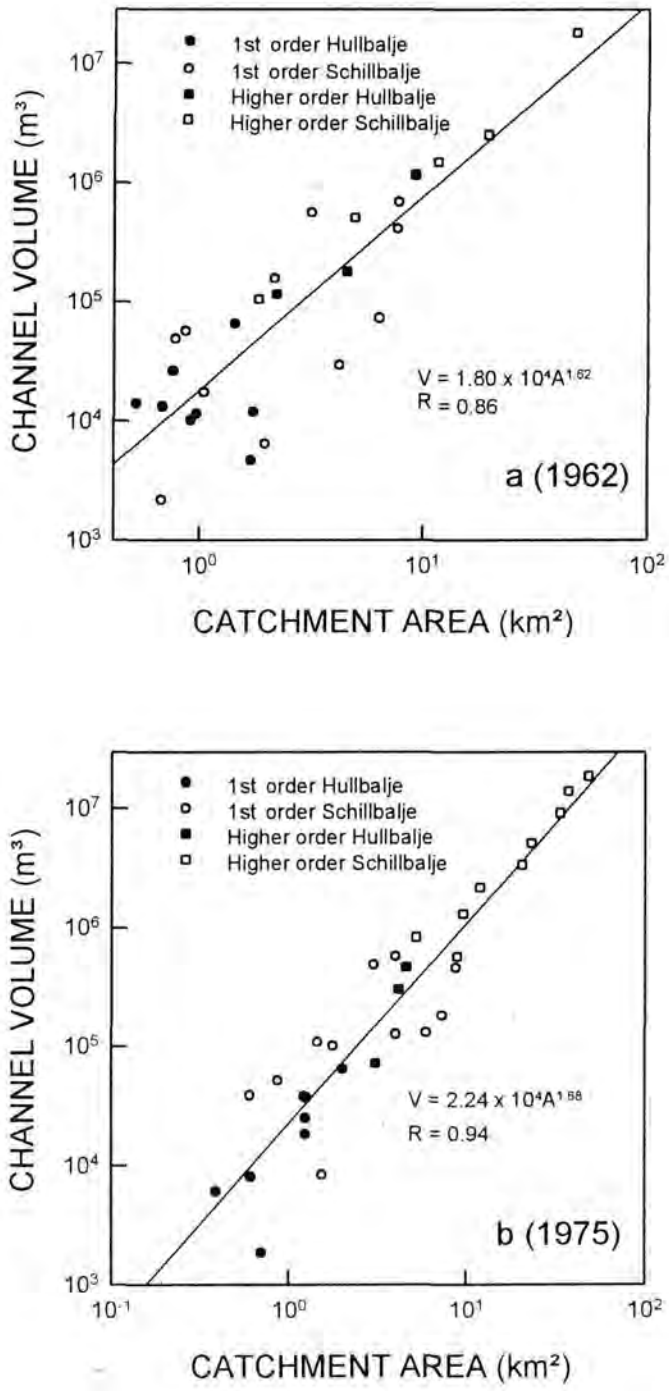

Fig. 3-6 Relationship between channel volumes and sizes of their catchment areas. Hullbalje drains the western sector of Otzum catchment area and Schillbalje drains the eastern sector.

The volume of a channel was found to be governed by the size of the catchment area. The channel volume is related to its catchment area through a power relationship as represented in Fig. 3-6 (a & b). The scatter of the data points of the different channel orders warranted a closer examination. Indeed, as can be seen in Fig. 3-7, the relationship between the volume of a channel and the size of its catchment area differs from one channel order to another. In comparison with small channels, higher order channels are shown to grow more rapidly in size as the catchment area expands. Since much of the volume of water drained by a small channel is in form of overbank flow, the channel itself needs little size adjustment. There are also clear differences between the channels of the western (Hullbalje) and eastern (Schillbalje) sectors. Larger channel volumes are predicted for the eastern parts than for the western ones of the Otzum tidal catchment. This implies that a large proportion of the discharge in the western part is in form of overbank flow. These empirical deductions are in concurrence with the fact that the tidal channel network is better developed in the eastern part than in the western part.

The channel volume-catchment area equations for the periods 1962 and 1975 are summarised in Table 3-1. The differences in the equations suggest a re-evaluation of earlier conclusions regarding the applicability of such empirical relationships. It is demonstrated by these results that the empirical equations are not only site specific but also dependent on the data base and scale. Thus, although PARTENSCKY (1980) asserts that the equation generated for the whole of the inner German Bight ($V = cA^{1.63}$, where V is volume, A is area and c is a constant) holds true for the individual catchment areas, this is in fact not a correct generalisation (Table 3-1). The exponent in the equations varies from -0.17 to 1.9 depending on the number of channels considered and their orders as well as the accuracy of the chart used. The overall equation for the 1975 topographic chart is:

$$V = 2.24 \cdot 10^4 A^{1.68} \qquad (2)$$

where, V is channel volume in m^3 and A is its catchment area in km^2.

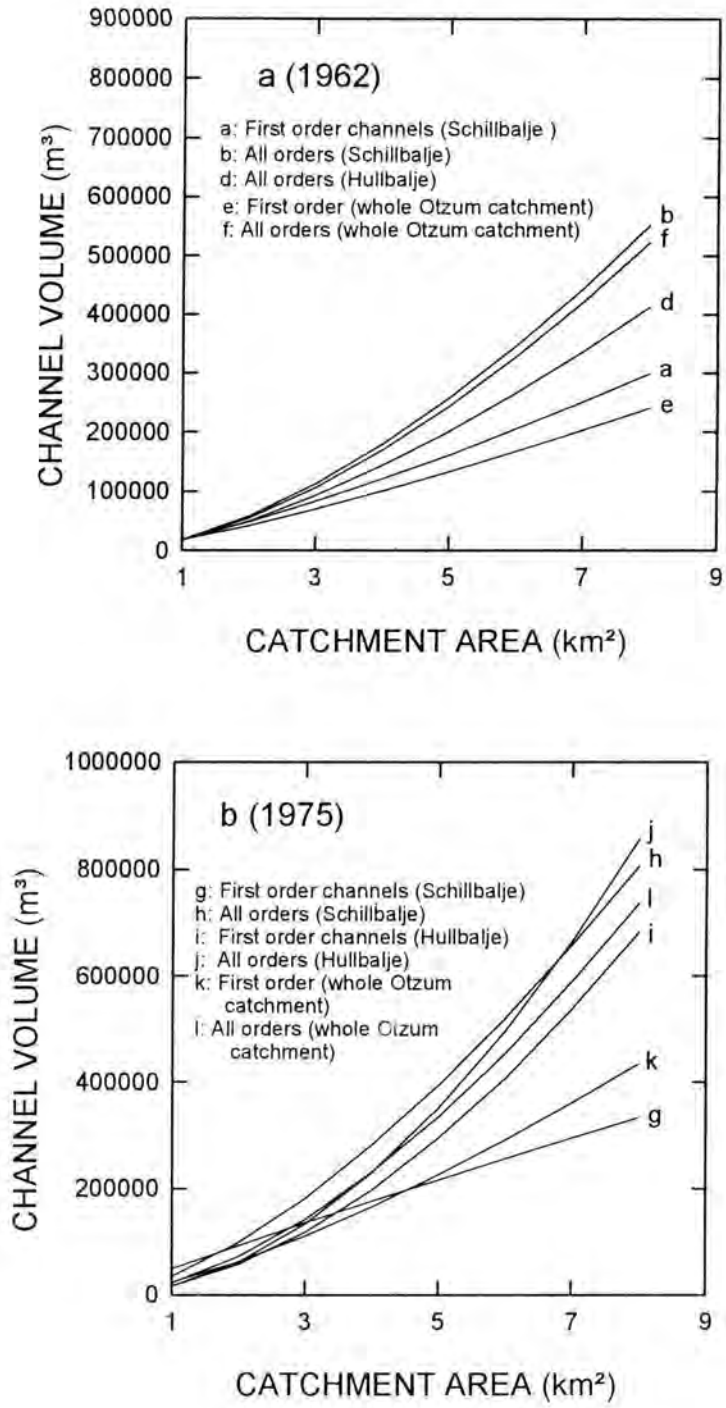

Fig. 3-7 Dependence of channel volume - catchment area relationships on channel order (size).

As shown above, equations representing only part of a catchment area (Table 3-1, Hullbalje & Schillbalje) deviate considerably from that of PARTENSCKY (1980). The range of variations in such power relationships is evident also in previous studies done within the German Bight region (RENGER & PARTENSCKY, 1974; RENGER, 1976; DIECKMANN, 1985).

Table 3-1 Summary equations of channel volume - catchment area relationships of various channels in the Otzum catchment.

Year	1st order channels	1st & higher order
	HULLBAJE	
1962	$V = 1.46 \cdot 10^4 A^{-0.17}$	$V = 1.75 \cdot 10^4 A^{1.52}$
	(R = -0.1)	(R = 0.80)
1975	$V = 1.65 \cdot 10^4 A^{1.79}$	$V = 1.65 \cdot 10^4 A^{1.90}$
	(R = 0.80)	(R = 0.92)
	SCHILLBALJE	
1962	$V = 2.0 \cdot 10^4 A^{1.30}$	$V = 1.90 \cdot 10^4 A^{1.62}$
	(R = 0.66)	(R = 0.85)
1975	$V = 4.91 \cdot 10^4 A^{0.92}$	$V = 3.42 \cdot 10^4 A^{1.52}$
	(R = 0.65)	(R = 0.91)
	OVERALL	
1962	$V = 1.79 \cdot 10^4 A^{1.25}$	$V = 1.80 \cdot 10^4 A^{1.62}$
	(R = 0.66)	(R = 0.86)
1975	$V = 2.37 \cdot 10^4 A^{1.40}$	$V = 2.24 \cdot 10^4 A^{1.68}$
	(R = 0.79)	(R = 0.94)

Volume (m^3), Area (km^2).

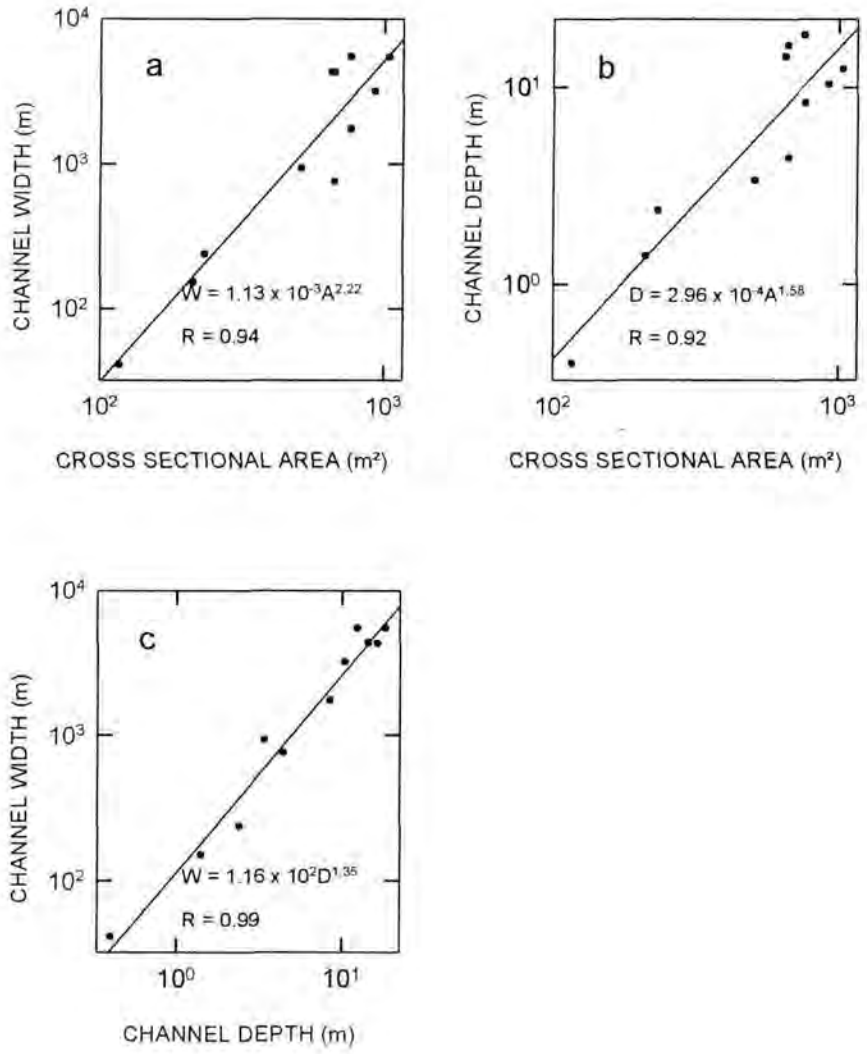

Fig. 3-8 Morphometric relationships in tidal channels.

3.5.3 Width - depth relationship

The cross-sectional area of a channel is a derived dimensional parameter parameter. The variations in the size of cross-sections depends largely on the width - depth relationship. Tidal channels are formed by erosion of the existing flats. These are then deepened and broadened as the channels become larger. As such, both the width and

depth of channels appear to be large for large cross-sections (Fig. 3-8 (a & b)). This proportional relationship means that large channels are wide and deep, whereas small channels are narrow and shallow. This interpretation is supported by Fig. 3-8 (c). The depths and widths of a channel at any cross-section are related to each other through a power function in which the width is more than 100 times as large as the depth. The equations are:

$$D = 2.96 \times 10^{-4} A^{1.576} \quad (3)$$

$$W = 1.13 \times 10^{-3} A^{2.22} \quad (4)$$

$$W = 1.16 \times 10^{2} D^{1.35} \quad (5)$$

where, D is depth (m), W is Width (m) and A is cross-sectional area (m^2).

3.5.4 Channel length

The length of a channel in a fluvial system is known to have a proportional relationship to the size of the catchment area (GREGORY & WALLING, 1973). In the Otzum tidal catchment the length of the channels is related to their catchment areas by a power equation of the form $L = a A^b$, where a denotes the Y-intercept and b is the slope of the regression (Fig. 3-9). Channels of different sizes (orders), however, provide different channel length - catchment area relationships, as expressed in Fig. 3-10. The equations of the different relationships are summarised in Table 3-2. The overall equation for the channels of the Otzum catchment is:

$$L = 0.81\ A^{0.87} \quad (6)$$

where, L is length (km) and A is catchment area (km^2).

From Table 3-2, it can be seen that the channels in the eastern part of the basin are characteristically longer than those in the western part, a feature already shown by the channel volume. This reflects once again the different hydraulic conditions prevailing in the two parts of the basin. The tidal wave which fills the basin from the NW introduces larger inflows into the Schillbalje than into the Hullbalje, thus inducing differences in the development of channel geometry.

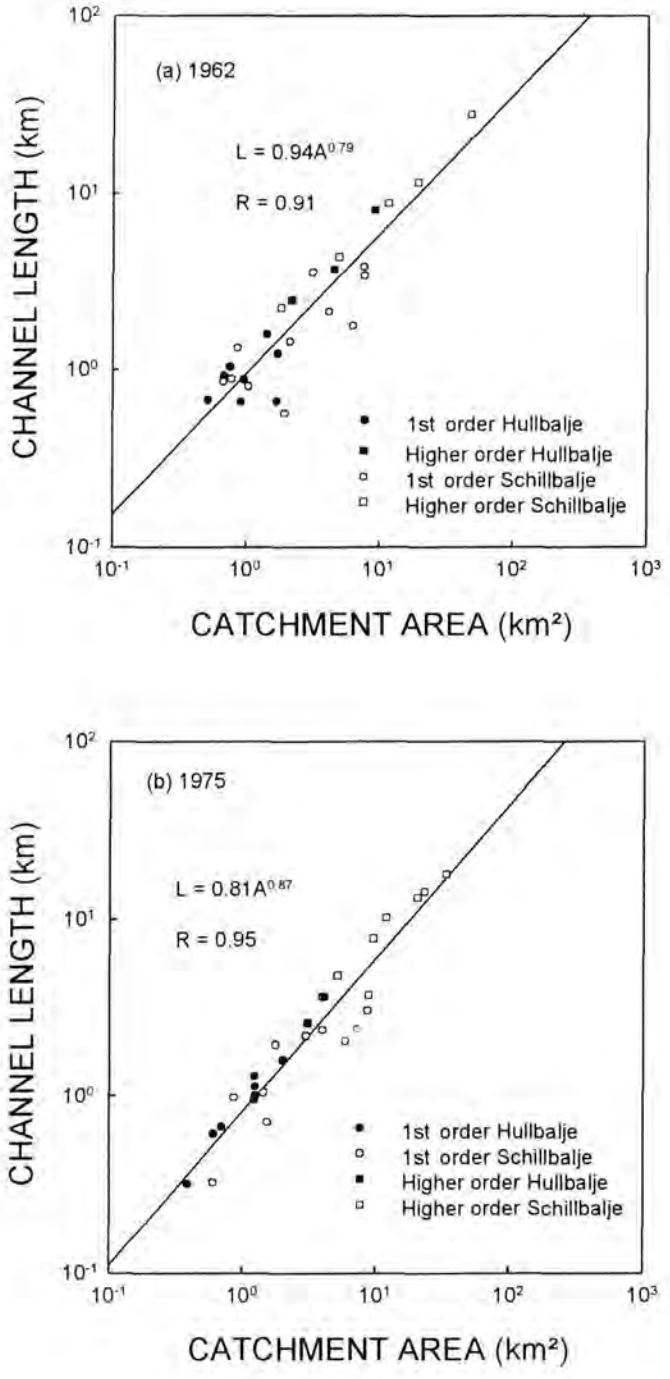

Fig. 3-9 Dependence of channel length on catchment area. The scatter in data points suggests dependence of regressions on channel ranking (open and filled symbols).

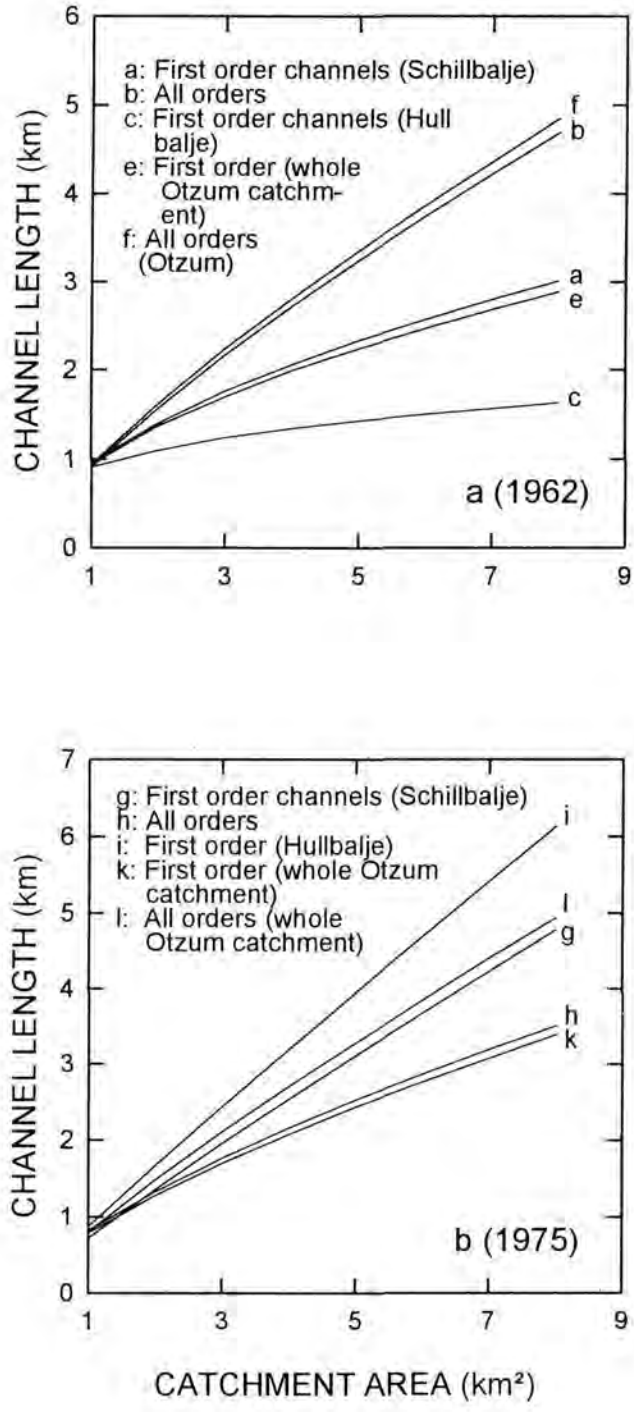

Fig. 3-10 Channel length - catchment area relationships for various channel orders in selected parts of the Otzum tidal catchment.

Table 3-2 Summary equations of channel length - catchment area relationships of tidal channels in the Otzum catchment.

Year	1st order channels	1st & higher order
	HULLBAJE	
1962	$L = 0.91\ A^{0.28}$	-
	(R = 0.39)	
1975	$L = 0.87\ A^{0.94}$	$L = 0.91\ A^{0.97}$
	(R = 0.97)	(R = 0.99)
	SCHILLBALJE	
1962	$L = 0.96\ A^{0.55}$	$L = 0.91\ A^{0.79}$
	(R = 0.77)	(R = 0.91)
1975	$L = 0.79\ A^{0.701}$	$L = 0.72\ A^{0.91}$
	(R = 0.85)	(R = 0.94)
	OVERALL	
1962	$L = 0.94\ A^{0.54}$	$L = 0.94\ A^{0.79}$
	(R = 0.78)	(R = 0.91)
1975	$L = 0.82\ A^{0.704}$	$L = 0.81\ A^{0.87}$
	(R = 0.90)	(R = 0.95)

Length (km), Area (km^2).

A comparison of fluvial and tidal catchments shows that the established relationship between the channel length and its catchment area for fluvial channels may be applied to tidal systems. Tidal channels plot within the same broad band defined by the upper and lower limits of meandering and straight channels, respectively (Fig. 3-11). The following equation representing the mean of both tidal and fluvial catchments was obtained:

$$L = 1.45\ A^{0.57} \qquad (7)$$

where, L is channel length (km) and A is catchment area (km^2).

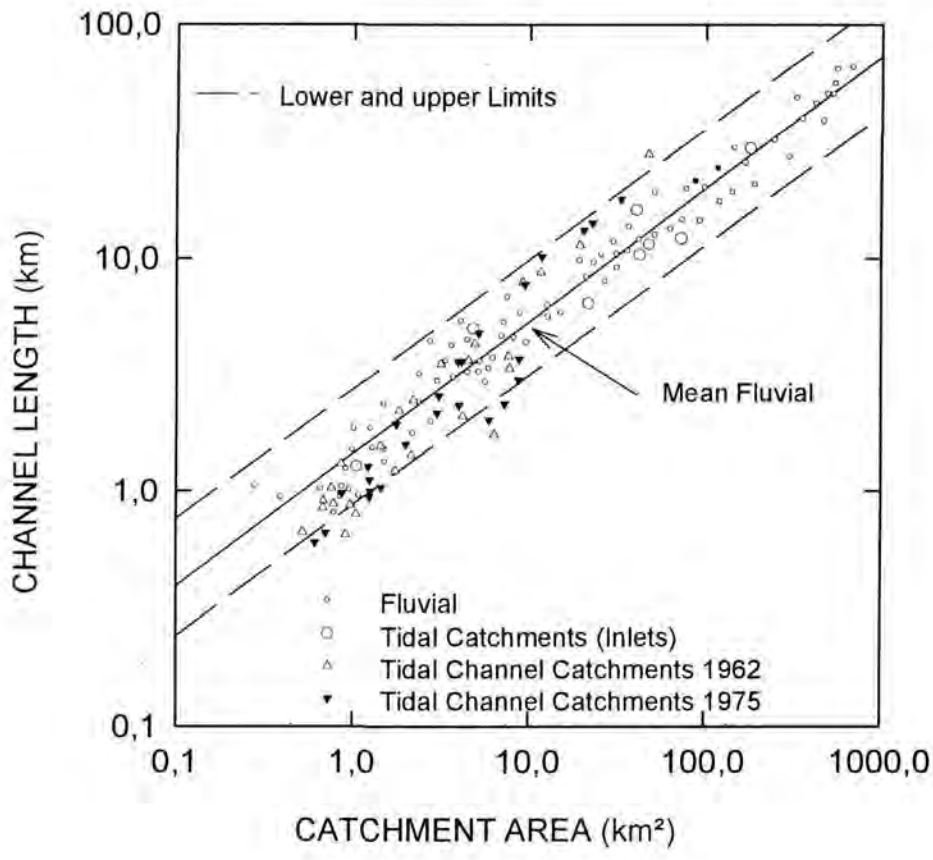

Fig. 3-11 Comparison of channel length - catchment area relationships in fluvial and tidal systems. Data plot in a narrow band bounded by an upper limit of meandering channels and a lower one representing straight channels.

The relationship between channel length and its catchment area has invariably been interpreted in terms of the density of the channel networks (km/km^2) (DIECKMANN, 1985). Thus, the mean equation for fluvial and tidal channels (Fig. 3-11) which is given by $L = 1.45\ A^{0.57}$ (L in km and A in km^2), means a density of 1.45 km/km^2.

This approach allows calculation of the channel network density for any given part of the catchment area, even as small as 1 m^2 (m/m^2).

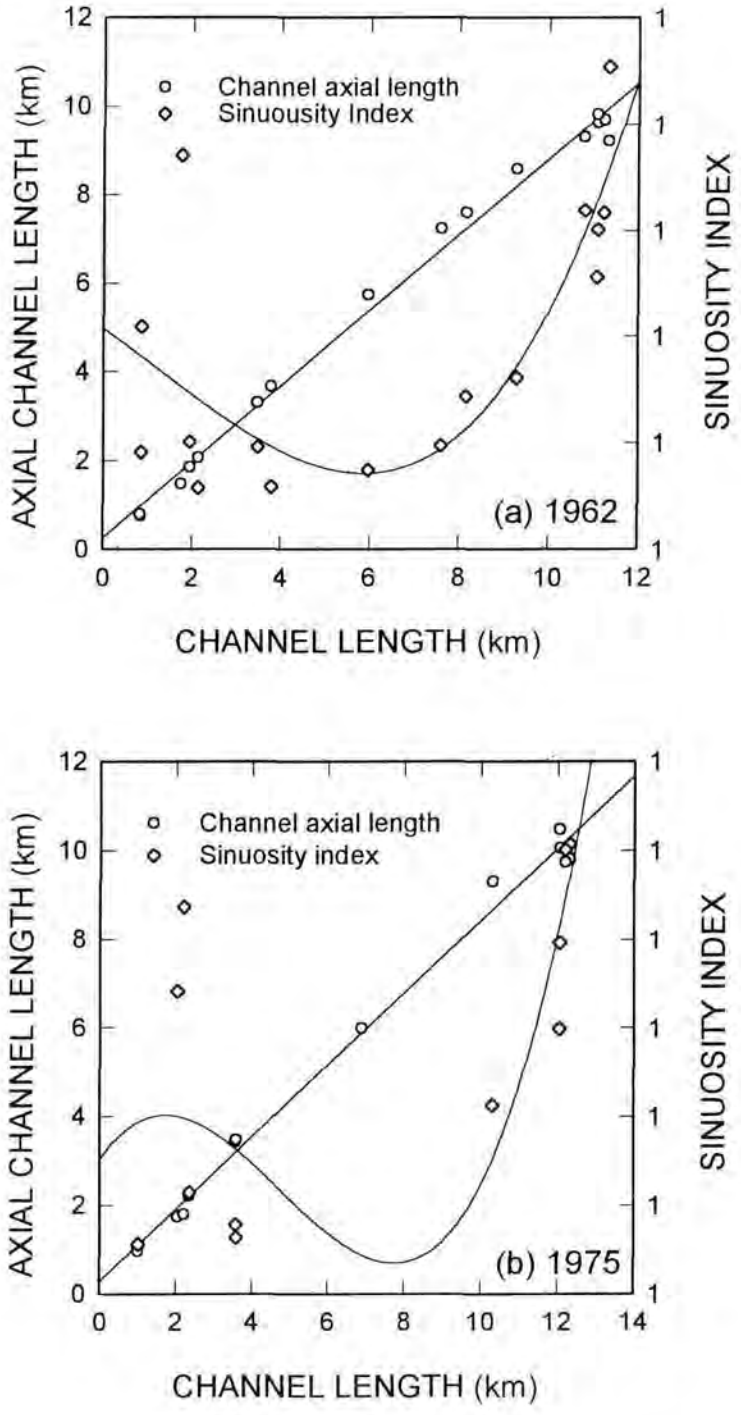

Fig. 3-12 How the tendency towards formation of meanders depends on channel length.

Given the scale of the topographic maps, however, the calculation of such small areas is unrealistic. To avoid this problem, the smallest measured catchment area and channel length should be defined in each case, so that channel network density calculations can be restricted to areas larger than these limiting values.

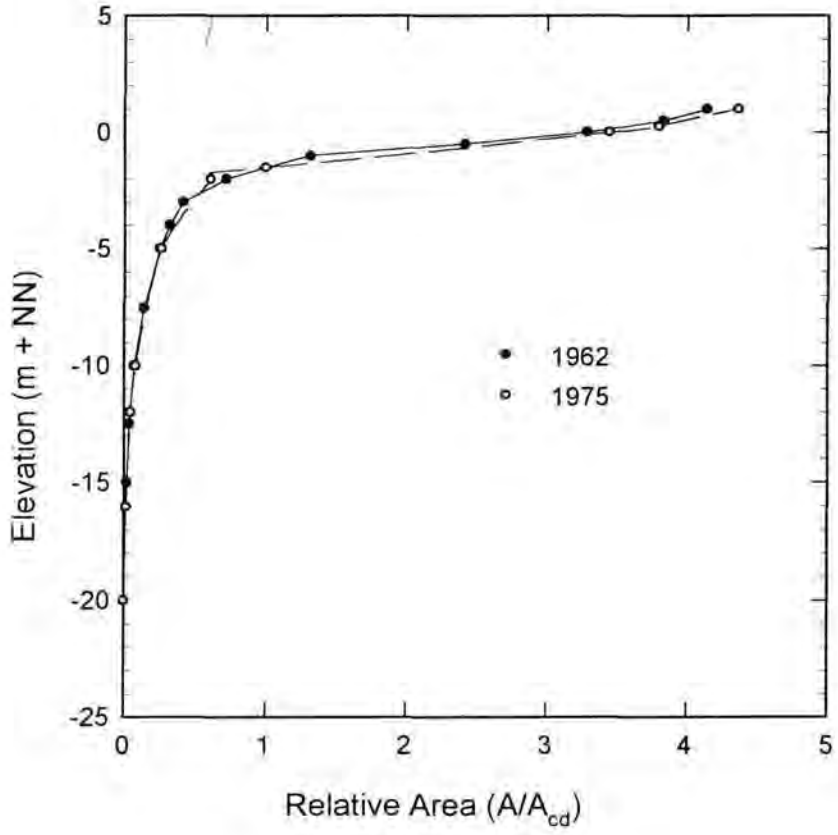

Fig. 3-13 Comparison of the area curves of the Otzum catchment between 1962 and 1975 indicating a positive mass balance.

3.6 Geomorphological changes

Changes in the topography, basin and channel geometry, and sedimentation contribute to the basin geomorphological changes. The various morphological changes that have

taken place in the Otzum tidal catchment area have been examined over the 13-year period from 1962 - 1975 with the help of the changes in the geomorphological parameters described in earlier sections.

3.6.1 Changes in the characteristic morphological parameters

The area and volume curves

The area distribution curve summarises the topographic distribution of the basin (catchment). Using such summary presentations for two consecutive periods, it is possible to compare the changes in elevation at different reference levels over a given time interval. In Fig. 3-13 the area distribution curves for the Otzum tidal catchment of 1962 and 1975 are compared. Above the chart datum (approx. NN - 1.5), the area curve for 1975 lies below the 1962 curve. A positive area under a given elevation over the given time interval indicates lateral expansion of the basin and hence, an increase in the sediment thickness underneath. This positive mass balance is clearly outlined when the changes in the basin volume are considered (Fig. 3-14). A decrease in the storage volume of the basin reflects sediment deposition. In Fig. 3-14 the volume curve for 1975 passes above the 1962 curve, which means that the storage volume under any given elevation in 1975 was less than in 1962. The trend of the curves relative to each other may be interpreted as typifying three distinct regions:

a) the channels between the depth interval NN - 3 to NN - 5 m are marked by shallowing;
b) shallower channels and low lying tidal flats (between NN - 3 m and NN - 0.5 m) appear to have experienced minor erosion; and
c) higher tidal flats (above NN) are marked by deposition.

The shallowing of the deeper channels together with deposition on the higher tidal flats more than compensate the erosion observed in shallow channels and on low lying tidal flats and hence reflects a positive mass balance.

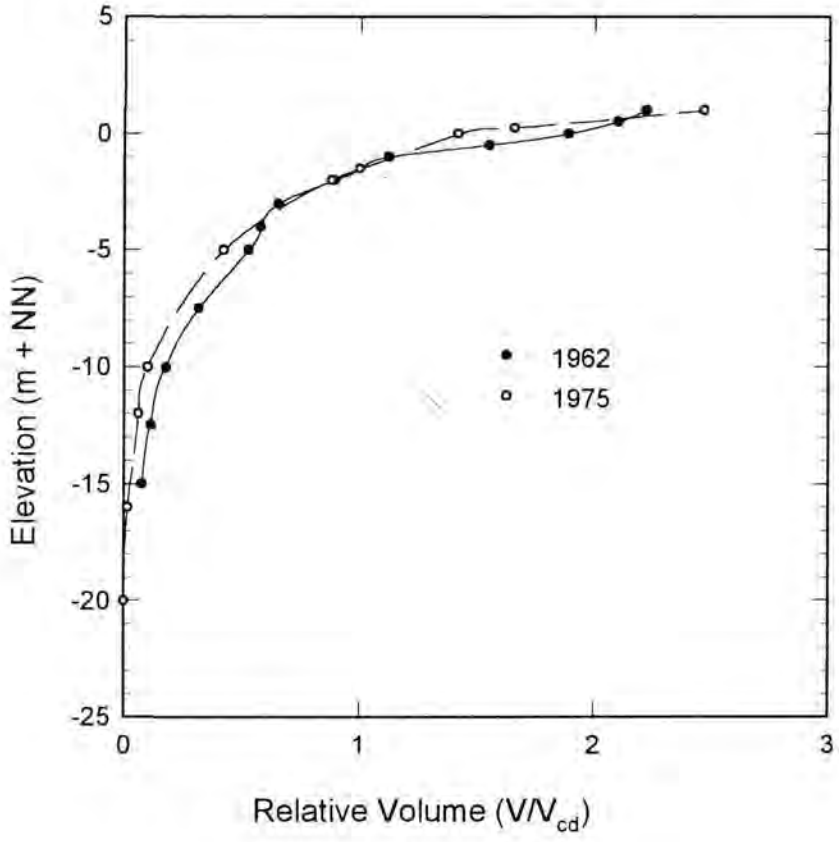

Fig. 3-14 Comparison of the volume curves of the Otzum catchment between 1962 and 1975 indicating decrease in basin volume corresponding to a positive mass balance.

Relationships between catchment area and channel dimensions

The various relationships between the size of the catchment area and channel size parameters also vary with time. Changes in the size of the catchment area, usually accompanied by changes in the tidal prism, would certainly result in changes in the channel dimensions or geometry (FITZGERALD et al., 1984a).

The differences in the channel volume - catchment area relationships for the period 1962/1975 are presented in Fig. 3-15. They are extracts from Fig. 3-7, the equations having been summarised in Table 3-1.

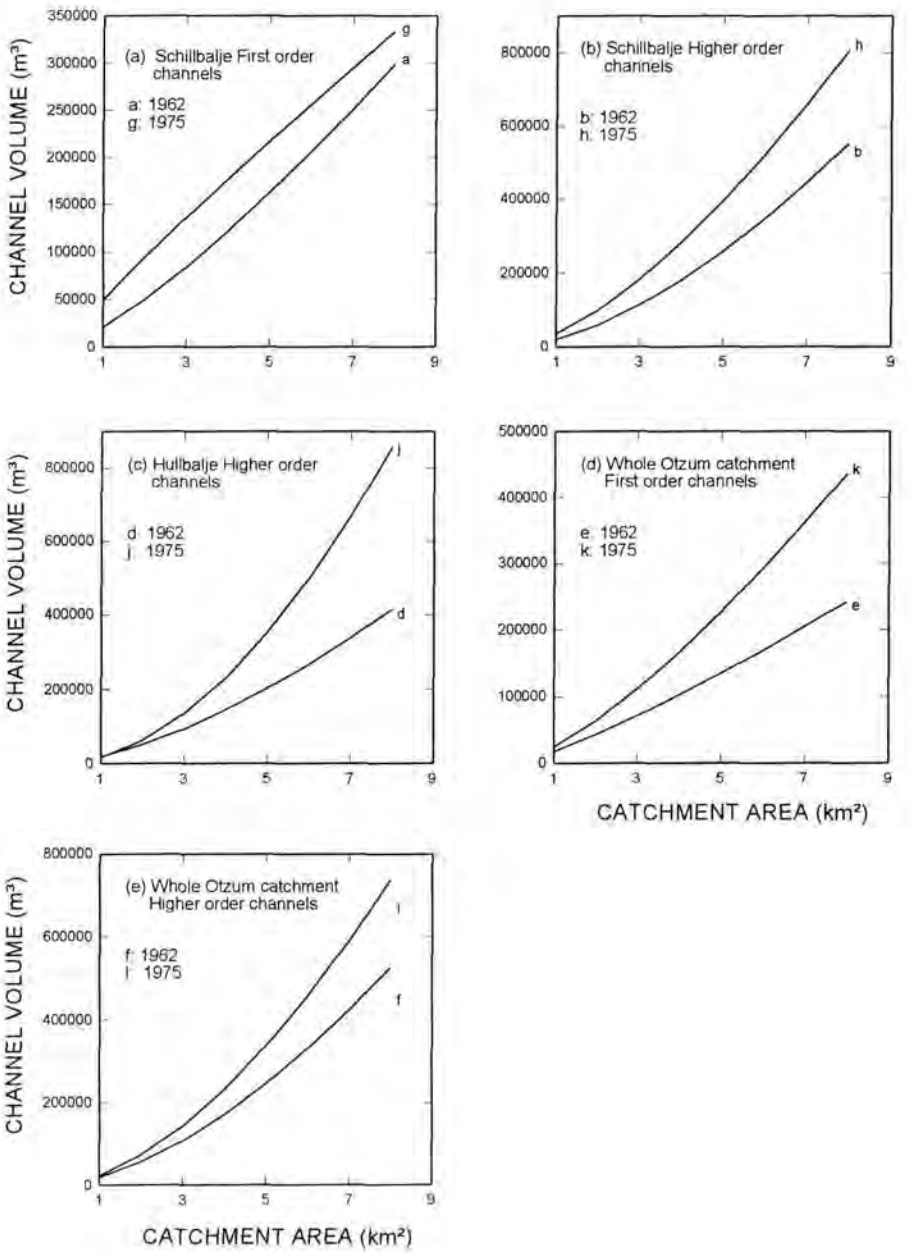

Fig. 3-15 Comparison of channel volume and catchment area over 13-year period showing a clear increase in channel volumes.

Irrespective of the channel order, it can be seen that between 1962 and 1975 there has been a general increase in the volume of the channels. Channel enlargement may be achieved through channel scouring (deepening and widening) as well as lengthening. The channel cross-section, width, depth and length relationships, as explained below, support this observation.

As noted earlier, the cross-sectional area of a channel is governed by the measures of width and depth. Since both width and depth of a channel tend to be large for large cross-sections (Fig. 3-8 (a & b)) and show a proportional relationship to each other (Fig. 3-8 (c)), it may be concluded that the increase in volume of the tidal channels over the 13-year time interval has been achieved mainly through widening and deepening of the channels, i.e. erosion of the tidal channels. The positive mass balance deduced previously must therefore, have been achieved largely through deposition on the tidal flats.

In Fig. 3-9 the channel length - catchment area relationships for the period 1962/1975 were graphically illustrated and also summarised in Table 3-2. The relationships for the time interval are also compared between channels of different orders (Fig. 3-16). It is evident from both figures that the relationships for 1975 generally predict longer channels than in 1962. A closer examination of the curves, however, reveals existence of cross-over points between the curves for 1975 and 1962. These cross-over points imply that, whereas longer channels were required to drain larger areas in 1975 than in 1962, smaller catchments required much shorter channels in 1975 as compared to 1962. These changes may have been caused by a number of factors:

a) Increase in the lengths of larger channels through erosion or development of meanders (FLEMMING & DAVIS, 1990).

b) Decrease in channel bifurcation resulting in large areas containing less effective (cumulative) channel lengths.

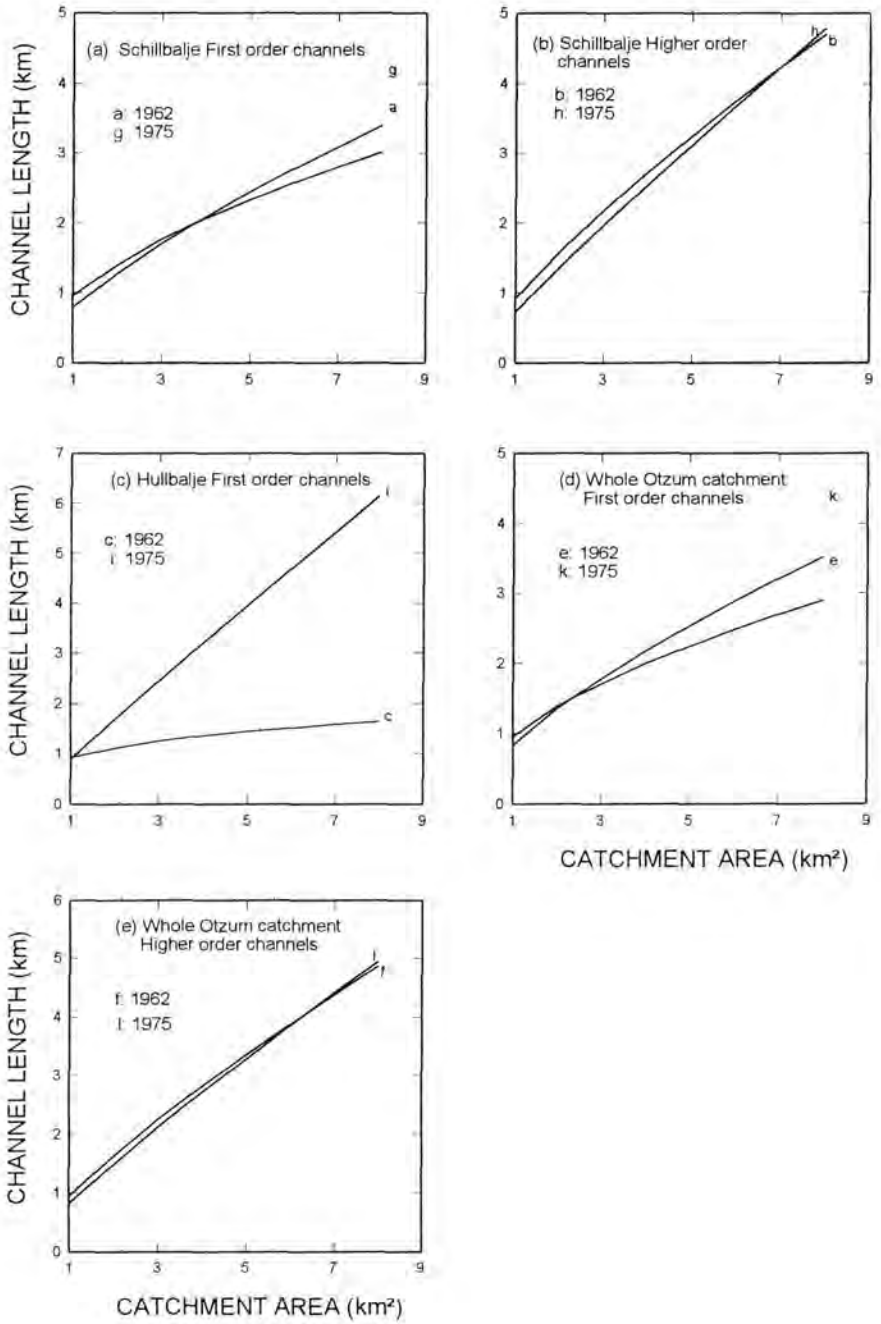

Fig. 3-16 Comparison of channel length against catchment area between 1962 and 1975. Cross over points show that, whereas longer channels were required to drain larger areas in 1975 than in 1962, smaller catchments required much shorter channels in 1975 than in 1962.

c) Straightening of meanders leading to reduction of the effective length, a fact supported by the findings that smaller channels tend to be straight, whereas the large ones tend to be sinuous (Fig. 3-12).

The growth of the tidal channels with time is not unexpected. Since the continuing eastward migration of the tidal water divide causes enlargement in the channel catchment areas, channels must re-adjust in sizes to accommodate the resulting increase in discharge volumes.

3.6.2 Channel migration

Examination of topographic maps or hydrographic charts reveals, among other things, the changes in the channel morphologies, positions and forms. An overlay of the hydrographic charts of the Spiekeroog backbarrier area for the years 1985, 1988 and 1991 (Fig. 3-17), for example, shows a significant change in the positions of channel thalwegs between 1988 and 1991. The Schillbalje (the main channel leading to the Otzum inlet behind Spiekeroog) is the only channel in the Otzum catchment area which appears to have occupied the same position over the 6 year period.

Although the main channel (Schillbalje) has remained relatively stable in the backbarrier area, instabilities have been registered in the inlet mouth. The deepest point of the inlet gorge (20 m) shifted northwards between 1962 and 1975. In this time interval the southern and northern parts of the inlet mouth have experienced deposition and erosion, respectively. Fig. 3-18 demonstrates the lateral and vertical shifts in the cross-sections across the deepest point. Whereas the shallowing (by 2 m) of the channel in the south was accompanied by a large channel displacement (225 m) towards the east, with the thalweg being totally abandoned, the channel deepening (by 5 m) in the north was accompanied by a smaller eastward displacement of the channel (175 m), with the thalweg being only partly abandoned. These adjustments clearly follow well established dimensional channel relationships. In the southern transect (Fig. 3-18 (b)), for example, the depth reduction was compensated by an increase in width.

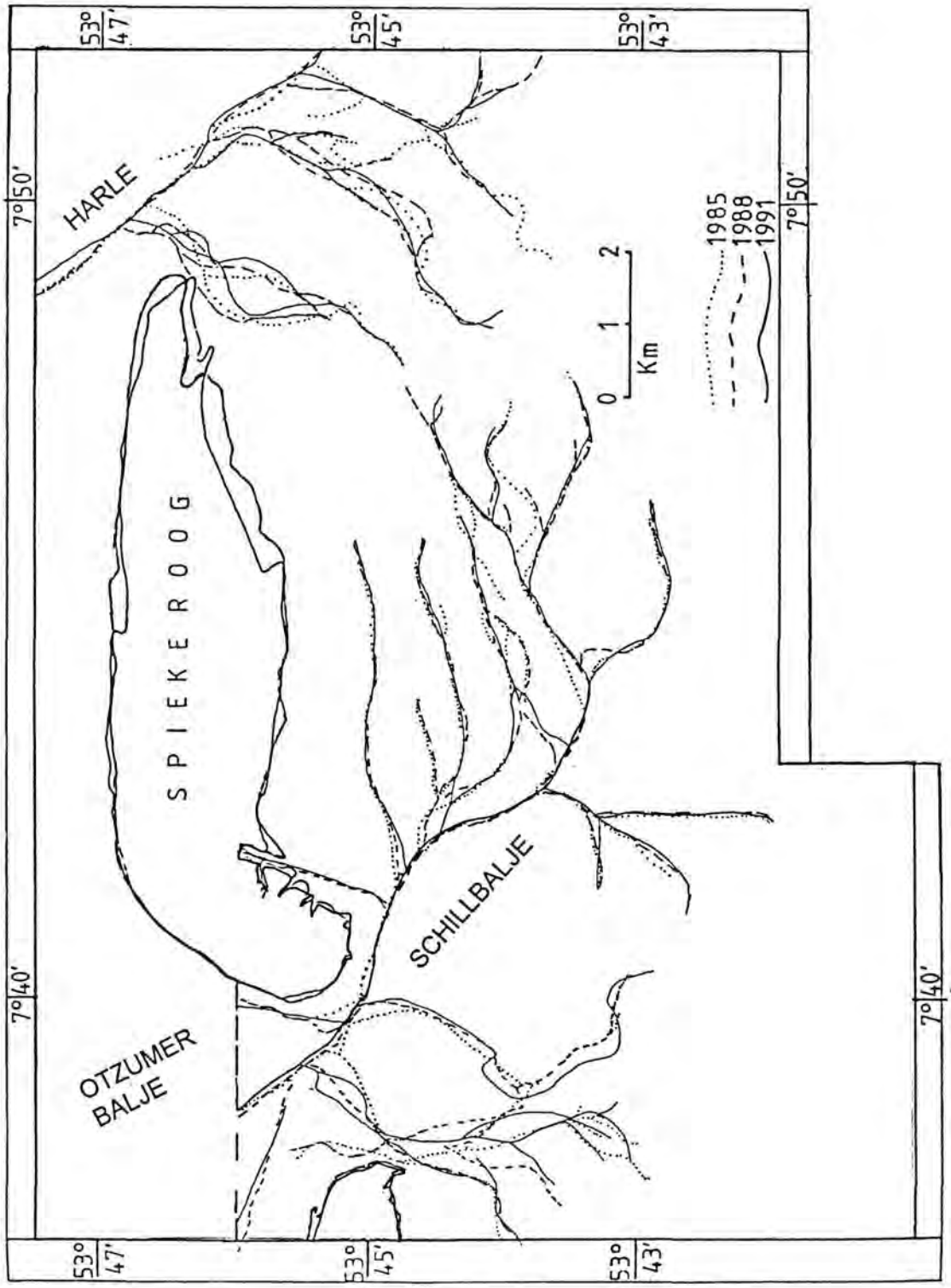

Fig. 3-17 An overlay of the hydrographic charts showing channel migration patterns.

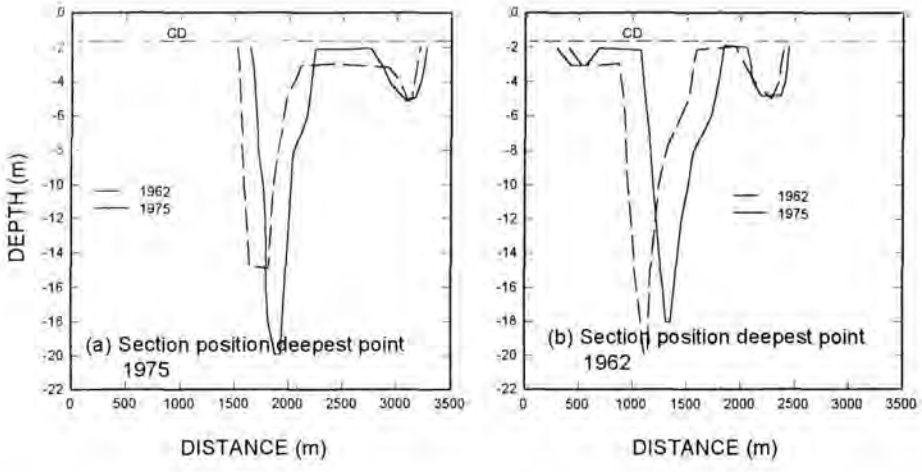

Fig. 3-18 Changes in the dimensions and positions of the Otzum inlet as illustrated by overlays of cross-sections through the deepest point of the channel gorge for the period 1962/1975.

The eastward migration of the inlet gorge seems to suggest an ultimate erosion of the western side of the island. This has indeed been the case in the past and further erosion had to be stopped through engineering measures. The western heads of both Wangerooge and Spiekeroog islands are reinforced. The eventual sequence of events, now that a further eastward migration of the inlet is unlikely, is not difficult to imagine. If the morphological equilibrium is further disturbed, re-adjustment of the gorge dimensions will be necessary and if this can not be achieved in its present location, a new channel may have to be established to the west of the old one. In this way the cycle is repetitive.

3.6.3 Migration of backbarrier shore of the island

The documented historical positions of the Frisian barrier islands point to a general south-eastward migration of the islands since their first appearance (HOMEIR & LUCK, 1969). This may, however, not be observable short time scales. Superposition of the 1985, 1988 and 1991 shorelines of Spiekeroog (Fig. 3-17) shows long stretches

of the open coast as well as the backbarrier shorelines to undergo erosion. Deposition is conspicuous only at the eastern head of the island, the so called "Ostplate", and a limited stretch on the backbarrier side. The erosion of the open coast shore is, despite a large supply of sand from the shore face, attributed to the presence of an efficient longshore sediment transport mechanism (FITZGERALD et al., 1984a & b). The longshore current which is directed towards the east in this region must, therefore, be responsible for the sand bypassing of the beach by way of the Harle inlet to deposit on the eastern margin and behind the island. In low lying parts of the dunes, as may be observed on existing aerial photographs, overwash processes take place.

With the rising sea level the mean high water mark rises on both sides of the island, allowing part of the salt marshes to become inundated. Thus, during stormy weather conditions erosion of the low-lying barrier island salt marsh becomes even more intensified. The net effect of these processes is the reduction of the island width and an increase in its length as a result of the eastwards directed sand transport along the open coast shore.

It may be concluded, therefore, that the path of the island migration towards the Southeast, if any, can in this case not be traced on the basis of short-term observations of the backbarrier shore alone. At present a net landward migration of the island is not apparent. A possible reason for this could be the after effects of massive human interventions over past centuries.

3.6.4 Mass balance

One of the oldest, but still reliable methods of determining the stability of catchment basins is a mass balance estimate. In establishing whether a basin is eroding or accreting, a number of methods may be used. Comparisons of cross-sections made across the central part of the basin for different times give an indication of the mass balance. In Fig. 3-19 the N-S cross-section through the centre of the Otzum tidal basin was measured for the years 1962 and 1975. Taking the deepest point to represent the axis of the basin, it can be seen that while the northern flank (towards the island) of the basin experienced erosion the southern flank accreted. Despite the

fact that the southern flank is narrow, its slope is steeper, a fact which reflects large sediment accumulations in the near-dyke region.

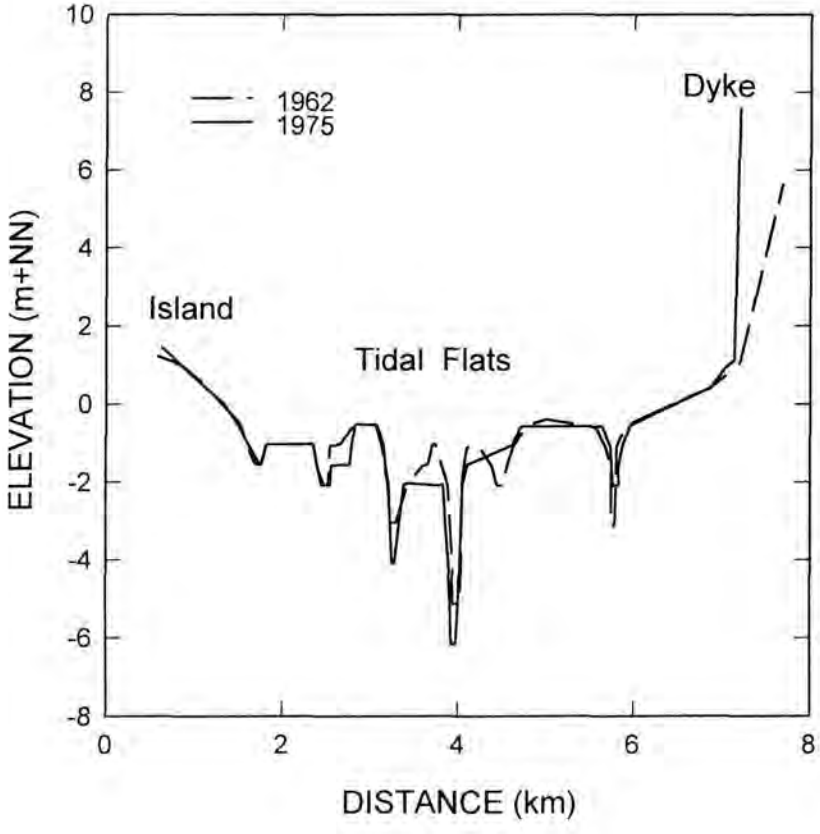

Fig. 3-19 Comparison of N-S cross-sections through the centre of the Otzum tidal catchment over 13-year period (1962 - 1975).

A better approach, however, is the superposition of topographic maps at the same scale and subsequent calculation of the topographic differences. This data forms the basis for the identification of areas of deposition and erosion (KNOP, 1963). In this case the 1962 and 1975 topographic maps of Spiekeroog (1 : 25000) were used. A transparent paper was overlaid on one of the maps and a 280m X 280 m grid map constructed. The ground elevation in each of the grids was entered and the same grid map overlaid on the other topographic map. The elevation differences registered were

multiplied by the grid area and summed to obtain the net sediment volume. In addition, an elevation difference map was constructed.

The mass balance map of the Otzum catchment area between 1962 and 1975 is presented in Fig. 3-20. A striking feature is the fact that major eroding areas tend to follow the channel outlines. This indicates that channels are eroding while higher intertidal flats continue to rise. The highest values of erosion and deposition were registered in the inlet mouth. As mentioned earlier (section 3.6.2), this is the region where the inlet has migrated eastwards. As such, the positive mass balance zones in this region represent earlier channel locations, whereas new channel locations are represented by negative mass balance. Furthermore, the fact that the channels are predominantly eroding corroborates the earlier findings that the increase in channel volumes as suggested by the channel volume - catchment area relationships were actually achieved mainly through widening and deepening of the channels i.e. erosion. Depositional and erosional scales are higher in the central interchannel region as compared to the basin flanks, i.e. along the island's backbarrier and mainland shorelines. This can, for example, be observed along a N-S transect through the middle of Spiekeroog. Whereas the northern basin flank along the island's backbarrier shoreline is characterised by a negative mass balance, a positive mass balance dominates on the southern flank (along the mainland's shoreline); negative mass balances also occur around Neuharlingersiel and halfway towards Harlesiel.

Over the 13-year period for which the mass balance was calculated a net positive sediment budget of about 1.5×10^6 m^3 was obtained. This gives a net sedimentation rate of about 16.3 cm/100 yr., a value well below the local sea level rise of about 24 cm/100 yr. (PELTIER & TUSHINGHAM, 1989). This implies that at present the basin does not receive a sufficiently high sediment supply to compensate sea level rise. This may have far-reaching consequences for the hydraulic stability of the catchment basin, especially if sea level rise should accrete as predicted (e.g. ETKINS & EPSTEIN, 1982; PELTIER & TUSHINGHAM, 1989).

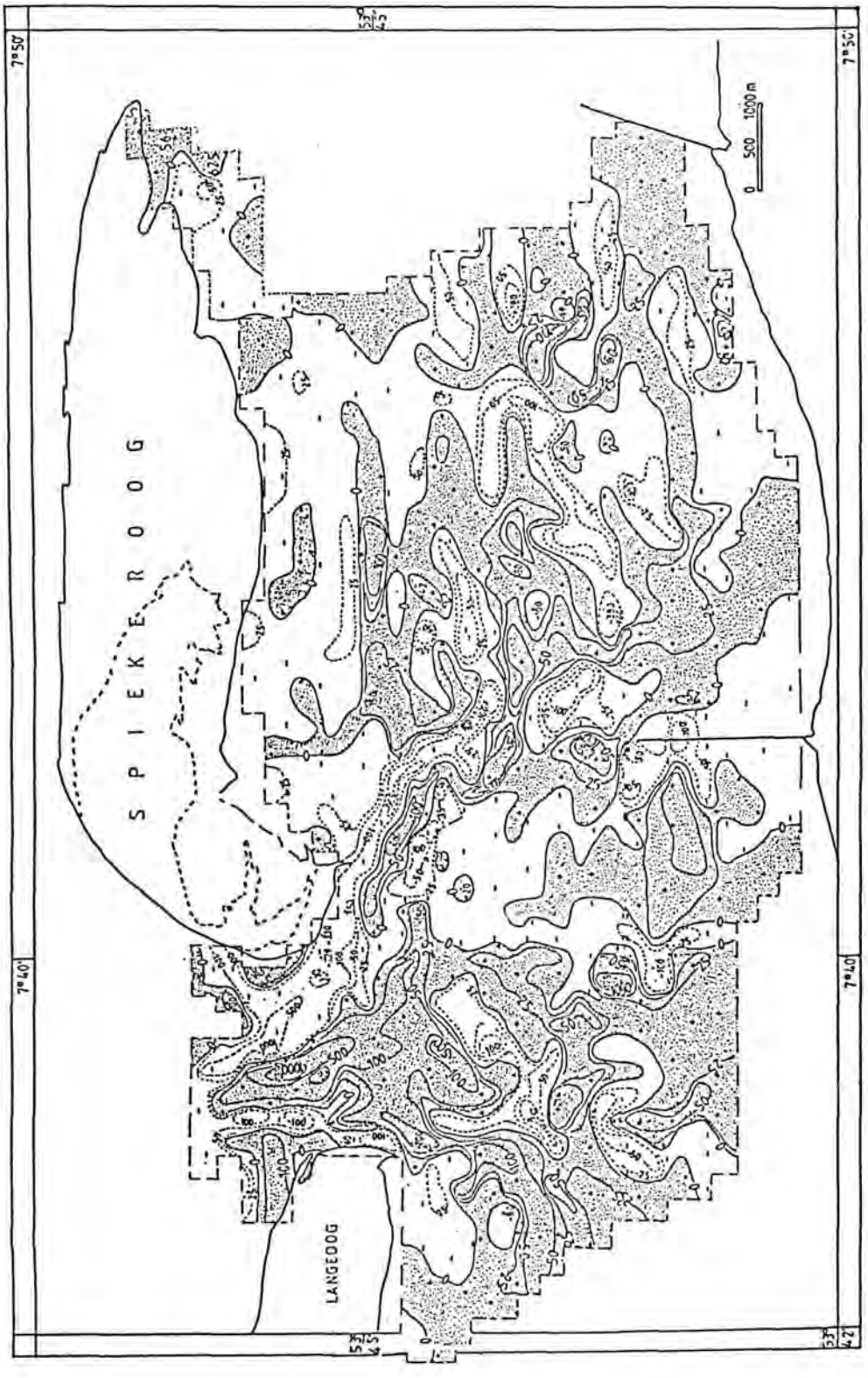

Fig. 3-20 Mass balance map of the Otzum tidal catchment over the period 1962/1975.

CHAPTER 4

SEDIMENT CHARACTER AND DISTRIBUTION

4.1 Data base

Since the aim of this study was to establish empirical relationships between the flow, the morphology and the sediments a close grid sampling of the sediments was necessary. The grid measured 0.25' longitude and 0.15' latitude, corresponding to a spacing of about 280 * 280 m (Fig. 4-1). Sample positions were fixed by means of a portable DECCA Navigator. The navigator was calibrated before each sampling campaign so that the position fixing parameters remained the same. Some 1300 samples were collected.

The samples were processed following standard laboratory procedures (e.g. CARVER, 1971). After desalination the mud content in the samples was determined by wet sieving. Sample splits of the remaining sand fraction were run through a high resolution (0.02 phi, where phi = $-\log_2 d_{mm}$), automatically recording settling tube system (BREZINA, 1979). The resulting settling velocities (psi = $-\log_2 V_{cm/s}$) were converted into equivalent settling diameters by means of a computer using a glass sphere standard.

Since the settling tube data is used to formulate a sediment transport hypothesis, a careful error assessment was carried out to make sure that the data were accurate. Two potentially serious sources of error are wrong calibration of the settling tube and overloading of the system with sediment leading to the development of convection currents (FLEMMING & THUM, 1978; BREZINA, 1979). Cross-checks of the results with glass bead standards ensured that there were no calibration errors. Settling convection was indeed observed when the settling tube analyses were repeated with bulk sample masses in excess of 1 g. Although this would introduce deviations of not more than 5%, great care was taken that sample masses did not exceed 1 g.

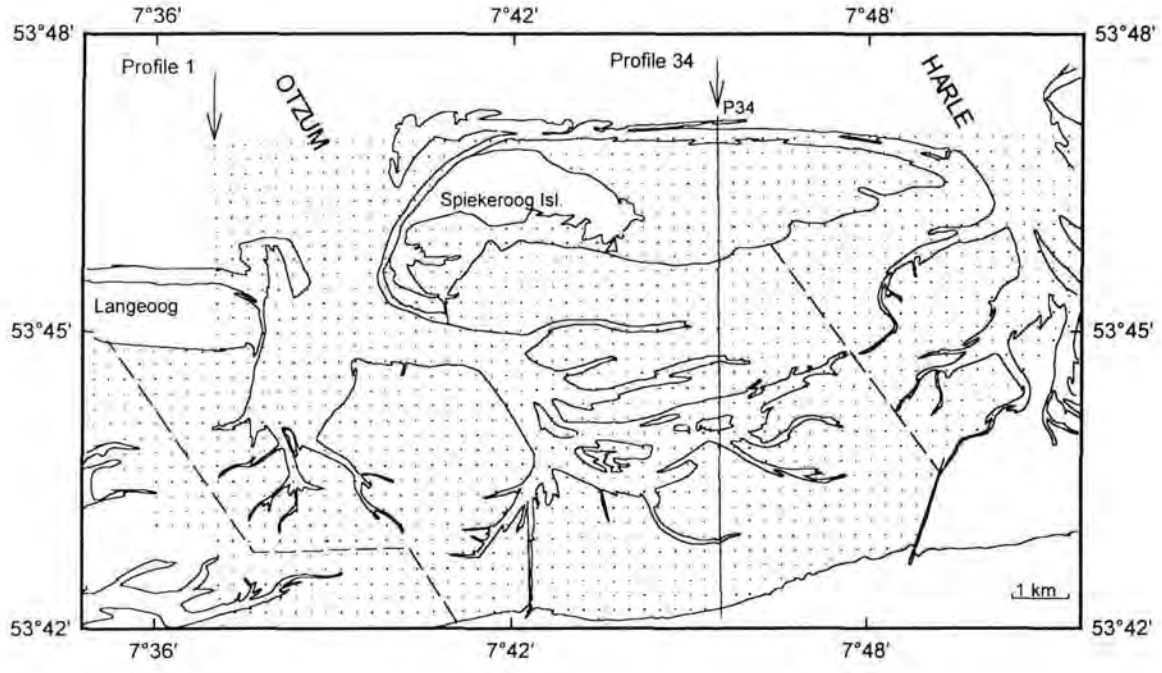

Fig. 4-1 Study area showing the sampling grid from which samples were collected.

4.2 Characteristic sediment parameters

A sediment has many properties, biological, chemical and physical. In order to characterise a sediment, a set of selected parameters are determined. traditionally, granulometric parameters are used to interpret provenance, transport and depositional processes. Such parameters are also useful in palaeoenvironmental reconstruction. The parameters include the mean or median size, sorting, skewness, kurtosis and the mode. In this study the parameters were calculated by computer both by the method of moments and percentile statistics (FOLK & WARD, 1957). The computer program also calculated settling velocity equivalents of these parameters. Other outputs

included the size frequency and cumulative frequency curves and the contribution of various size fractions to the sample.

4.2.1 The relationship between size and settling velocity parameters

Whereas the grain size parameters refer directly to the grain size distribution characteristics, their settling velocity equivalents relate to the behaviour of the sediment grains depositing from suspension. In modern settling tube systems, however, the grain size statistics are computed alongside their settling velocity equivalents by the accompanying software. It is therefore of interest to know whether it is possible to establish simple relationships between the settling velocity parameters and their grain size equivalents and thus apply a common descriptive classification (FOLK & WARD, 1957) using settling velocity summary statistics. The relationship between the mean settling velocity and the mean grain size is none other than the well established Stoke's law as shown by the plot of the two parameters (Fig. 4-2). As evident from Table 4-1, a simple relationship between the Wentworth size scale and an equivalent mean settling velocity scale is not possible. As a result, the descriptive textural classification schemes used in the phi system can not be directly applied to the psi system. A general descriptive classification scheme for statistical parameters derived from psi-distributions is thus lacking.

The remaining moments of settling velocity and size distributions (sorting, skewness and kurtosis), however, appear to be comparable. ANTIA (1993), with the aim of establishing a functional scaling of the summary statistics of the grain settling velocity distribution which may be compatible with the scaling of their grain size equivalents, suggests that the phi-sorting (size) should be multiplied by a factor of 1.7 in order to obtain its equivalent psi-sorting (settling velocity). Observing no marked differences between the skewness and kurtosis of the phi and psi-distributions, no changes in their scaling was suggested. A re-evaluation of these results using a new set of data from the backbarrier area led to the following conclusions:

- The conversion of the phi-sorting into its psi equivalent is linear (Fig. 4-3). By looking at the ratio between the two parameters at the sorting intervals defining its descriptive classification (Table 4-2) the factor increases steadily from as low as 1.37 at phi-sorting 4Φ to 1.57 at phi-sorting 0.35Φ reaching 2.1 at phi-sorting 0.1Φ.

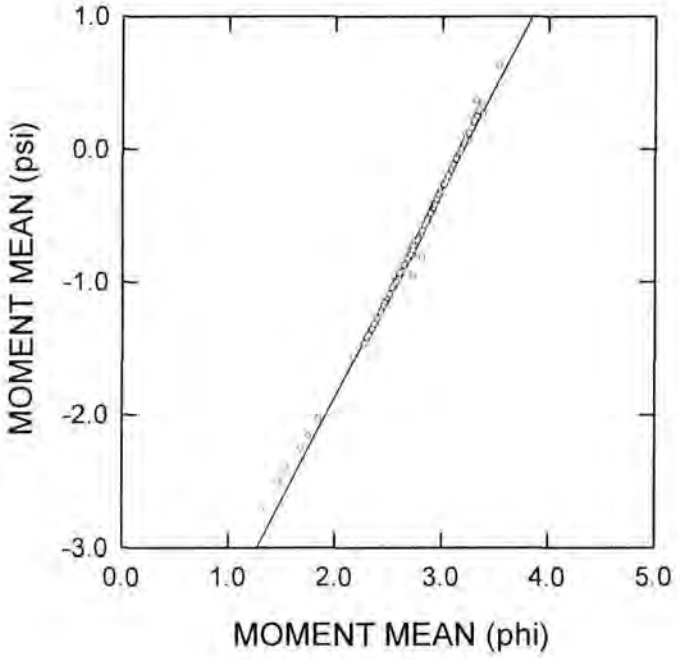

Fig. 4-2 Relationship between the mean of phi and psi-distributions.

- The skewness of the settling velocity distribution (psi-skewness) is generally higher than the skewness of the size distribution (phi-skewness), being related to each other through a simple linear relationship (Fig. 4-4). At phi-skewness values exceeding 0.3 the trend reverses giving smaller psi values. The skewness range is thus smaller in case of the psi scale. However, the evident shift in the absolute limits of psi-skewness towards more positive values at phi-skewness < 0.3 renders the scaling inferior to the symmetrical phi-skewness scale.

- The kurtosis shows a close similarity between the two distributions (Fig. 4-5).

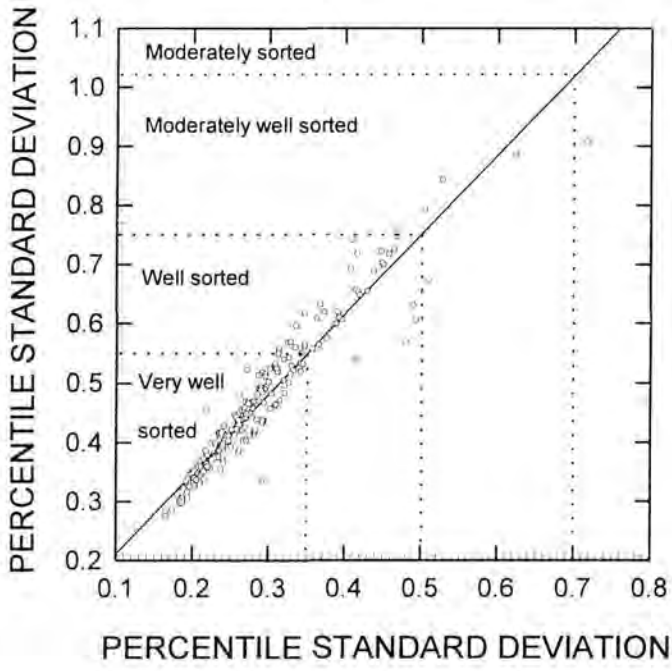

Fig. 4-3 Comparison between the descriptive classifications of phi and psi sorting. The conversion factor between the two increases as the sorting (phi) worsens.

4.2.2 The choice between moments and graphic methods

The summary statistics, namely the mean (also median and mode), sorting, skewness and kurtosis are used in describing the size distribution of the sediment. Since the method of moments gives different results from the percentile or its slightly simplified graphic derivation, it remains a matter of necessity to state which of the two methods has been adopted. Despite the implied freedom of choice of the method some facts may override the decision. FOLK & WARD (1957) made some improvements to the graphic methods of INMAN (1952) and their comparison of the graphic and moments methods are very instructive. Apart from establishing a descriptive classification of sediment parameters, they found that the method of moments provides the most

accurate values of mean and sorting and that the moment skewness is generally 4.35 times as high as the inclusive graphic skewness.

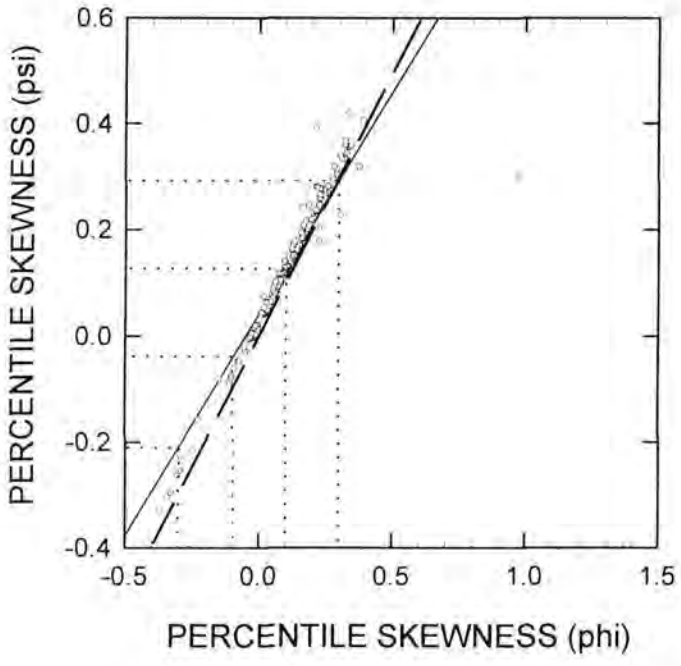

Fig. 4-4 Comparison between phi and psi skewness. Psi skewness shows a positive shift in its values at skewness < 0.3 phi.

The relationships between measures of the moment and the percentile statistical methods are here re-evaluated using data from a N-S band transect, about 2 km wide and 6 km long running through the central region of the Otzum tidal catchment area. Whereas the moment mean is very similar to the percentile mean (Fig. 4-6), the moment sorting is typically higher than its percentile equivalent, especially in the very well sorted category (Fig. 4-7). The regression equations, with very high degrees of correlation (R = 0.99), may be used for interconversions between moments and graphic measures. The moment skewness (Fig. 4-8), on the other hand, shows a very poor correlation (R < 0.5) with its percentile counterpart, with an evident shift in the moment skewness towards more positive values as previously mentioned. Thus, neither the factor of 4.35 as suggested by FOLK & WARD (1957) nor the regression

obtained here gives a satisfactory basis for comparing the two skewness values. A plot of the moment kurtosis against the percentile one (Fig. 4-9) likewise shows a poor correlation (R = 0.58), with moment values of up to 15. The following are the interconversion equations:

Moment mean = $0.03 + 1.005M_Z$, R = 0.99
Moment std = $0.09 + 0.86\sigma_I$, R = 0.99
Moment sk = $0.33 + 1.9SK_I$, R = 0.48
Moment kurt = $-3.28 + 5.9K_G$, R = 0.58

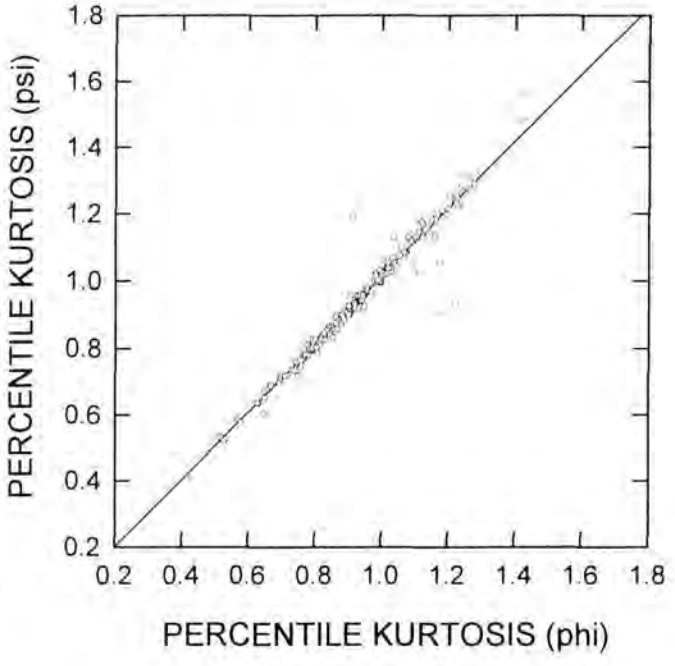

Fig. 4-5 Comparison between phi and psi kurtosis. The two show a close similarity.

In order to maintain consistency with the established descriptive classification the sorting, skewness and kurtosis values used here therefore, refer to the inclusive percentile methods (FOLK & WARD, 1957). The means, on the other hand, were calculated using the method of moments.

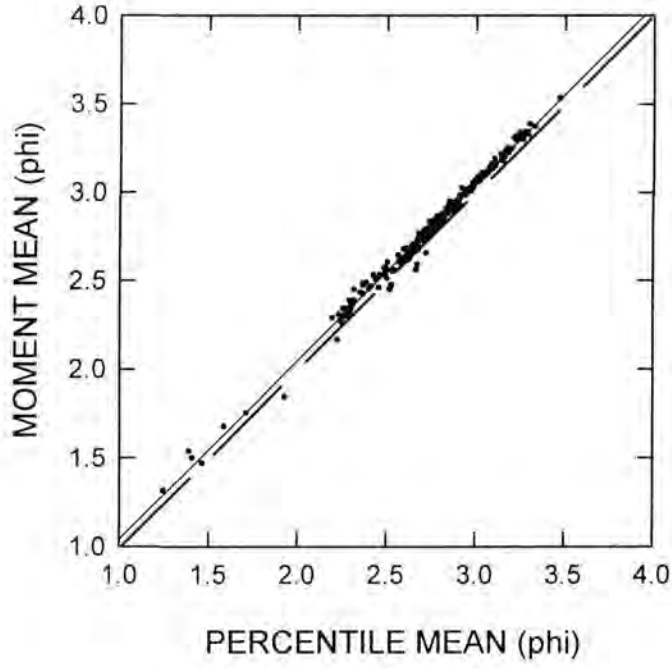

Fig. 4-6 Comparison between the moment and percentile mean.

4.3 Areal distribution of the grain size parameters

In the interpretation of palaeoflow and palaeoenvironmental conditions, spatial distribution patterns of the various summary grain size statistics are commonly used, namely that of the mean, sorting, skewness and kurtosis. These patterns form in response to the varying hydrodynamic conditions of the environment as well as the source characteristics and as such describe the environmental differentiation in an area. The changing hydrodynamic conditions along the transport path is usually indicated by the progressive change in the sediment textural parameters, as represented by the size sorting models of SAHU (1964), McLAREN (1981), McLAREN & BOWLES (1985). In many cases, however, multisource factors have also been identified, as documented for example in the mixing models of FOLK & WARD (1957), FOLK & ROBLES (1964), FLEMMING (1988).

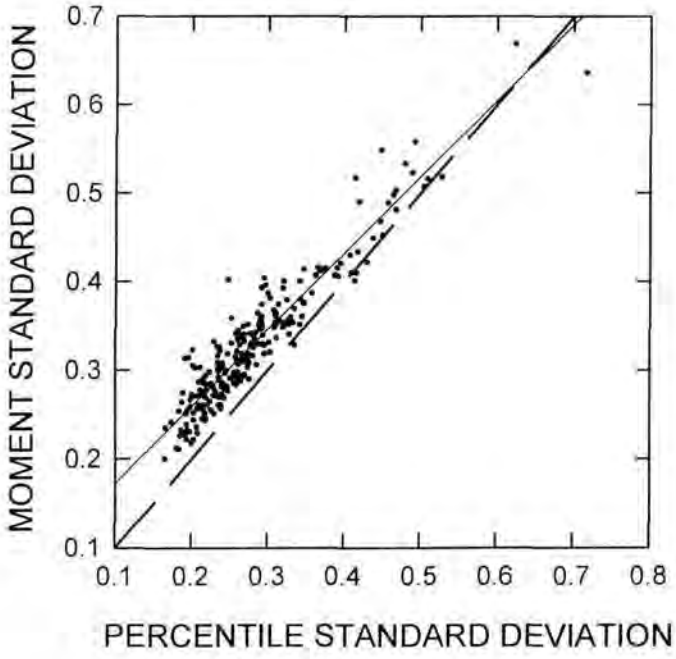

Fig. 4-7 Comparison between moment and percentile sorting. Generally, moment sorting gives higher values than the percentile ones.

The interpretational approaches of grain size parameter trends have nevertheless been accompanied by differences of opinion. In early studies, single parameter trends, e.g. that of the mean diameter, were used to deduce the transport pathways. Whereas, for instance, the average size has been held to decrease in the direction of transport (e.g.PETTIJOHN et al., 1972; SELF, 1977), the converse has also been claimed (McCAVE, 1978). Today, single parameter trend analyses are yielding to multiparameter trend analyses (FOLK & WARD, 1957; McLAREN, 1981; McLAREN & BOWLES, 1985; GAO & COLLINS, 1994). The spatial distribution of grain size fractions as tracers of hydraulic energy conditions may, in fact, be even more useful than the traditional measure of the size distribution.

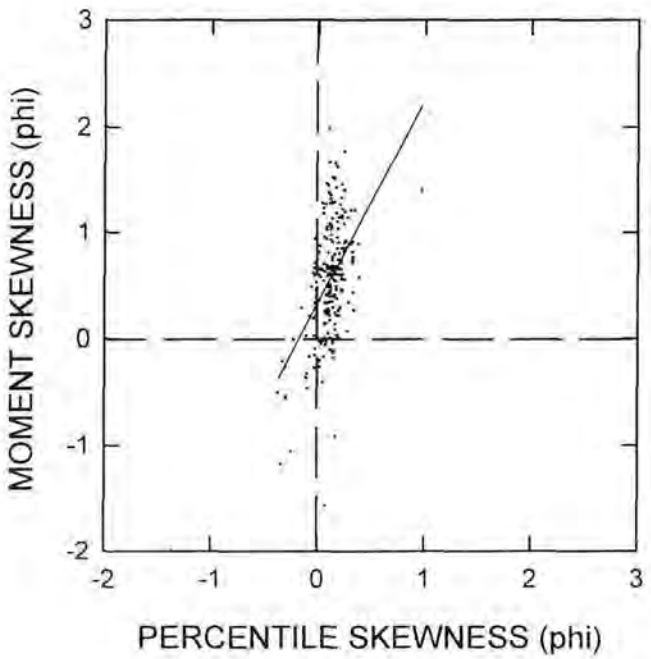

Fig. 4-8 Comparison between moment and percentile skewness. There is a very poor correlation between the two.

Bivariate and ternary diagrams have also been used to interpret the palaeoenvironmental conditions. These are graphic representations of multivariate analyses of textural parameters, sediment types or their compositions. The delimitation of the different depositional environments is done by drawing lines either defined by well established empirical relationships (e.g. the C-M diagram of PASSEGA, 1957; 1964) or arbitrarily drawn through the data set to demarcate distinct point clusters. In cases where the point clusters overlap, this procedure may become conjectural.

The shape of grain size distribution curves (curve shape clustering) has also been used as an indicator of the depositional environment. Individual curve shape clusters commonly delineate distinct areas within a sample grid and hence are thought to

reflect particular hydrodynamic conditions (e.g. NOTA, 1958; VAN ANDEL & VEEVERS, 1967; NOTA, 1968; LORING & NOTA, 1973). In some cases the variations in the shape of the curves are understood to be a result of mixing or truncation processes (SPENCER, 1963).

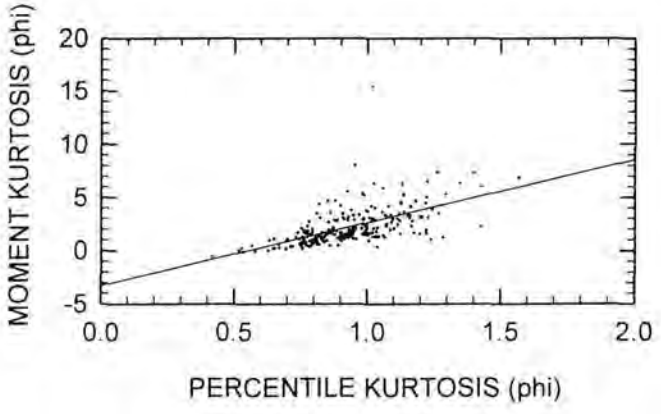

Fig. 4-9 Comparison between moment and percentile kurtosis. Their correlation is poor, with somewhat erratic values in the former.

4.3.1 Mean grain size

The mean is a mathematical average of the grain diameters of a sample. The percentile mean is given by:

$M_Z = 1/3\ (\Phi_{15.866} + \Phi_{50} + \Phi_{84.134})$, where Φ_x is the phi value of the x^{th} percentile on the cumulative curve. It should be noted that the graphic statistical procedure of FOLK & WARD (1957) is a simplified form of the percentile statistical procedure, developed to allow statistical derivation to be made from graphic size data presentations whereby the decimals of the percentile values in the formula above are rounded off to give the graphic mean.

Sands have their mean grain sizes ranging between -1 and 4 phi (2 - 0.063 mm), classified as shown in Table 4-1.

For sediment deposited in a fluid medium the mean is an average measure of the maximum fluid kinetic energy which, in turn is related to the current velocity (e.g. INMAN, 1949; MENARD, 1950; BAGNOLD, 1968). By plotting the sample mean diameters at their geographic locations, an areal distribution map of the sediment is produced. Fig. 4-10 represents the sediment (sand) distribution map (in phi) of the Spiekeroog backbarrier area which encompasses the Otzum tidal catchment area and the western part of the Harle inlet including the inlet mouths. The coarse fraction (< 4 phi) is largely made up of medium to very fine sands, with the mean grain size varying between 3.5 phi near the dyke to < 1.0 phi in the tidal inlets. On the basis of a contour interval of 0.25 phi the area can be divided into two regions namely, 1) the backbarrier area away from the inlet mouth regions, characterised by a mean diameter range of 2 to 3.5 phi distributed in shore parallel 0.25 phi interval zones, and 2) the inlet mouth regions which are characterised by a mean grain size range of 1 - 2 phi, the contour resolution of which drops drastically from 0.25 phi through 0.5 to as poor as 1.0 phi.

Whereas the high contour resolution is tentatively interpreted as indicating a highly sensitive energy level differentiation (transport sorting), the poor contour resolution encountered in the inlets is largely a provenance factor. The inlet throats are over 20 m deep and are cut into coarser (fine - medium) Pleistocene sands. Since the tidal flow velocities diminish away from the inlet throats, these sands are not transported far, but become re-distributed in and around the inlet mouth region without much size sorting. These provenance and transport sorting effects will be analysed further in the sections dealing with sorting, skewness and transport modes.

The high contour resolution which has been interpreted as indicative of a highly effective energy differentiation in effect depicts a shore-normal energy gradient. Starting from the very low energy environment near the mainland dyke, the energy level and hence the mean grain size increases seawards. The shore-normal energy

gradient is even more clearly defined when the dominant size fractions (making up more than 50% of the total sample) are plotted together (section 4.4.3)

Table 4-1 The Wentworth size classification scheme for sands.

phi	mm	psi (24°C)	cm/s	Wentworth classification
-1	2.00	-4.81	28.0	
-0.75	1.68	-4.58	24.0	
-0.50	1.41	-4.39	21.0	
-0.25	1.19	-4.17	18.0	
0.00	1.00	-3.91	15.0	Very coarse sand
0.25	0.84	-3.70	13.0	
0.50	0.70	-3.32	10.0	
0.75	0.60	-3.17	9.0	
1.00	0.50	-3.00	8.0	Coarse sand
1.25	0.42	-2.58	6.0	
1.50	0.35	-2.32	5.0	
1.75	0.30	-2.00	4.0	
2.00	0.25	-1.58	3.0	Medium sand
2.25	0.21	-1.26	2.4	
2.50	0.18	-1.00	2.0	
2.75	0.15	-0.76	1.7	
3.00	0.13	-0.14	1.1	Fine sand
3.25	0.11	+0.32	0.8	
3.50	0.09	+0.74	0.6	
3.75	0.07	+1.32	0.4	
4.00	0.06	+1.74	0.3	Very fine sand

The characteristics and the genetic model of this energy gradient will be dealt with later. It should be pointed out here that the shore-normal (N-S) energy gradient marking the central basin does not coincide with the main tidal flow direction (NW-SE), a feature requiring closer analysis.

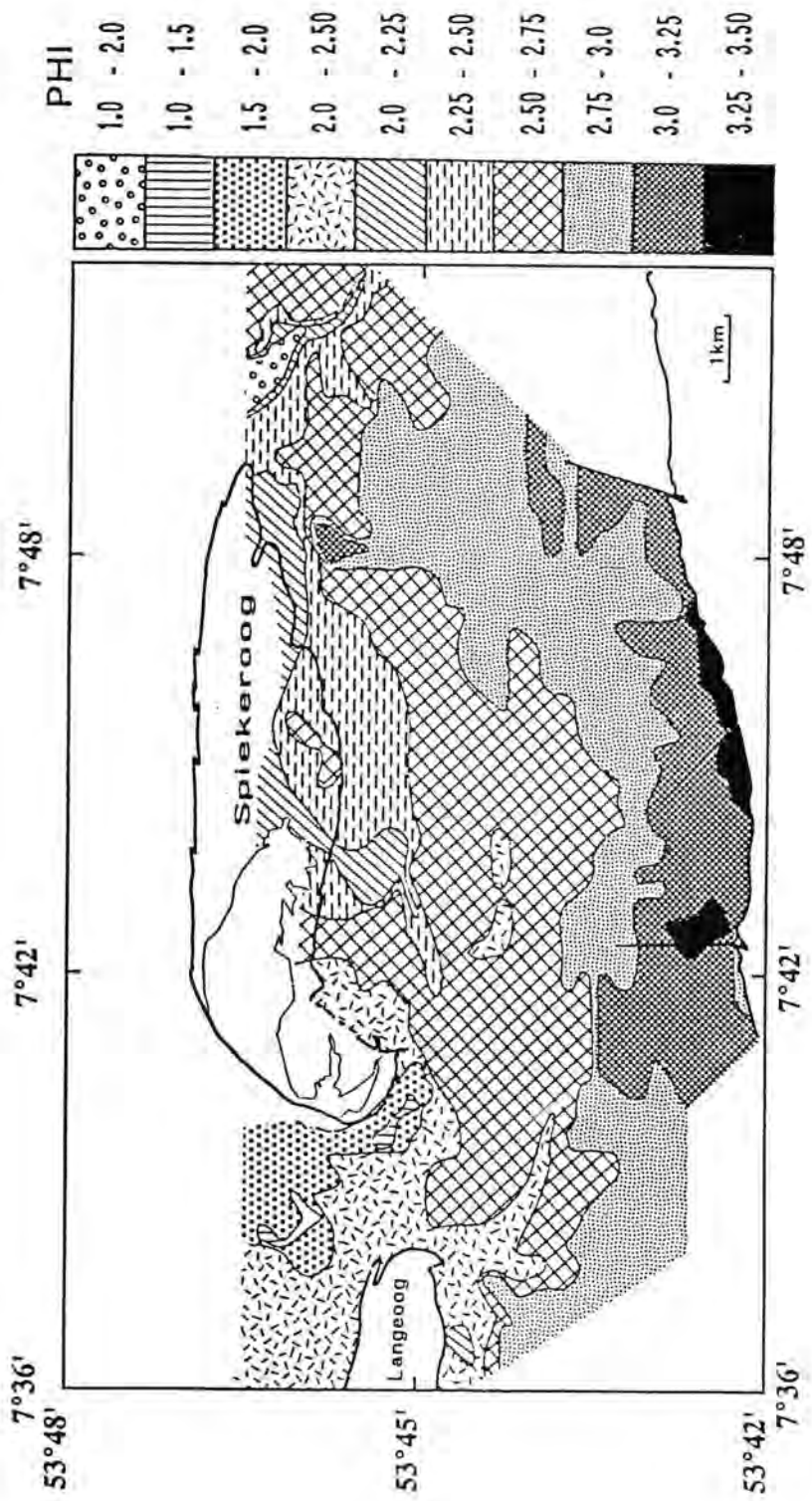

Fig. 4-10 Spatial distribution of the sand fraction (< 4 phi) in the backbarrier area of Spiekeroog island.

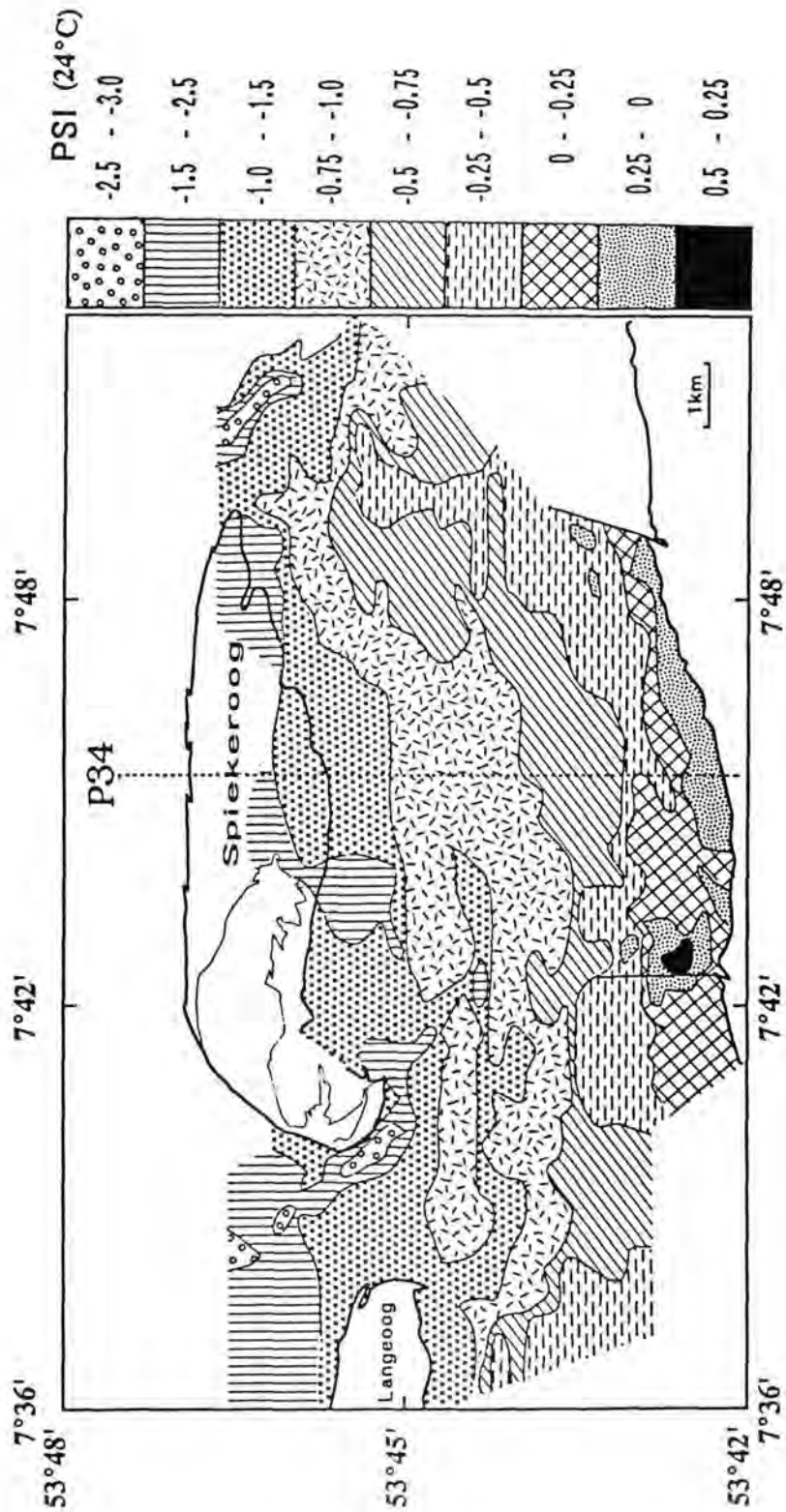

Fig. 4-11 Spatial distribution of the grain mean settling velocities of the sand fraction in the Spiekeroog backbarrier area. Note the similarities with Fig. 4-10.

4.3.2 Mean settling velocity

The spatial distribution of the mean grain settling velocity is presented in Fig. 4-11. An areal separation of the settling velocities similar to that of the mean grain size is evident. There is, however, a slight difference in the contour resolution with the settling velocity distribution map providing a better resolution in the fine-grained region and poorer in the coarser. Landwards of the central region (mean 2.5 -2.75 phi or -0.75 - -1.0 psi) the mean settling velocity shows 5 separate 0.25 psi zones as compared to only 3 (0.25 phi) on the mean grain size (settling diameter) map. This is due to the fact that the relationship between the phi and psi scale is not linear, as clearly inferable from Fig. 4-2. The relationship between the mean settling diameter and the mean settling velocity shows that as the sediment gets coarser ($<$ 2.5 phi) the mean settling velocity increases more rapidly. This means that for a given range of mean grain size the corresponding range of settling velocities is comparatively wider and hence results in a poorer contour resolution. Conversely, as the sediment gets finer ($>$ 3 phi) the settling velocities decreases more slowly, resulting in a better contour resolution. These results confirm the Stoke's law principle and underlines the good calibration of the settling tube used in this study.

4.3.3 Sorting

The sorting of a sediment is mathematically represented by the standard deviation, a measure of the spread of a distribution from the mean. The inclusive percentile standard deviation (sorting) is calculated from the cumulative curve, thus:

$$\sigma_I = 1/4\ (\Phi_{84.134} - \Phi_{15.866}) + 1/6.6\ (\Phi_{95} - \Phi_5)$$

The descriptive classification of sediment sorting is given in Table 4-2.

Table 4-2 The classification of sediment sorting as established by FOLK & WARD (1957).

σ_I	Degree of sorting
< 0.35	Very well sorted
0.35 - 0.50	Well sorted
0.50 - 0.70	Moderately well sorted
0.70 - 1.00	Moderately sorted
1.00 - 2.00	Poorly sorted
2.00 - 4.00	Very poorly sorted
> 4.00	Extremely poorly sorted

The areal distribution of the sample standard deviation is plotted on Fig. 4-12 and contoured following the classification of FOLK & WARD (1957). It can be seen that the surficial sediments of the Spiekeroog backbarrier area are mostly very well sorted (sorting < 0.5). Moderately to poorly sorted sediment (σ_I > 0.5) occur only in the inlet mouth regions and behind the island in sheltered, high elevation channel bank areas.

As demonstrated by many workers, the sorting evolution of a sediment is in most cases simple to reconstruct. The sorting normally improves as the sediment becomes finer in the direction of transport. This observation, however, is mostly restricted to the sandy sediments (FOLK & WARD, 1957; McLAREN & BOWLES, 1985). In the study area the sorting trends thus indicate a general transport direction towards the coast. The poor sorting in the sheltered areas (channel confluences, etc.), channel banks and high elevation regions is a result of mixing of different sand populations brought about by sediment influx from different sources. According to SAHU (1964) sorting is hydraulically considered to represent a measure of the energy fluctuations of the depositing agent. In the sheltered areas coarser sediment component reflects supply by overwash processes and subsequent mixing with sediments deposited in the course of the normal energy gradient.

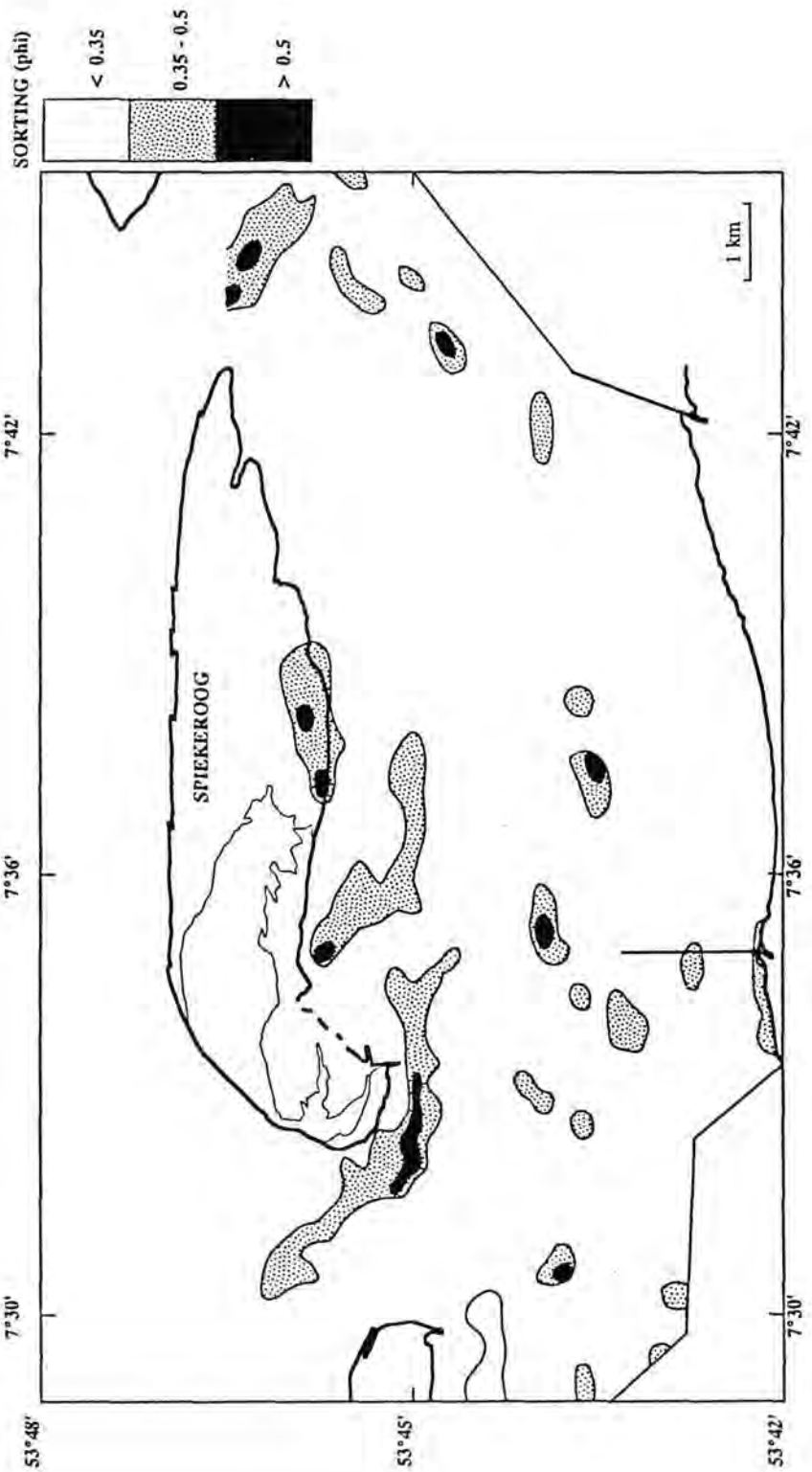

Fig. 4-12 Distribution of the sediment sorting in the backbarrier area of Spiekeroog island.

4.3.4 Skewness

The frequency curve of a grain size distribution is either symmetrical or asymmetrical about the mean. Non-symmetrical distributions are said to be skewed. Skewness is a measure of the direction and magnitude of the asymmetry. Skewed distributions are also said to be non-normal. The inclusive percentile skewness is computed from the cumulative curve as follows:

$$SK = \frac{(\Phi_{84.134} + \Phi_{15.866} - 2\,\Phi_{50})}{2(\Phi_{84.134} - \Phi_{15.866})} + \frac{(\Phi_{95} + \Phi_{5} - 2\,\Phi_{50})}{2(\Phi_{95} - \Phi_{5})}$$

The descriptive classification of the skewness measure is presented in Table 4-3.

Table 4-3 Descriptive classification of the skewness sign and magnitude.

SK	Description
-1.0 - -0.3	Very negatively skewed
-0.3 - -0.1	Negatively skewed
-1.0 - +0.1	Nearly symmetrical
+1.0 - +0.3	Positively skewed
+3.0 - +1.0	Very positively skewed

4.3.4.1 Skewness interpretation

The true meaning of the skewness has been elusive. SPENCER (1963) notes the lack of proper understanding or emphasis on the significance of this measure until the paper by FOLK & WARD (1957) where it was mainly associated with mixing processes between different hydraulic populations. Nevertheless, a survey of some more recent publications dealing with skewness shows an array of confusing interpretations.

FOLK & WARD (1957) interprets the negative and positive skewness values as due to the presence of "tails" of coarse and fine sediments, respectively. However, the presence of a tail is not always readily visible from the frequency curve i.e. in many cases, especially near-symmetrical distributions, the tails simply show similar extensions. KOMAR (1976) interprets a positive skewness as an "overabundance" of fines and the negative skewness as an overabundance of coarse material. As indicated by the equation above, the skewness sign shows on which side (fine or coarse) of the median (Φ_{50}) the mean diameter is situated. Thus, if the mean (phi) is larger than the median, a positive skewness is registered and vice versa. Since the mean is the arithmetic dividing line between the fine and the coarse grain size classes of a sample, a positive skewness means that the fines contribute less than 50% of the available size classes and hence, an overabundance of coarse size classes, which contradicts KOMAR's (1976) view. CLARK (1981) suggested that a negative skewness may be interpreted as a "lack" of fine material brought about by the truncation of the fine tail. This interpretation should not be equated with that of KOMAR (1976). Truncation of the fine tail has long been recognised as a cause of negative skewness (FOLK, 1966). According to McLAREN (1981), a positive skewness indicates an "abundance" of coarse grains with a "tail" in the direction of fines, a negative skewness hence indicating an abundance of fines with a tail in the direction of coarser fractions. This view has recently been echoed by McLAREN & BOWLES (1985) and ANTIA (1993).

4.3.4.2 Evolution of skewness

Opinions differ as to how the skewness sign evolves. Mixing processes, whereby two or more normal sub-populations are mixed resulting in a non-normal (skewed) sediment, has been extensively documented in the literature (e.g. FOLK & WARD, 1957; SPENCER, 1963; FOLK & ROBLES, 1964; FLEMMING, 1988). The eventual skewness sign will then depend on the grain size spectra and relative proportions of the mixing components. The various modes of mixing and the resulting skewness has been re-addressed by ANTIA (1993).

Changes in the hydrodynamic regime along the transport path result in a progressive change in the sediment textural parameters. The model of McLAREN (1981) and McLAREN & BOWLES (1985) utilises a multiparameter analysis in their size sorting model. In his purely deductive model of grain size trends from source to deposit McLAREN shows the changes in the skewness sign as the sediment is eroded, transported and finally deposited. His results can be summarised by a number of cases as represented in Fig. 4-13:

Case I (Total deposition): Here a hypothetical normally distributed source is eroded. Since the finer particles have higher probability of getting eroded, the sediment in transport achieves a negative skewness, is better sorted than the source and is finer grained. The eroded sediment is then deposited without further modification. The remaining lag deposit (Case II) becomes positively skewed and coarser than the original source.

Case III (Selective deposition): In this case we observe the effect of a filtering processes. The coarser sediments deposit first or have a higher probability of depositing than the fines. As a result the negatively skewed sediment in transport will be positively skewed upon deposition. The mean size of the deposit, however, may be finer or coarser than the source. A coarser mean will result if erosion involves size classes coarser than the mean. Although this model is purely deductive, it has a strong theoretical base and is supported by a number of field examples.

The model of McLAREN (1981) was later modified by McLAREN & BOWLES (1985). In the modified version use was made of what they called transfer functions which, in simple terms, are comparisons of grain size distributions of sediment in transport with their source. They found that the transfer functions were negatively skewed, better sorted and finer than the source and concluded that the resulting deposit will retain the same characteristics (Fig. 4-14). One important point to note here is the fact that the derived transfer functions do not say anything about the depositional mechanism, i.e. whether it is total or probabilistic. This model, though extensively applied has been questioned by GAO & COLLINS (1991), who also suggested a number of modifications.

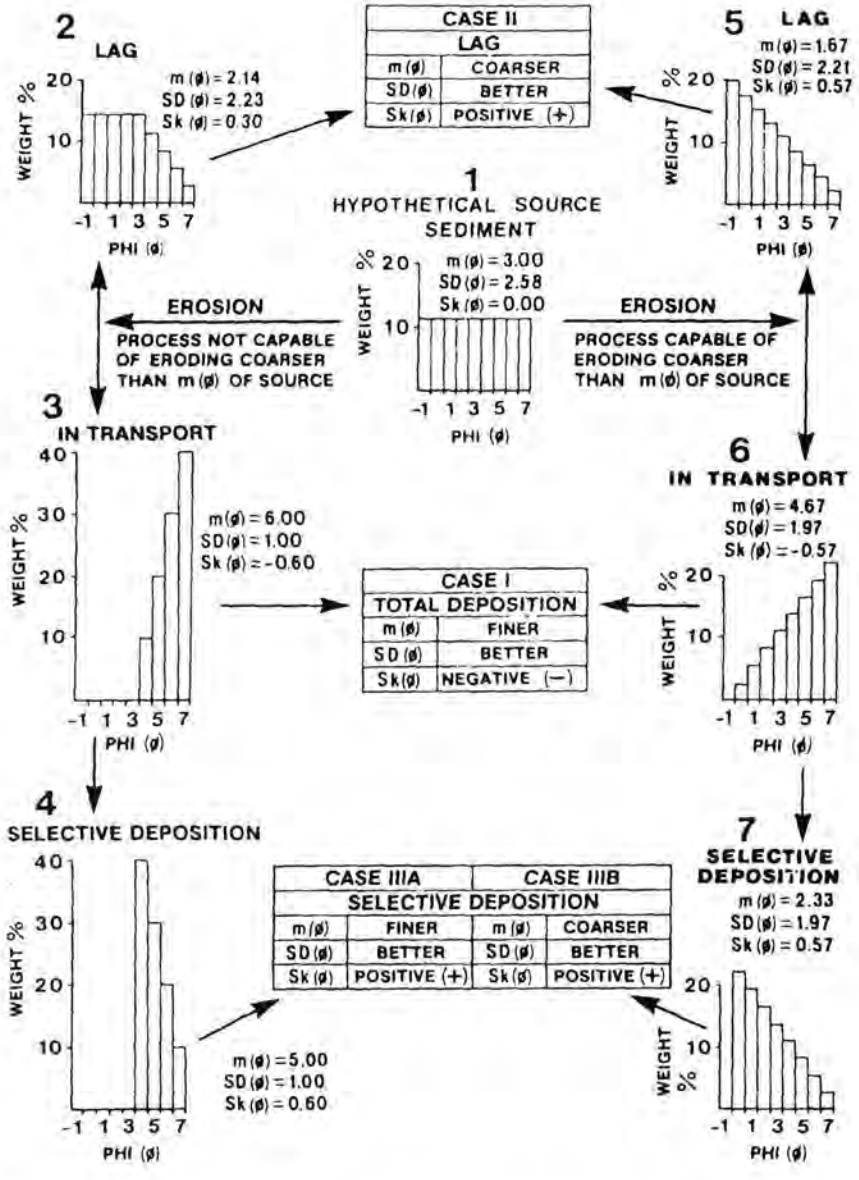

Fig. 4-13 The deductive model of skewness evolution according to McLAREN (1981).

The skewness-sign evolution model of ANTIA (1993) considers both mixing (miscible as well as immiscible sub-populations) and truncation (probabilistic and total) (Fig. 4-15). Whereas his first four cases (case 1-4) represent variants of the mixing model, the last two (cases 5-6) are a replica of McLAREN's (1981) model of erosion of a symmetrically distributed source material (progressive size sorting model). It is not difficult to predict the evolution of both the sorting and mean size from case 1 to case 4 if a secondary mode sediment is mixed with a primary mode. The sorting becomes poorer, the mean diameter becomes finer with the addition of fines and coarser if

coarse fractions are added (FOLK & ROBLES, 1964). This model shows how incomplete simplified theories of grain size trend analyses, as e.g. applied by McLAREN (1981), McLAREN & BOWLES (1985) and GAO & COLLINS (1991, 1992, 1994) in reality are.

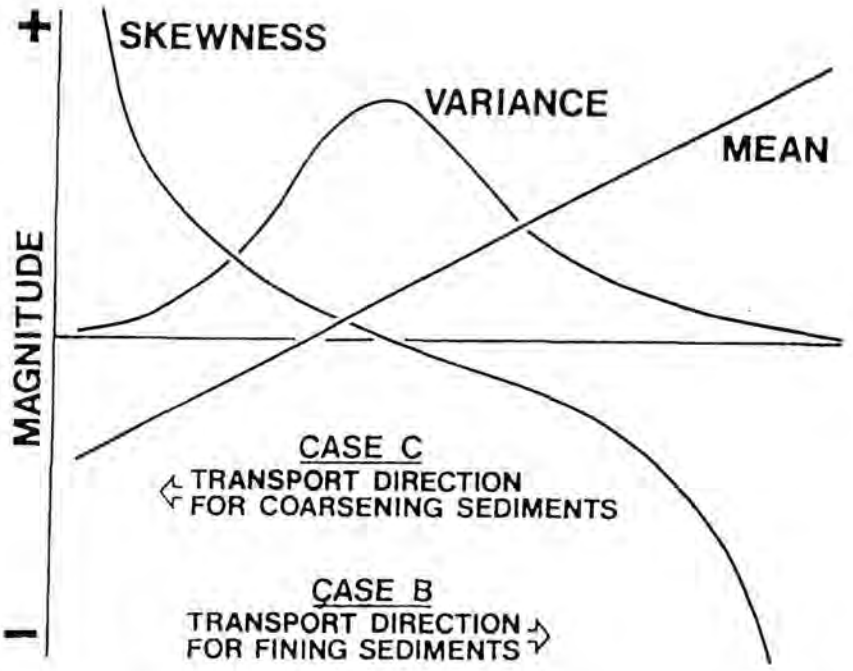

Fig. 4-14 The model of skewness change between source and deposit (McLAREN & BOWLES, 1985).

4.3.4.3 Spatial distribution of skewness

Figure 4-16 shows the skewness distribution which has been contoured following the descriptive classification. Regions characterised by either negative or positive skewness are clearly outlined. The inlet mouth region depicts a cross-channel variation of the skewness which is centred on a negative skewness zone flanked on either side by zones of positive skewness, followed again by negative skewness towards the island beaches. The beaches of the islands, with the exception of minor

positively skewed zones along the Spiekeroog backbarrier beach, are essentially negatively skewed.

Away from the inlet mouth the skewness becomes increasingly more positive, to attain maximum values of more than $+0.3\Phi$ near the mainland coast. This trend supports the McLAREN (1981) model of skewness evolution along the transport pathway. In the previous sections it was demonstrated that the inlet mouth area acts as a source of sediment. In the direction of decreasing tidal flow velocities of this area the sediment becomes finer, better sorted and relatively more positively skewed. The net landward sediment transport by the tides, which was revealed by the positive mass balance discussed previously (chapter 3), is thus responsible for the observed skewness trend.

McLAREN (1981) and McLAREN & BOWLES (1985) suggest a positively skewed lag deposit. If the fines are probabilistically removed from an originally symmetrical source deposit, the lag will in no doubt contain an overabundance of coarse grains and hence attain a positive skewness. If the original source sediment was already positively skewed the magnitude will be amplified, whereas it will be diminished if the source was negatively skewed (ANTIA, 1993). Although McLAREN & BOWLES (1985), like McLAREN (1981) suggest that the sediment in transport is negatively skewed (supported by flume and field observations), they do not, unlike McLAREN (1981), make any suggestions as to what happens to this sediment during and after deposition. In effect, deposition is selective (probabilistic) at a given energy level, with coarser grains depositing more readily than the fines. Each deposit then serves as a source to its immediate down-stream neighbour. In this way the transfer functions would still result in progressively more positively skewed sediments along the transport path. LANCASTER (1986), in his work on linear sand dunes in the Kalahari, observed that sands become finer, better sorted and more positively skewed in the direction of transport. These observations strongly suggest that the model of McLAREN & BOWLES (1985) merely represents a special case of many possible alternatives. Ofcourse, local exceptions are always possible since processes like mixing of different populations and total deposition of the sediment load without

sorting may take place, thereby locally affecting the skewness sign and disrupting the directional trends (e.g. FLEMMING, 1988).

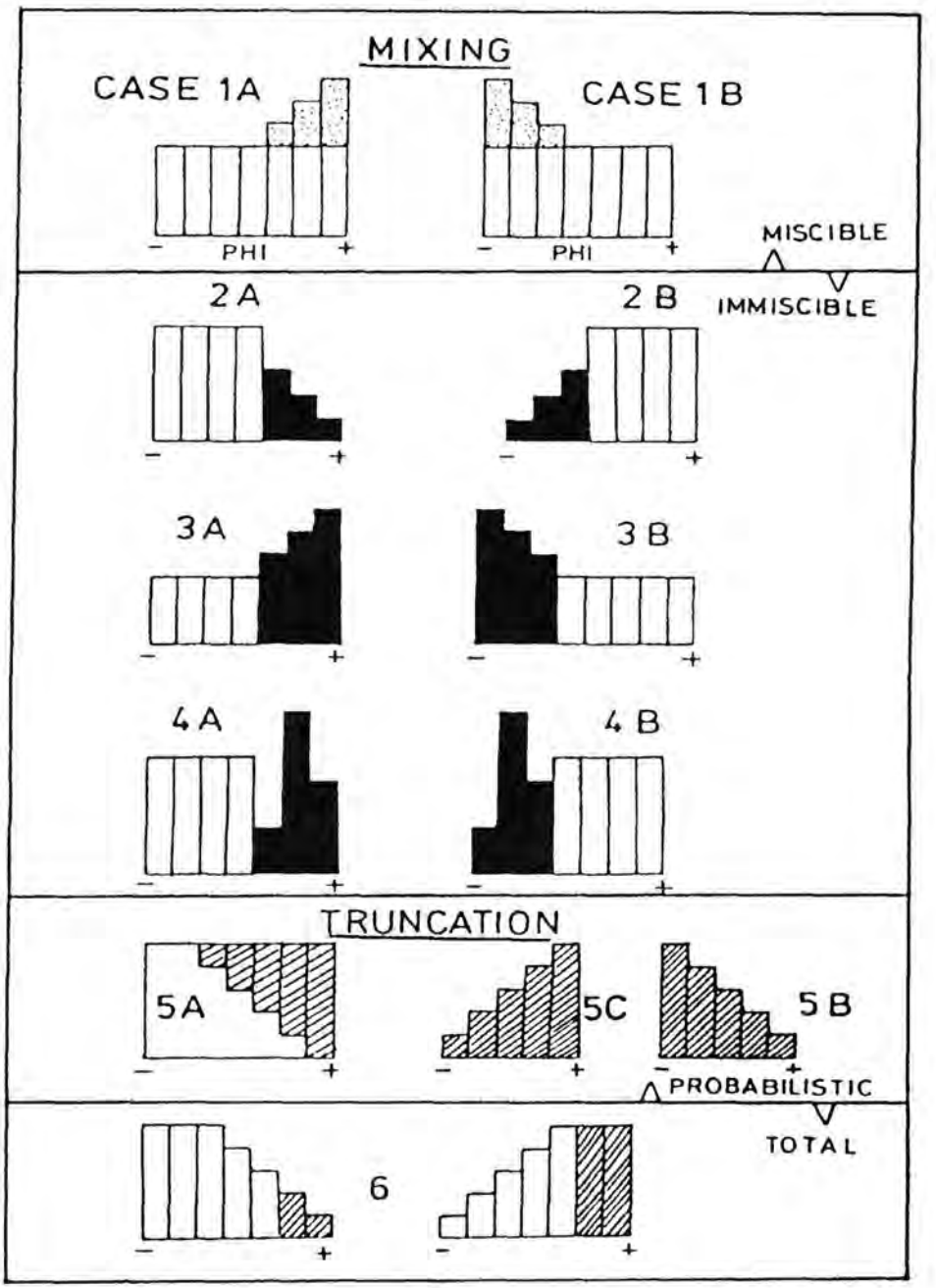

Fig. 4-15 The deductive model of skewness-sign evolution taking into account mixing and truncation of various sub-populations (ANTIA, 1993).

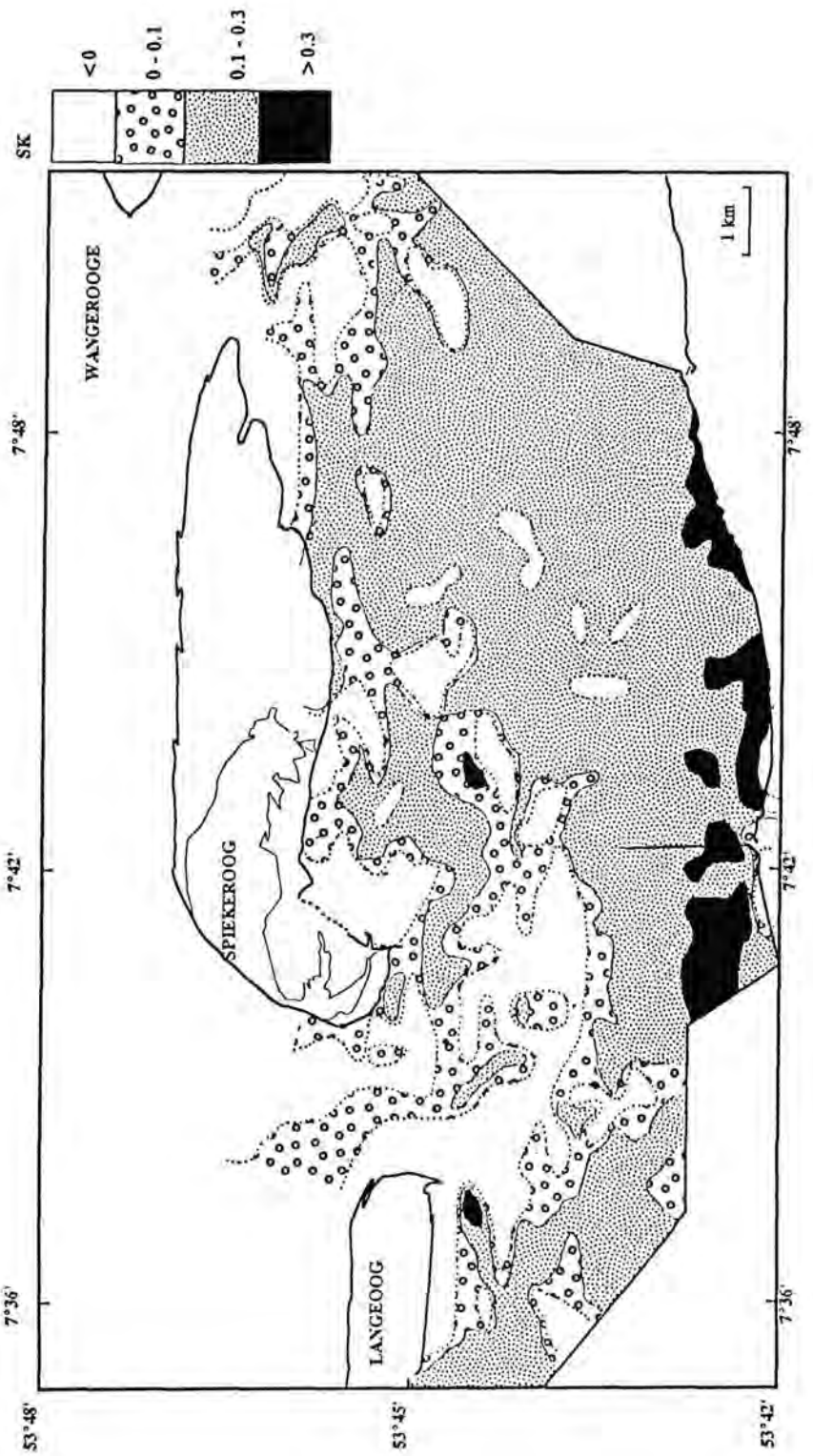

Fig. 4-16 Skewness distribution in the Spiekeroog backbarrier area.

4.3.5 Kurtosis

Kurtosis is a measure of the peakedness of a grain size frequency curve. The percentile kurtosis is calculated thus:

$$K_G = \frac{(\Phi_{95} - \Phi_5)}{2.44\,(\Phi_{75} - \Phi_{25})}$$

The descriptive classification of kurtosis is presented in Table 4-4.

Table 4-4. Descriptive classification of kurtosis.

K_G	Description
< 0.67	Very platykurtic
0.67 - 0.90	Platykurtic
0.90 - 1.11	Mesokurtic
1.11 - 1.50	Leptokurtic
1.50 - 3.00	Very leptokurtic
> 3.00	Extremely leptokurtic

Normal distributions have kurtosis values of 1.0 and curves with higher or lower values are strictly non-normal, although the distributions can be symmetrical. The physical significance of the parameter, therefore, is to distinguish between normal and non-normal distribution. Apart from its useful application in combination with the skewness sign in discriminating sediment types, e.g. dune sediment from beach sediments (FOLK, 1966), it offers little help in understanding transport mechanisms. Some studies, however, have shown that there is a close relationship between the kurtosis value and the sorting coefficient (e.g. FOLK & WARD, 1957). Very well sorted sediments should therefore show higher kurtosis values, the range of which reflects how close to normality the sediment is.

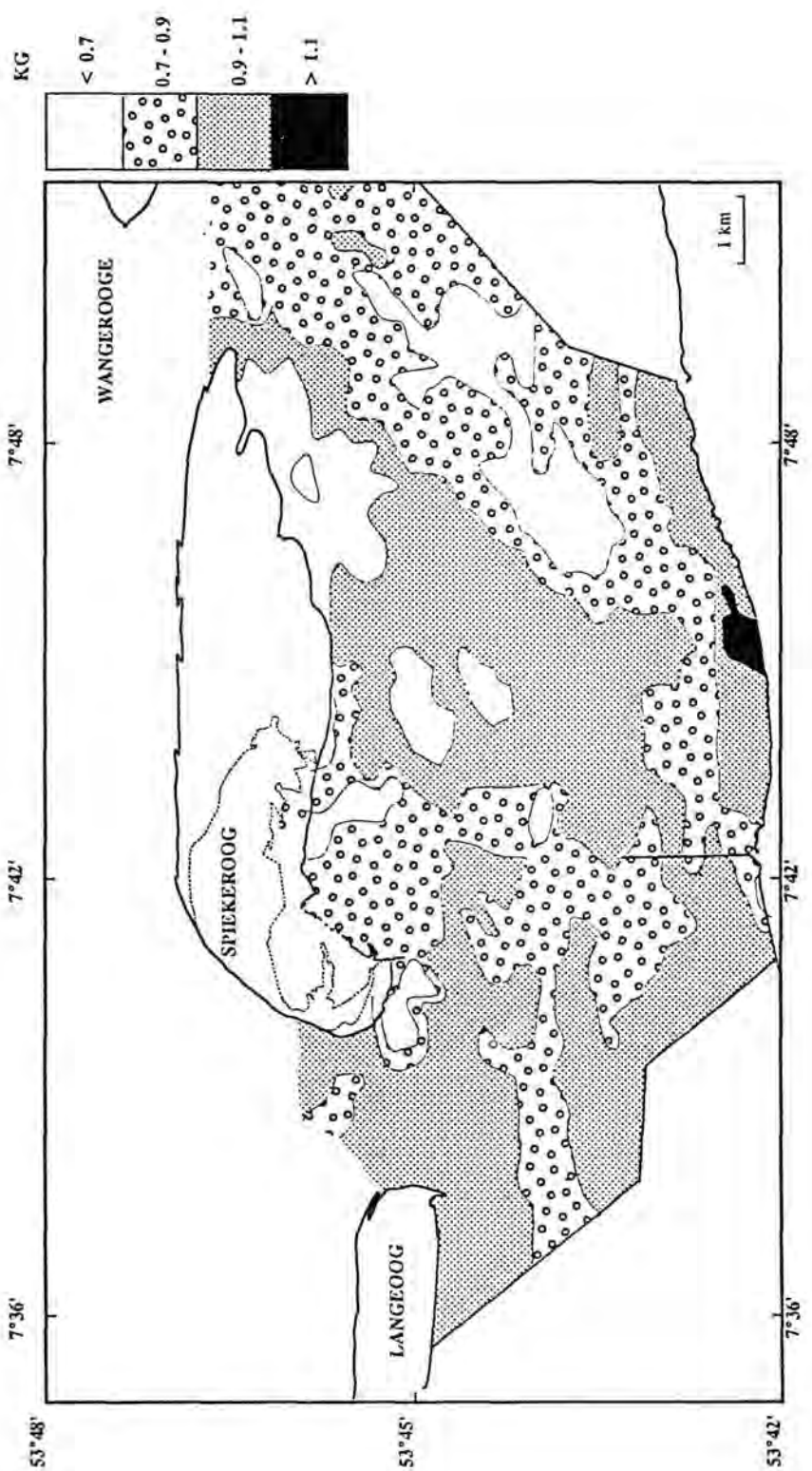

Fig. 4-17 Kurtosis distribution of the Spiekeroog backbarrier sediments.

The areal distribution of kurtosis is presented in Fig. 4-17. The region can be described as being mainly composed of patykurtic - mesokurtic sediments. Isolated patches of very platykurtic sediments within the platykurtic bands are not uncommon. The same is true of isolated cases of leptokurtic sediments within bands of mesokurtic sediments. As shown below, the areal distribution of this parameter, like the other textural parameters also appeared to be geomorphologically influenced.

In the Otzum inlet three kurtosis bands are found. A zone of very high kurtosis values (mesokurtic - very leptokurtic) is found in the inlet throat area. Both seawards and landwards of this zone a NW-SE oriented band of platykurtic sediments is found. Further landwards of the central zone, the platykurtic band turns NE-SW along the high tide water divide between the Schill and Hull channels. The platykurtic bands are surrounded by bands of mesokurtic sediments. A similar pattern is repeated in the Harle inlet, with the exception that the central zone with high kurtosis values is missing. It is presumed to exist further northwards in the inlet. The platykurtic bands closely correspond to similar bands of well - moderately sorted sediments. The surrounding mesokurtic sediments are correspondingly very well sorted.

The central tidal flats, bounded to the south by the dyke and to the north by the island, show a N-S alternation of mesokurtic and platykurtic sediments. The near-dyke region is largely mesokurtic with a minor core of leptokurtic sediments at the centre. These sediments are very fine, very well sorted and the most positively skewed. The next mesokurtic band, which occupies the whole central interchannel region, is separated from the near-dyke band by a narrow band of platykurtic sediments. This narrow band correlates with the change in slope between the southern flank (near-dyke region) and the central part (interchannel region) of the basin. Towards the island the mesokurtic character gives way to platykurtic sediments which occupy most of the backbarrier shoreline. Mesokurtic sediments also occur to the south of the eastern island head (Ostplate) and in the central section.

Significantly, the N-S bands of kurtosis values occur in the same number and pattern as those of the mean grain size map at 0.25 phi intervals (Fig. 4-10). This attests

further to the fact that sub-populations or grain size fractions which are separately deposited are hydraulically different.

4.4 Distribution of individual grain size fractions

Besides high-resolution grain size analyses, the settling tube also provides information on percentage contribution by weight of the various size fractions at 0.25, 0.5 and whole phi intervals. When these percentages are plotted areally for each of the fractions, maps showing the distribution of particular size classes are obtained. The spatial separation between the fractions is a clear indication of the lateral separation of the effective energy levels in the area. Grain size fractions (or settling velocity fractions) are therefore important fingerprints of relative energy levels in the study area. This fact is demonstrated below using the size fractions 1 - 1.5, 1.5 - 2, 3 - 3.25 and 3.25 - 3.5 phi.

4.4.1 The 1 - 1.5 and 1.5 - 2 phi fractions

These fractions form relatively coarse deposits in high energy environments. Samples containing appreciable amounts (> 5% by weight) of the 1 - 1.5 phi fraction thus do not occur on the tidal flats. Instead, they are restricted to the inlet mouth (Fig. 4-18). Nevertheless, the contribution of this fraction is typically less than 50%, the highest recorded value being 66%.

The 1.5 - 2 phi fraction, although concentrated in the same areas as the previous fraction, forms wider belts and contributes more than 50% to the sediment (Fig. 4-19). Values of 5 - 25% occur widely on the interchannel flats. In the main channels concentration bands of 25 - 50% extend southwards of the inlet mouth. This lateral shift in the areal extent of this fraction reflects a landward decrease in energy away from the inlet mouth, i.e. in a SE direction in this region.

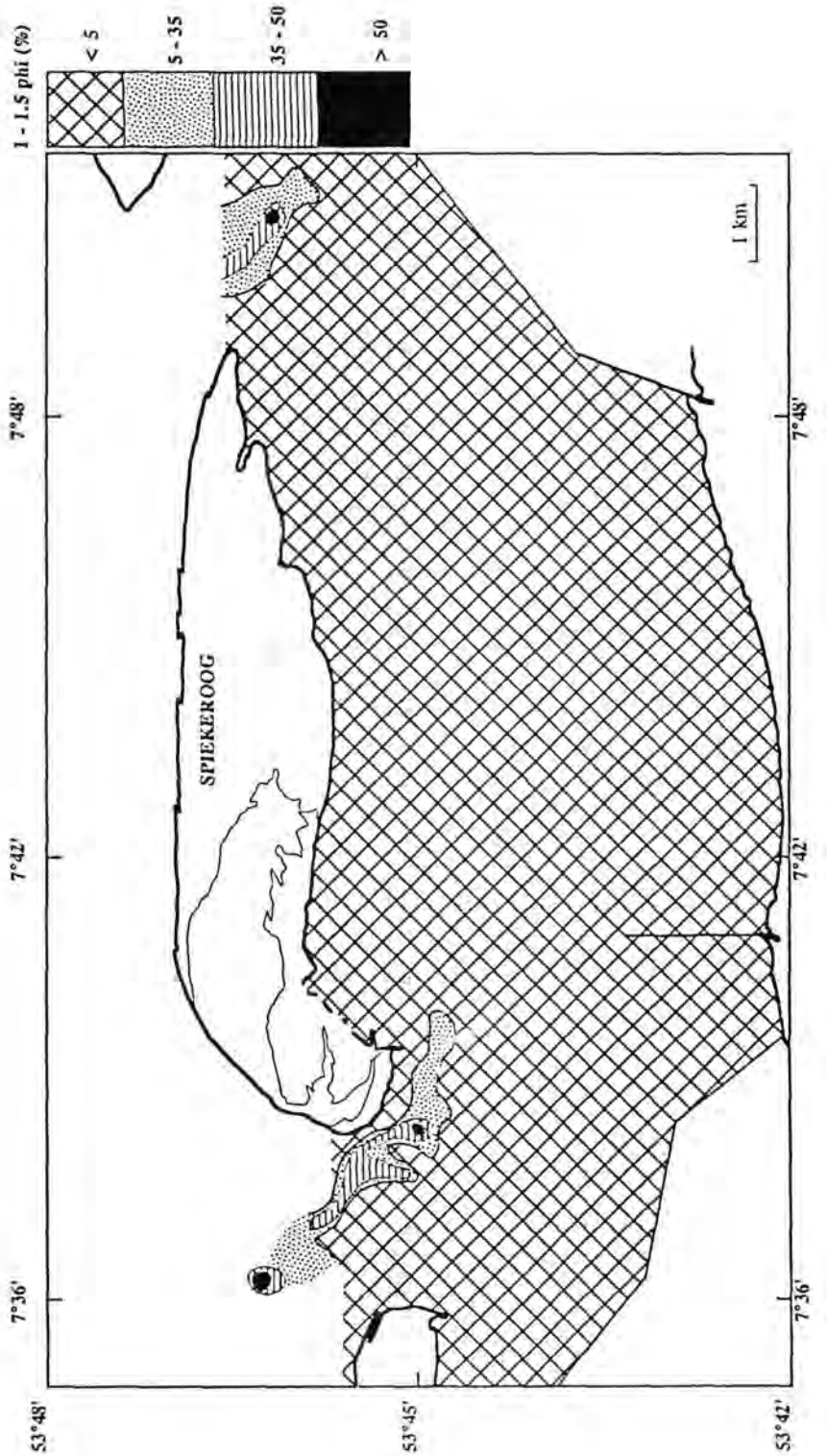

Fig. 4-18 Spatial distribution of the 1 - 1.5 phi size fraction in the Spiekeroog backbarrier area.

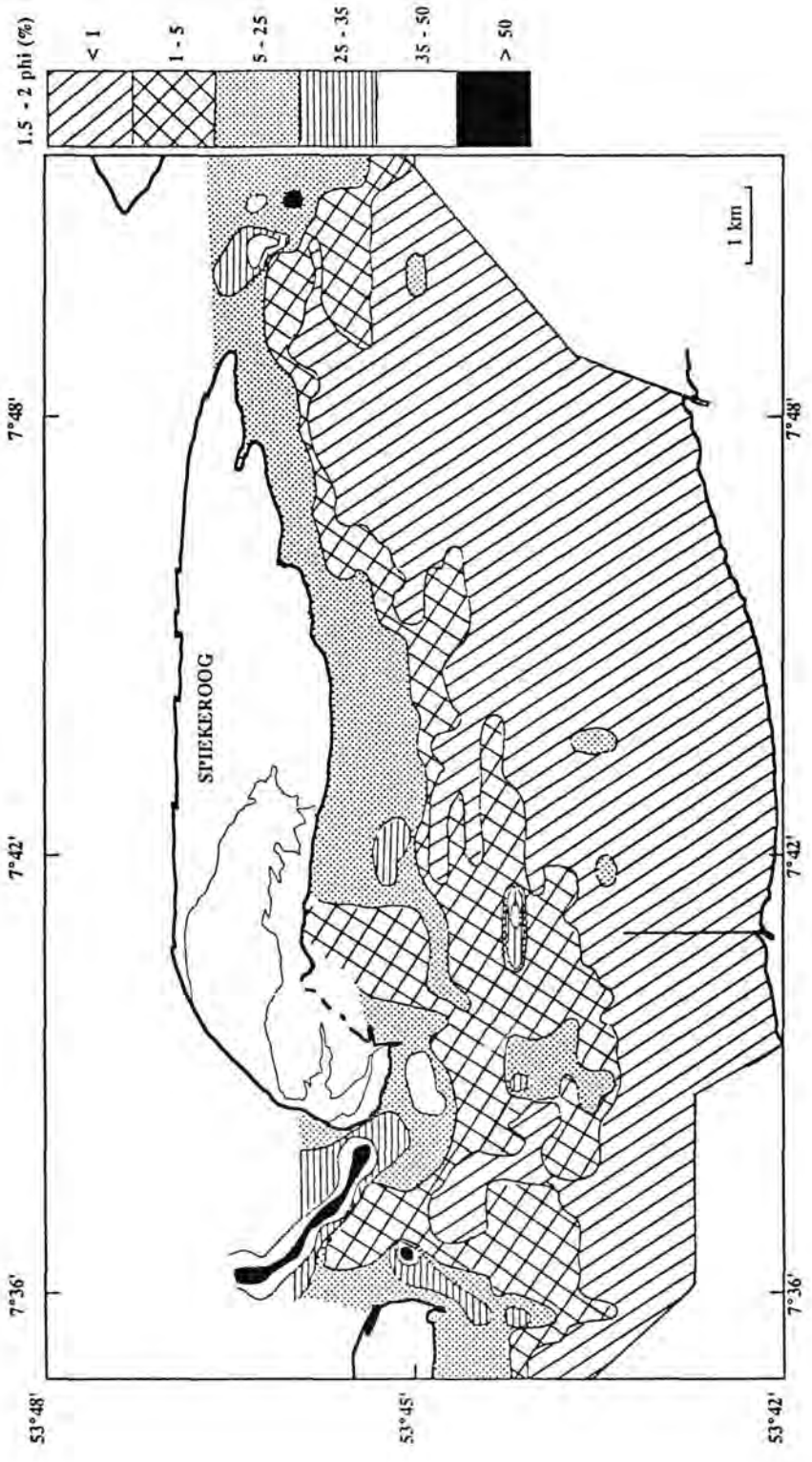

Fig. 4-19 Spatial distribution of the 1.5 - 2 phi size fraction in the Spiekeroog backbarrier area.

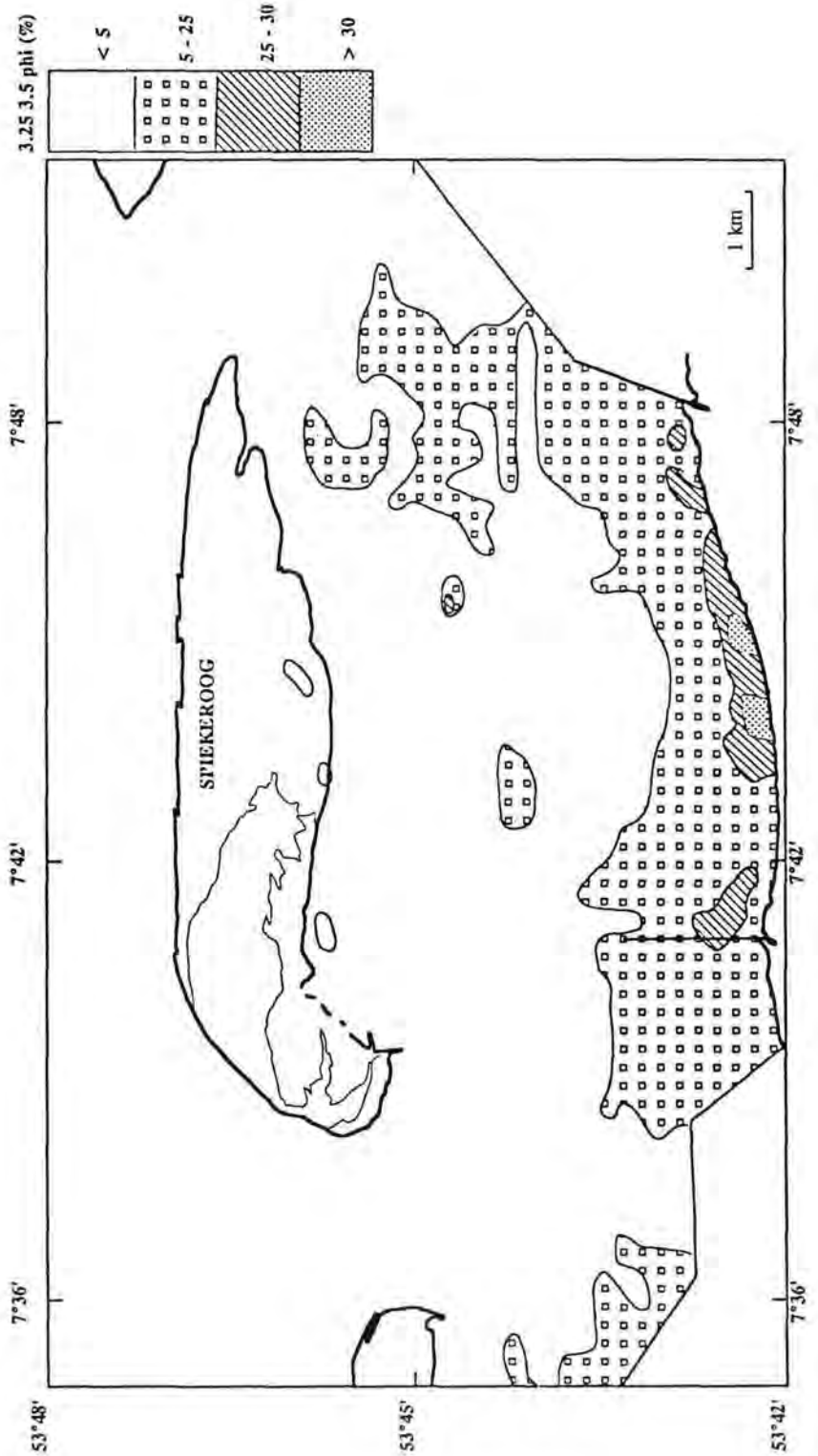

Fig. 4-20 Spatial distribution of the 3.25 - 3.5 phi size fraction in the Spiekeroog backbarrier area.

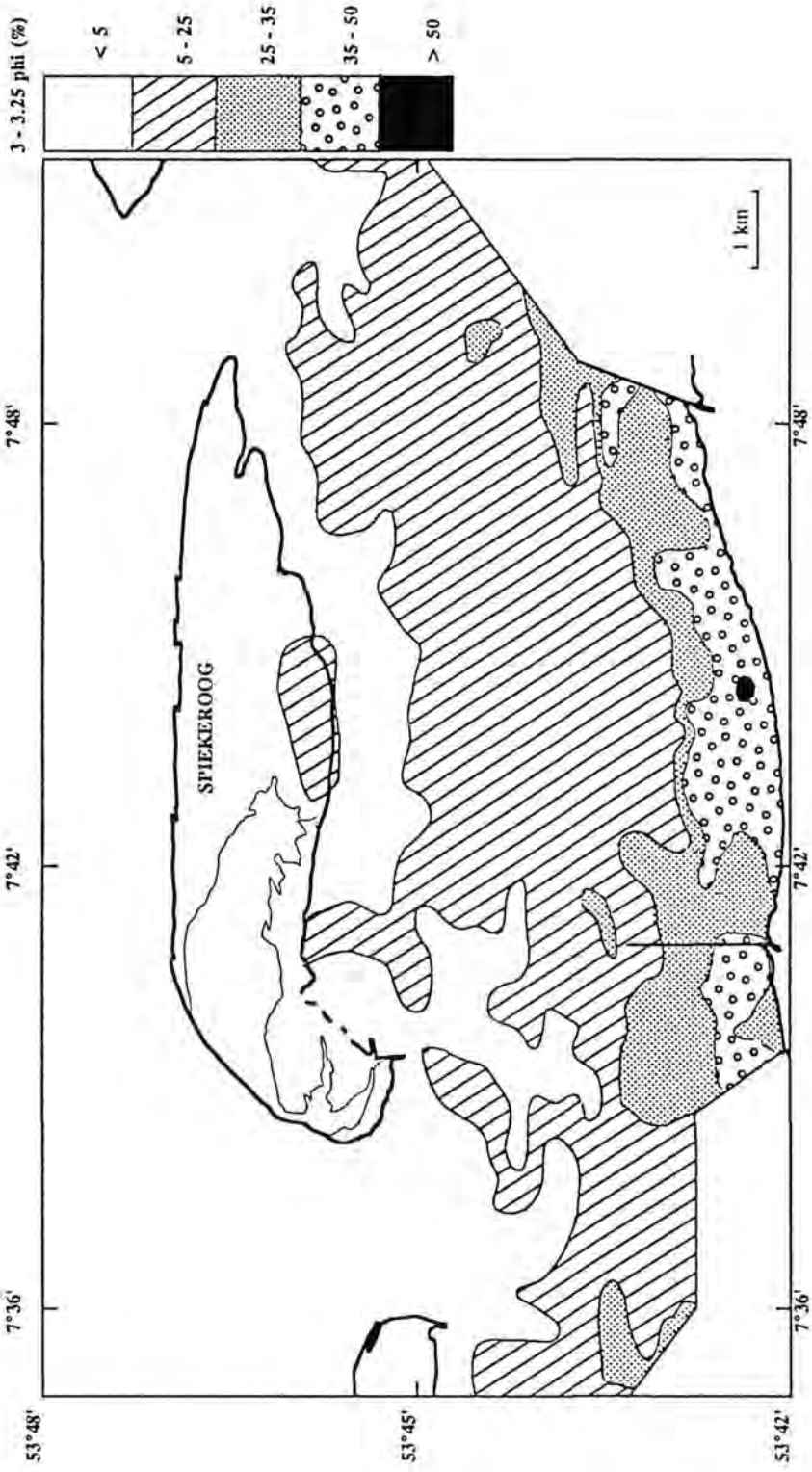

Fig. 4-21 Spatial distribution of the 3 - 3.25 phi size fraction in the Spiekeroog backbarrier area.

4.4.2 The 3 - 3.25 and 3.25 - 3.5 phi fractions

In contrast to the fractions discussed above, these fine fractions are typically found in the less exposed low-energy environments. The 3.25 - 3.5 phi fraction is highly concentrated (25 - 40%) in a narrow belt near the dyke (Fig. 4-20). This is a zone of high elevation in which tidal action is less effective. Seawards of this zone the energy level increases and the contribution of this fraction to the bulk sediment drops to 5 - 25%. Outside this region isolated patches of this fraction (< 5%) occur in sheltered areas behind the island.

With the exception of the inlet throat areas, the 3 - 3.25 phi fraction is widely distributed (Fig. 4-21). Its contribution ranges from 5 - 25% on the tidal flats and 35 - 50% along the dyke. It is evident here that the two fractions exhibit similar concentrations near the dyke, with a tendency of the coarser of the two to extend further seawards. This points to a seaward increase in the energy level.

The depletion in the mass content of the 3.25 - 3.5 fraction, as compared to the 3.0 - 3.25 (coarser fraction) along the dyke, indicates that the near-dyke energy level is too high for the settlement of the finest sand fractions. The dyke thus appears to have interrupted the energy gradient, leading to the elimination of the finest very fine sands. If the dyke was absent these very fine sands would presumably have occurred in high concentrations landwards of the present dyke (FLEMMING & NYANDWI, 1994).

4.4.3 Dominant grain size fractions

The above discussion can be summarised by a map in which the dominant grain size fractions are plotted together. Dominant fractions are those contributing more than 50% to the sediment. Such concentrations are only found in 0.5 phi and larger size fractions. The resulting map (Fig. 4-22) shows the backbarrier tidal flats to be characterised by three distinct shore-parallel, overlapping dominant-fraction zones. Two additional zones are defined within the inlet mouth areas. The dominant fractions

are the 3.5 - 3, 3 - 2.5, 2.5 - 2, 2 - 1.5 and 1.5 - 1 phi size classes, listed in order of increasing energy.

Assuming the most abundant size classes to reflect local hydraulic equilibrium with the hydrodynamic regime, the resulting zonation pattern defines a land-to-sea energy gradient, as deduced earlier from the mean grain size map. The overlap zones between adjacent size classes highlight the progressive nature of this energy gradient. They occur largely as transitions between the interchannel region (high energy) and the high elevation regions (lower energy) adjoining both the island and the mainland coast (dyke).

4.5 Mud content

On the basis of the sand content in tidal flat sediments, REINECK & SIEFERT (1980) and REINECK et al. (1986) have defined three sediment types, namely sand flats (> 90% sand), mixed flats (50 - 90% sand) and mud flats (< 50% sand). By implication, this classification can also be inversely defined on the basis of mud content, Thus, sand flats contain < 10% mud, mixed flats 10 - 50% mud, and mud flats > 50% mud. The choice of the former classification in the German literature is the lack of a precise definition of the term mud in German. These sediment types have been found to form coast-parallel belts in which the mud flats occupy the near-coast areas. Seawards of the mud belt lies a mixed flat belt followed by pure sand flats. That tidal flats of non-dyked coastlines prograde shorewards into progressively finer sediments, culminating in thick mud deposits and extensive salt marshes is a long established fact (e.g. REINECK & SINGH, 1973; ELLIOT, 1978). Such a coast-perpendicular gradient has been widely documented in other coastal settings (e.g. HÄNTZSCHEL, 1955; VAN STRAATEN & KUENEN, 1957; VAN STRAATEN, 1961; EVANS, 1965; REINECK, 1967, 1972; KELLERHALS & MURRAY, 1969) and is unequivocally considered to reflect the existence of a well developed energy gradient.

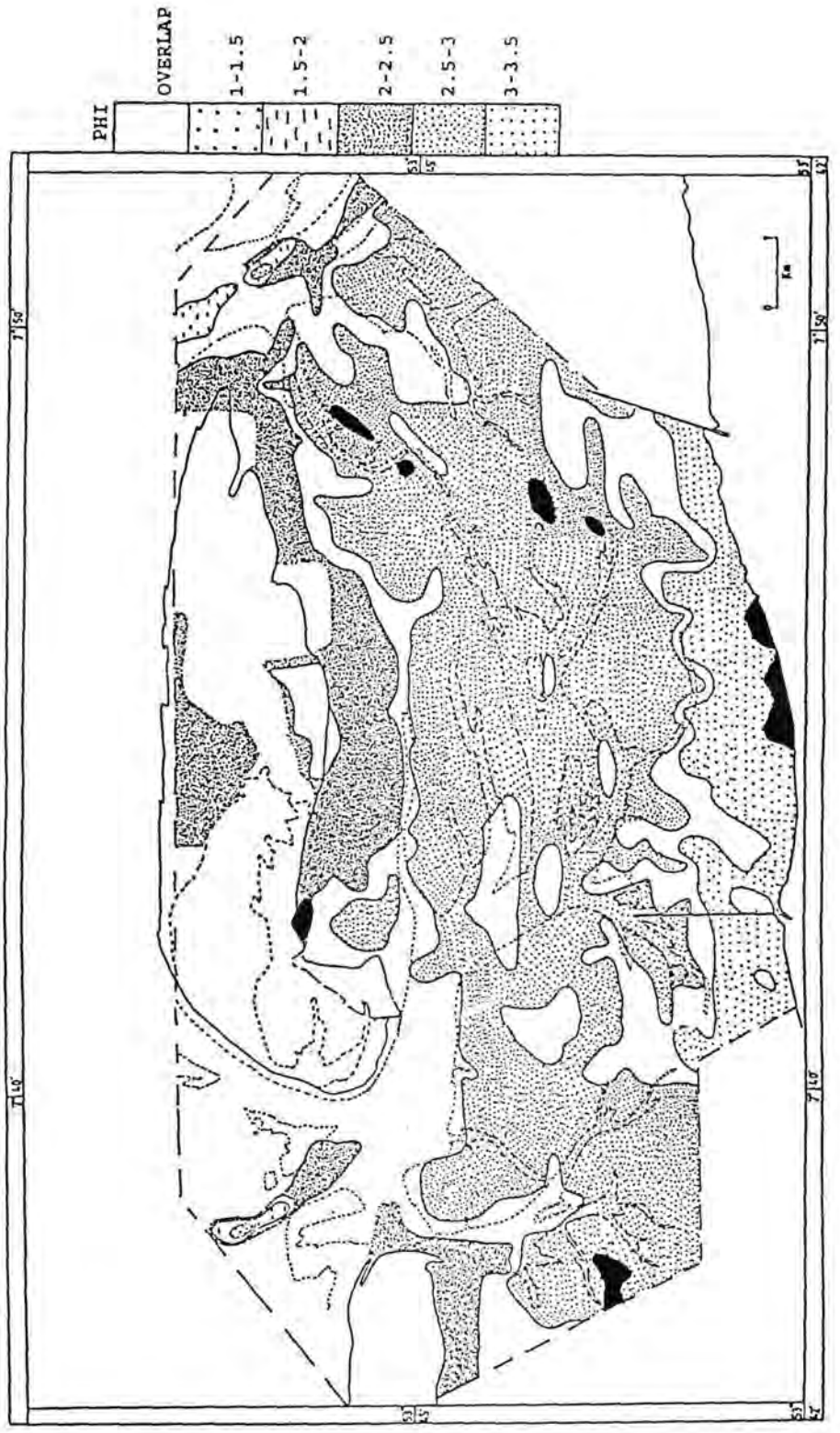

Fig. 4-22 Distribution of the dominant grain size fractions and mud patches in the Spiekeroog bacbarrier area. The dominant-fraction zones reflect energy level variation.

4.5.1 Mud distribution and mode of deposition

The occurrence of mud deposits (> 50% mud) in relation to the distribution of sand is presented as mud patches in Fig. 4-22. As it can be seen, mud only occurs in isolated patches, hardly showing any clear relation to the energy gradient. However, the distribution of the mud content in the sediment, as shown in Fig. 4-23 does show some obvious trends:

a) High mud contents are registered along high tide water divides.
b) The mud patches are always surrounded by mixed flats, followed by sand flats.
c) The mud content increases shorewards (Fig. 4-24).

The scatter plot of Fig. 4-24 represents sediment samples along a N-S transect centred at P34 (see Fig. 4-1). Together with the general landward fining of the sediment reported earlier, a corresponding increase in mud content is evident. With the exclusion of the interchannel samples (open circles) a very good linear correlation (R = 0.87) between the mean grain size and the amount of mud contained is obtained. The interchannel region is characterised by lower mud contents and a somewhat poorer correlation (R = 0.73) between the sand grain size and the mud content. Whereas the shoreward increase in mud content corresponds to the general energy gradient, a feature attributing to the predominance of hydrodynamically controlled deposition, the other trend suggests topographic control on deposition.

4.5.1.1 Effect of topography

The enrichment of mud in areas of high elevation clearly points to a correlation between water depth and mud deposition. At high tide the water depths on the high tidal flats remain shallower than on the lower flats and the tidal channels. At high water slack, when the turbulence has considerably diminished, settling of suspended mud aggregates takes place. Since the duration of the slack water condition is short, larger amounts of mud can settle to the bottom on the shallower, high elevation flats. As the water depth increases away from these areas, mud deposition decreases

correspondingly. The high-tide water divides, which are regions of shallower water depths, are thus characterised by high mud contents.

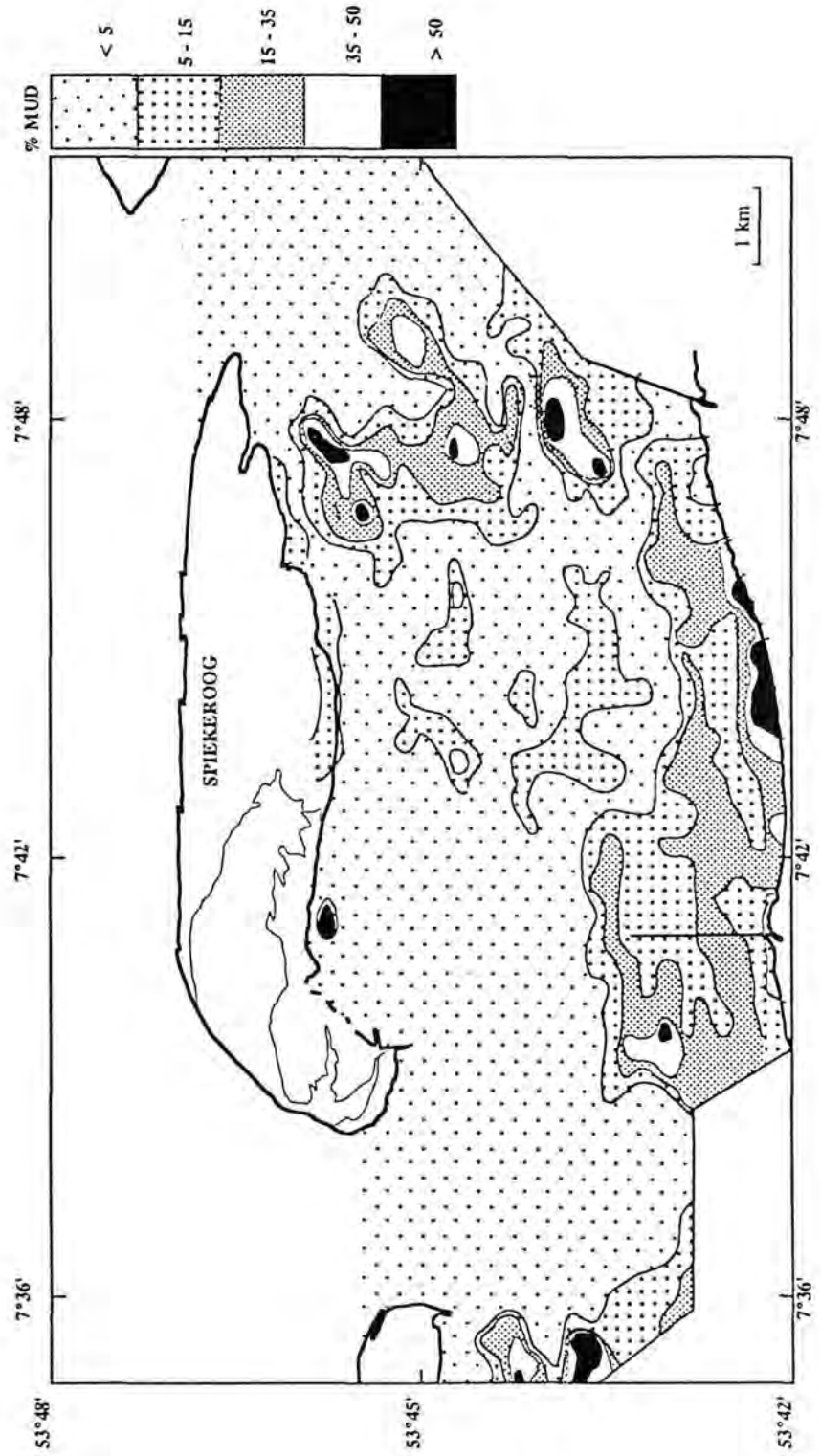

Fig. 4-23 Distribution of the mud content in the Spiekeroog backbarrier sediments.

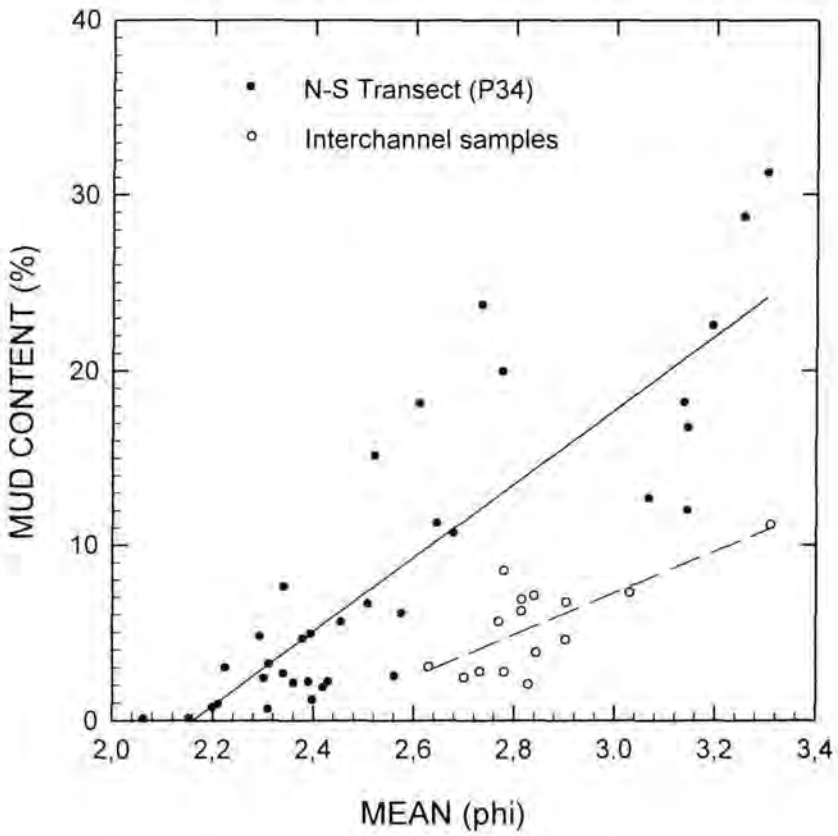

Fig. 4-24 Land-to-sea variation of mud content with sediment size in the Spiekeroog backbarrier area.

Biological enrichment

Mud deposition by bottom filter feeders in form of faecal pellets and pseudo-faeces has long been recognised as one of the mechanisms by which mud is enriched on tidal flats (e.g. FOX & COE, 1943; VERWEY, 1952). FLEMMING (1991) observes that the mud deposits occurring away from the dyke in the Spiekeroog area occur as surface coatings on shell beds (mussel beds), an association which indicates that they are biologically deposited. Similar observations have been made elsewhere

(NIEMEYER, 1972; BEUKEMA, 1976). Other studies, however, have shown that the faecal pellets produced by bottom filter feeders rarely settle long on the bottom before they are recycled, thus making it difficult to ascertain the biological contribution (SMETACEK, 1980; PEINERT et al., 1982; TEN BRINKE & DRONKERS, 1993).

The occurrence of mussel beds is known to be limited to muddy areas of the backbarrier tidal flats (EHLERS, 1988), especially at elevations above mean low tide level (FLEMMING et al., 1992). These are clear evidence that topography controls not only the deposition of mud on high tidal flats but also the distribution of the organisms that contribute further to the enrichment of mud.

Flocculation

Since the mud is closely related to the finest fractions of the sand fraction (FLEMMING & NYANDWI, 1994), there must be some form of similarity in the hydraulic behaviour of this sand and the mud. The mud-rich areas are essentially associated with very fine sands (Fig. 4-25). Due to flocculation the increased effective settling velocity of the mud flocs leads to their deposition along with coarser sand fractions in relatively higher energy zones. However, whereas very close to the dyke (lowest energy level) the high mud content appears to correlate well with the 3.0 - 3.5 phi sand fraction (occurring at concentrations of over 50%), the next finer sand fraction (3.5 - 4 phi) is highly depleted (Fig. 4-26). This leads to the conclusion that the near-dyke mud represents the coarser tail of the aggregate grain size spectrum, all smaller aggregates being eliminated in the same way as the finest sands (FLEMMING & NYANDWI, 1994).

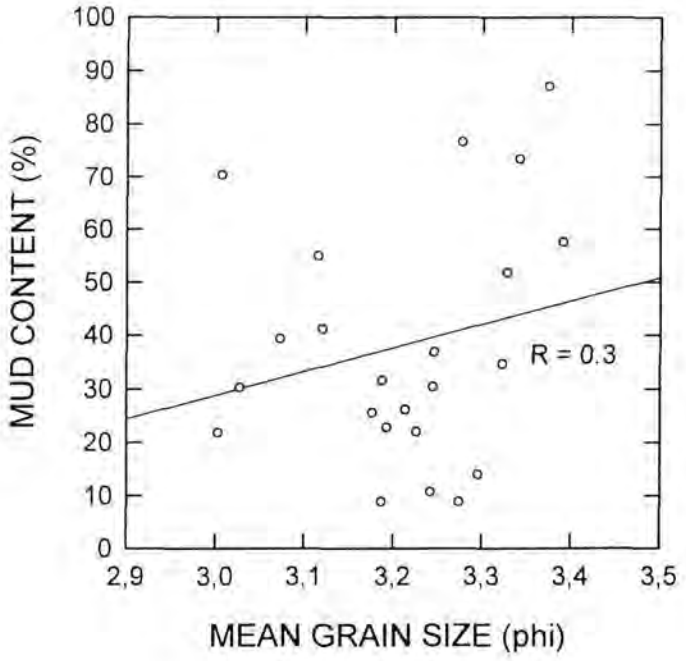

Fig. 4-25 Correlation between mud content and the mean grain size of the sand fraction in the mud-rich near-dyke area. Although the mud content increase generally with decreasing mean of the sand fraction, the poor correlation suggests energy incompatibility between the two.

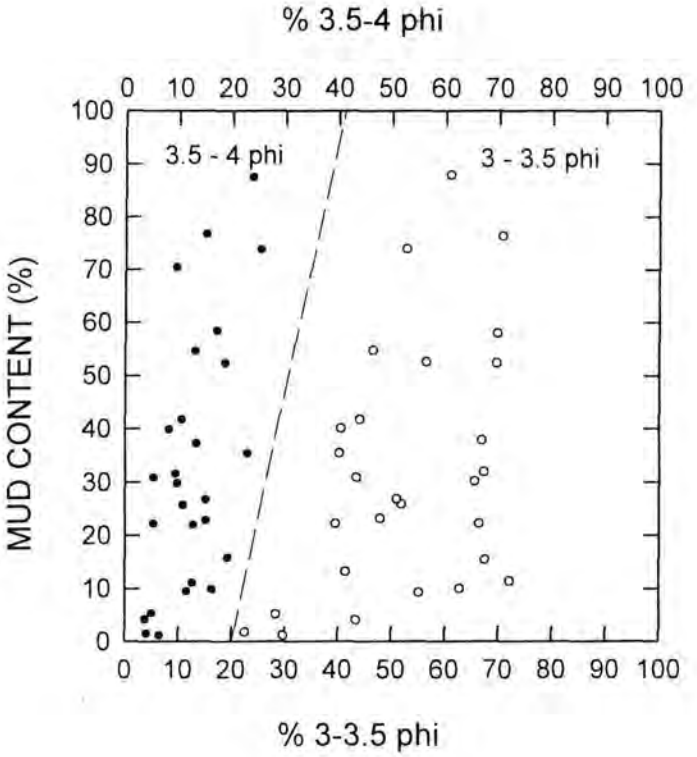

Fig. 4-26 Correlation between mud content and the fine sand fractions. There is a clear depletion of the finest sand fraction (3.5 - 4 phi).

CHAPTER 5

DEPOSITIONAL ENVIRONMENTS AND THE ENERGY GRADIENT

In the preceding chapters a shore-normal energy gradient was inferred in addition to the NW-SE aligned tidal gradient (following the main tidal channel axis or tidal flow direction). The occurrence of this seemingly flow direction-unrelated shore-normal gradient could not be anticipated and thus merits further investigation. Whereas its character in relation to the general geomorphology of the backbarrier area is closely examined in this chapter, its origin is investigated in chapter 6. The influence of the energy gradient on the depositional environments and transport pathways of the sediment is also addressed.

5.1 Basin structure

The Spiekeroog backbarrier tidal basin, which comprises also the Otzum tidal catchment area to the west and part of the Harle tidal catchment area to the east, is flanked on its seaward side by the Spiekeroog island and to the south by the mainland. Although the inlets (main channels) generally run in a NW-SE direction, the tidal channels behind the island are generally E-W oriented. A N-S cross-section through the central region of the basin and the island shows the basin to be characterised by three physiographic units, namely a northern (Region C) and a southern (Region A) regions which flank a central interchannel region (Region B) (Fig. 5-1). Whereas the flanks slope towards the centre of the basin, the central interchannel region is characterised by an alternation of tidal flats and channels. On the basis of ground elevation and vegetation cover, Regions A & C may be referred to as higher (flank) tidal flats transforming into marshes, as opposed to the low (interchannel) flats of Region B. Unlike the mainland coast (dyke), not only marshes with creeks and pools are developed on the island, but also isolated dunes of varying ages.

On account of the clear-cut grain size trends (chapter 4), it might be expected that the three physiographic units above represent different depositional units (environments). Based on these trends the hydraulic energy levels and depositional processes responsible for these units are examined in detail.

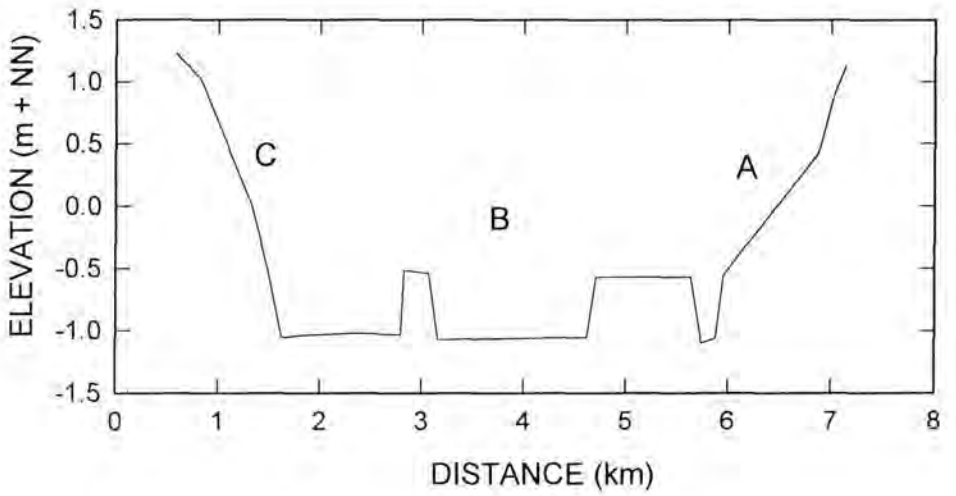

Fig. 5-1 N-S cross-section through the Spiekeroog backbarrier tidal basin showing the basin form above chart datum.

5.2 The energy gradient

Ideally, the most accurate way of characterising the energy conditions and its spatial distribution (i.e. gradient) in a modern tidal environment would be through the measurement of flow velocities. However, monitoring of tidal flow conditions covering many stations simultaneously is in most cases both logistically and financially prohibitive. In absence of this, hydraulic proxies such as median size (SPENCER, 1963; SHI, 1992) or mean grain settling velocity may be used to infer related energy levels. The energy gradient is then reconstructed by the variation of the parameter, either with distance or with water depth in a given direction. Since the

water depth varies very little across the tidal flats, it has been decided to use distance as the independent variable.

The mean grain settling velocity has been chosen because it is related to the level of turbulent energy. The logarithm of the settling velocity, defined as psi = $-\log_2 V_{cms}$-1, is used as an equivalent of the phi-based grain size scale. In chapter 4 it was shown that the mean settling velocity (psi) distribution map depicts a similar pattern as that of the mean grain size (phi).

When the mean settling velocity (psi) is plotted with distance, a scatter diagram is obtained which is best described by a polynomial curve fit (Fig. 5-2). The polynomial has the form:

$$Y = a_0X^n + a_1X^{n-1} + \ldots + a_{n-1}X + a_n$$

Where, Y and X are the dependent and independent variables, respectively as defined before. It can be seen that the more the energy gradient is subdivided (in this case due to topographical variations), the higher the order of the polynomial describing it. Order 10 polynomials were found to give excellent fits ($R > 0.95$). Nevertheless, the polynomial per se has little physical meaning. The separate segments of the polynomial, on the other hand, appear to be meaningful because they correlate with the topographic variations. The data points representing the individual segments may then be linearly fitted to produce discreet gradients (Fig. 5-3).

In order to understand the physical significance of the numerous gradients one needs to look at the linear fit of the whole data. (Fig. 5-4). The steadily seaward increasing energy level, as indicated by the overall energy gradient, supports the observed grain size (Fig. 4-10) and settling velocity (Fig. 4-11) distributions. The line segments are thus interpreted as representing local energy gradients which are nothing else but an indication of the interruption of the energy gradient by the bottom morphology. This is demonstrated by the fact that Profile P34 (Fig. 5-3 (a)) running through the outer region of less developed tidal channels shows less subdivisions (straight line segments) of the energy gradient than profile P31 (Fig. 5-3 (b)) which runs through the inner region of the tidal channels.

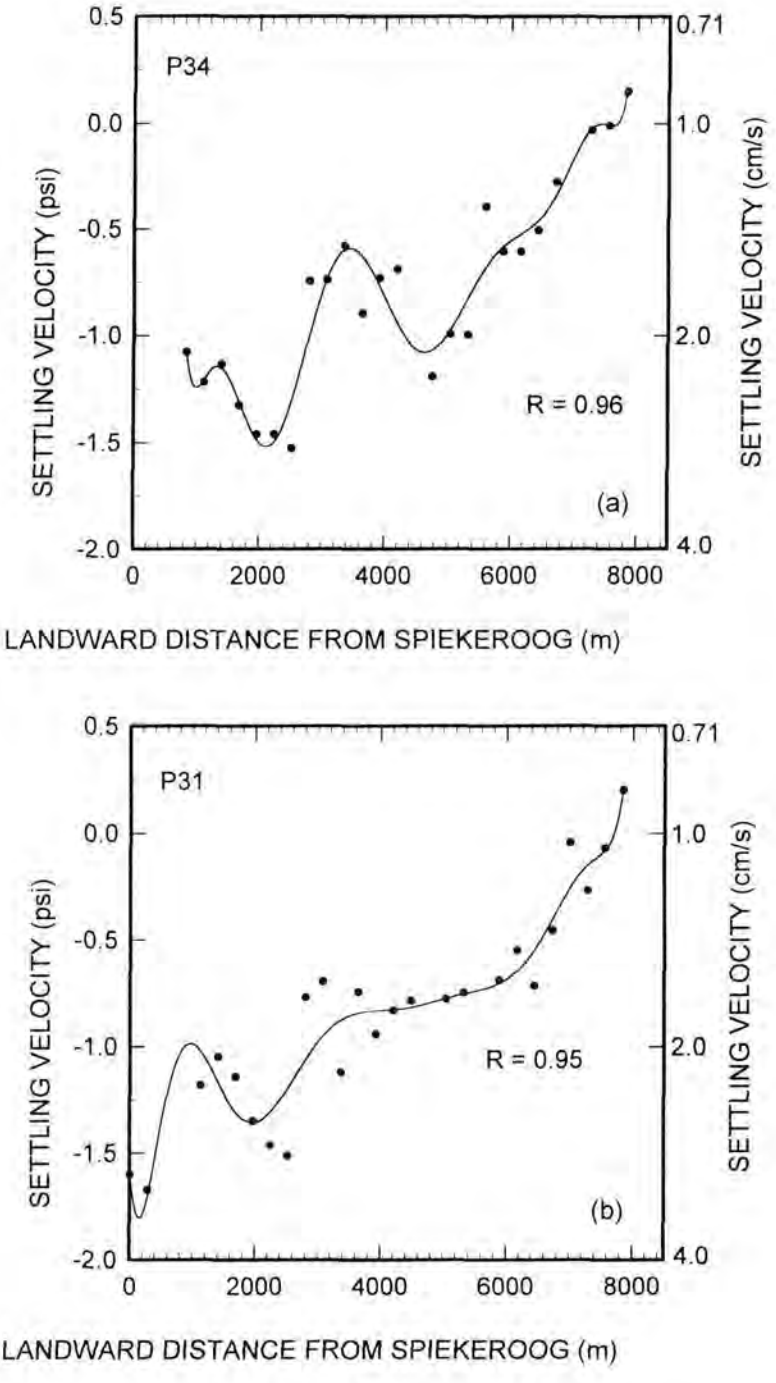

Fig. 5-2 Polynomial curve fitting of the energy gradient across the Spiekeroog backbarrier tidal flats. Although profile P34 (a) is situated 840 m to the east of Profile P31 (b) the energy gradient is similar.

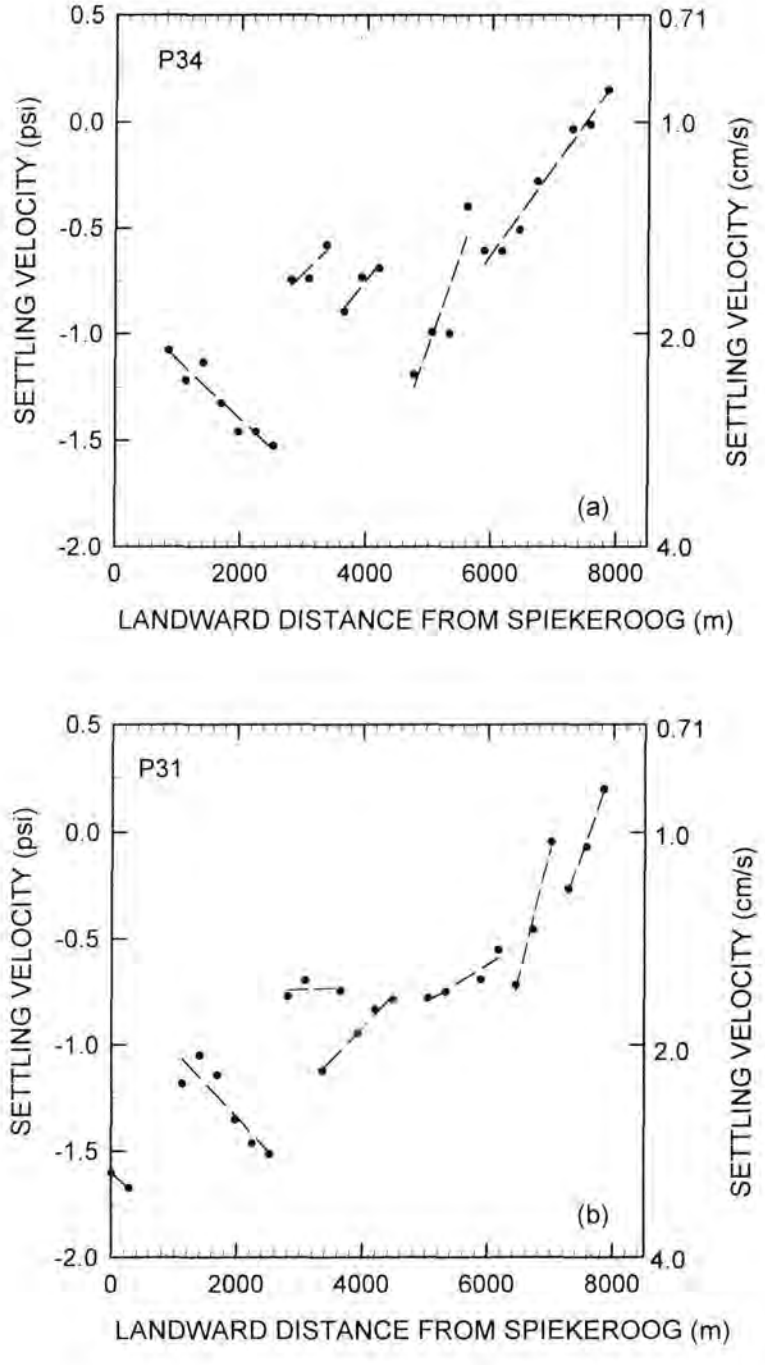

Fig. 5-3 Break-down of the polynomial into its constituent linear segments which appear to correlate with the physiographic units of the basin. Profile P34 running through the outer region of less developed tidal channels shows less subdivisions of the energy gradient than profile P31 which runs through the inner region.

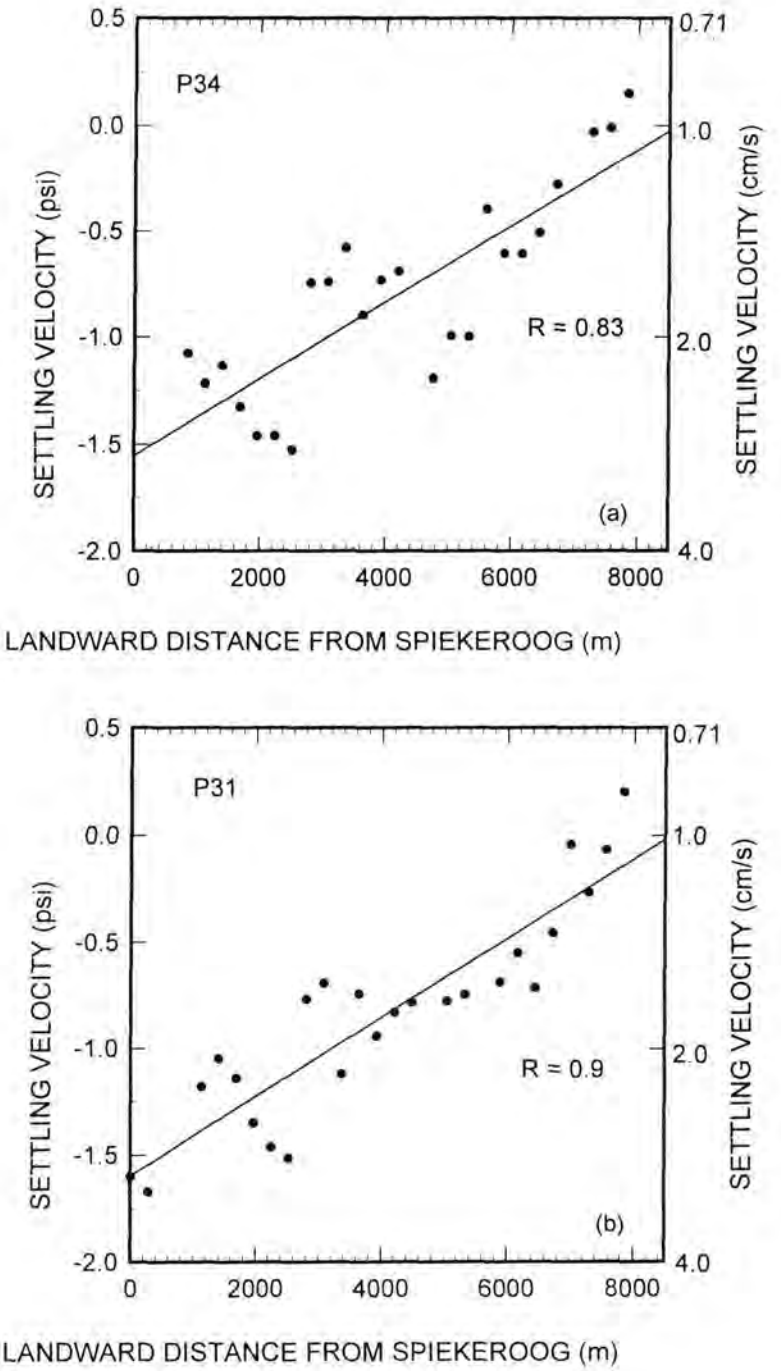

Fig. 5-4 Linear fit of the energy gradient indicating a steadily seaward-increasing energy gradient.

5.2.1 The energy compartments

By compartmentalising the energy gradient in regions of similar sub-energy gradients, three compartments are defined, within which better correlation coefficients are obtained (Fig. 5-5). These energy compartments relate to the three previously defined sedimentologic-geomorphologic regions in the following ways:

a) Compartment I represents the southern flank region (A) with only a minor interruption in the energy gradient.

b) Compartment II represents the interchannel region (B) with a number of energy gradients.

c) Compartment III (a & b) represents the northern flank region (C).

The inverse gradient in Compartment IIIA (Fig. 5-5b), which corresponds to a seaward decreasing energy level, is explained by the geomorphology of the area. This compartment represents the first kilometre from the last tidal channel towards the island - a region in which currents are expected to decrease away from the tidal channel as the ground elevation also increases. In addition, the increasing vegetation density towards the island dampens the waves and slackens the currents, resulting in decreasing energy levels and hence the fining of the sediment. Some distance into the island marsh zone the sediment becomes coarser again (Compartment IIIB) as the influence of overwash processes from the island shore slowly increases. This region of the backbarrier is essentially a marsh area with numerous creeks, pools and vegetated sand bodies which give way nothwards to isolated dunes. As such, a line transect through this area reveals rather more elaborately the textural variations than does the areal distribution map. The reason as to why Compartment III on Fig. 5-5(a) is not sub-divided lies on the fact that the intertidal zone is wider in this region.

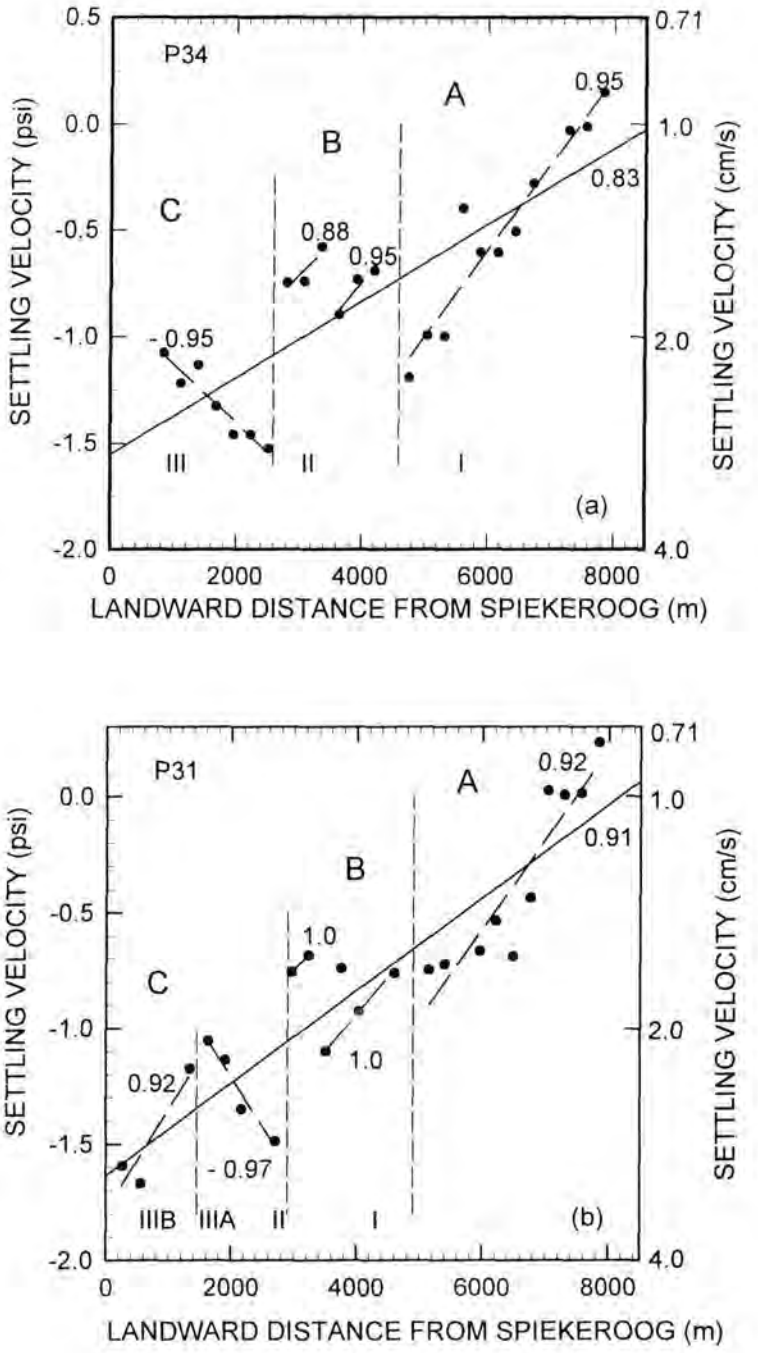

Fig. 5-5 Energy compartments as defined by different segments of the linear energy gradient. The compartments correlate well with the established sedimentologic-physiographic units.

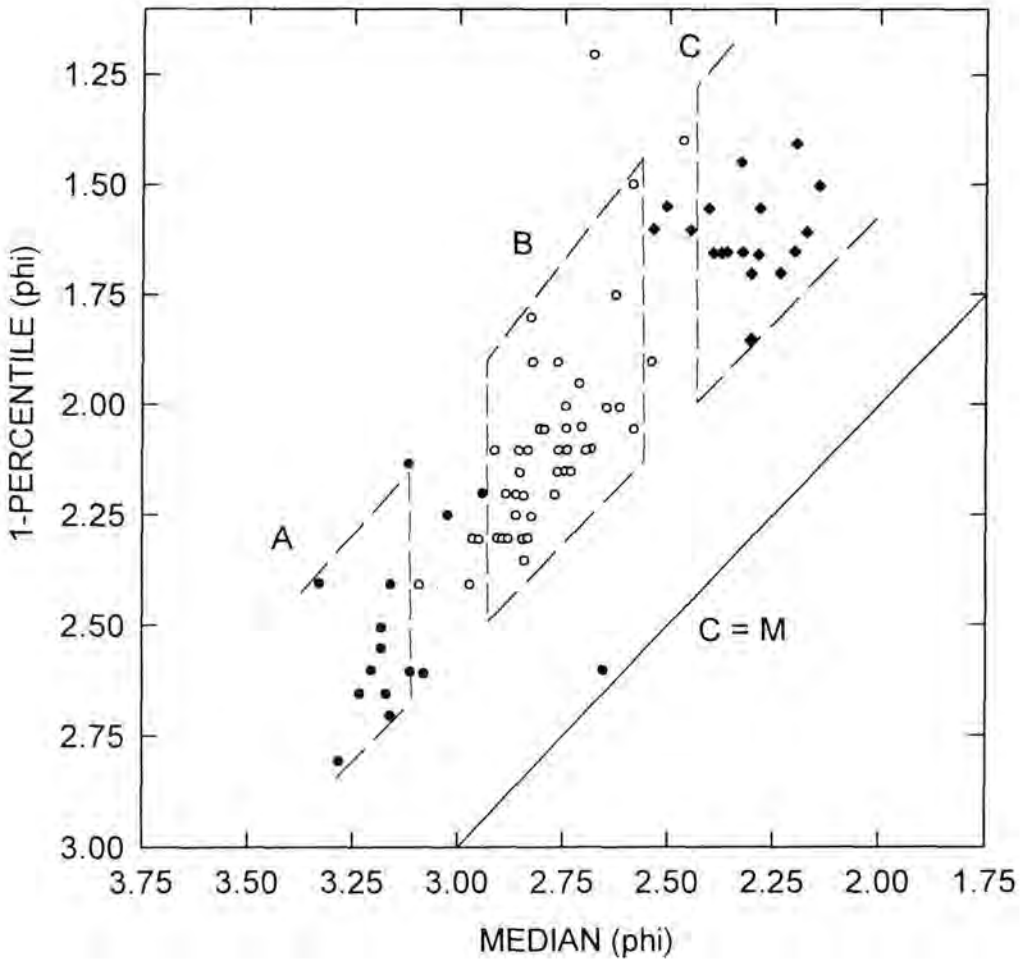

Fig. 5-6 C-M diagram of a selected transect (1 km wide belt transect). Three sediment facies (A, B & C) are obtained, which correspond to the previously defined physiographic units of Fig. 5-1 (Regions A, B & C, respectively).

5.2.2 Sediment facies

The relationships between any pair of the grain size parameters represented as scatter diagrams are useful in determining provenance, transport as well as depositional environment characteristics in a range of sediment types (FOLK & WARD, 1957;

PASSEGA, 1957; 1964; STEWARD, 1958; FLEMMING, 1977; SHI, 1992). Mathematical combination of the four size parameters (mean, standard deviation, skewness and kurtosis) gives rise to six relationships (scatter diagrams). The interpretation of scatter diagrams, however, is not always straight-forward and simple because the resulting patterns deduced rarely follow any established mathematical rule. Against this background, efforts are directed towards determining and interpreting any observable patterns. The sample set used is a 1 km wide N-S belt transect centred around profile P34 (Fig. 4-1).

A plot of the sample set on a C-M diagram shows three separate groups (Fig. 5-6). The same groups are identified when the degree of sorting is plotted against the mean size (Fig. 5-7). These groups or facies clearly represent the three different physiographic environments established earlier, i.e:

a) Group A sediments are from the tidal flats adjoining the mainland coast (Region A).

b) Group B are from the interchannel central area (Region B).

c) Group C are from the tidal flats transgressing on to the island and its dunes (Region C).

On the scatter diagram of skewness against mean (Fig. 5-8) the three facies established above are still evident. From the island of Spiekeroog southwards the three groups are separated from each other by forming bands of increasing skewness with decreasing grain size. The first group (Group III) shows an initial decrease in skewness values towards slightly negative values (with decreasing mean grain size) before switching to an increasing trend outlining a V-shaped pattern. This trend reflects the fact that the island's southern (land side) beaches which are mainly negatively skewed are bounded northwards by coarser, symmetrical to slightly positively skewed sediments and southwards by finer, positively skewed sediments. Away from this initial sub-group, skewness increases once again with decreasing

mean grain size. The trend does not differ in the successive groups. These groups have been identified by the fact that they form clusters of areally separated sediments, i.e. the interchannel and southern flank facies, here denoted as groups II & I, respectively. The line of lowest skewness values in Fig. 5-8 depicts the landward increasing positive skewness, as observed earlier (Chapter 4). FOLK & WARD (1957) show the relationship as being strongly sinusoidal and not linear. This, however, is not a discrepancy, but an artefact of the grain size range investigated. Their data had a larger grain size range (-3 to +3 phi). The mean grain size range of 2 - 3.5 phi in their study shows a similar skewness relationship as observed above.

The scatter diagram of kurtosis against mean represents the first case in which the pattern in the relationship is both difficult to determine and to interpret. The pattern becomes clear only upon drawing the boundaries between the groups (Fig. 5-9). The three sediment groups can still be distinguished, the kurtosis generally decreasing with decreasing grain size in groups I, II & IIIb. The sub-group IIIa shows an opposite trend, representing the subordinate group of samples with increasingly poorer sorting seawards of the island's backbarrier shore described in Fig. 5-5. The skewness-kurtosis relationship, by comparison, is not at all clear. The samples from the different groups do not form separate clusters (Fig. 5-10). Not unexpectedly, kurtosis generally decreases as the sediment gets more poorly sorted (Fig. 5-11). Since the textural relationships are inherently multidimensional, they should actually be viewed in three-dimensional plots. Thus, when considering the relationship between mean diameter, skewness and kurtosis, then it becomes clear that the poor grouping in the kurtosis/skewness plane is simply explained by the fact that the samples representing the individual groups, and which are separated in a three-dimensional projection, are here projected together onto a two-dimensional plane.

The same argument applies to the relationship between the sorting coefficient and the sample skewness, which can also not be understood without taking into consideration the relationship between sorting and the mean grain size. In Fig. 5-12 the scatter of skewness versus sorting may best be seen as being enveloped by a circle. The few samples falling outside of this circle actually belong to Group IIIa, a set of relatively poorly sorted ($\sigma > 0.35$) island dune samples which have been described earlier. In

this plot too, the sediment facies can not be recognised because of the two-dimensional superimposition of sample points separated in three dimensions. These results lead to the conclusion that in two dimensions only those scatter plots incorporating the mean diameter along one axis allow the recognition of sedimentary facies and their interpretation.

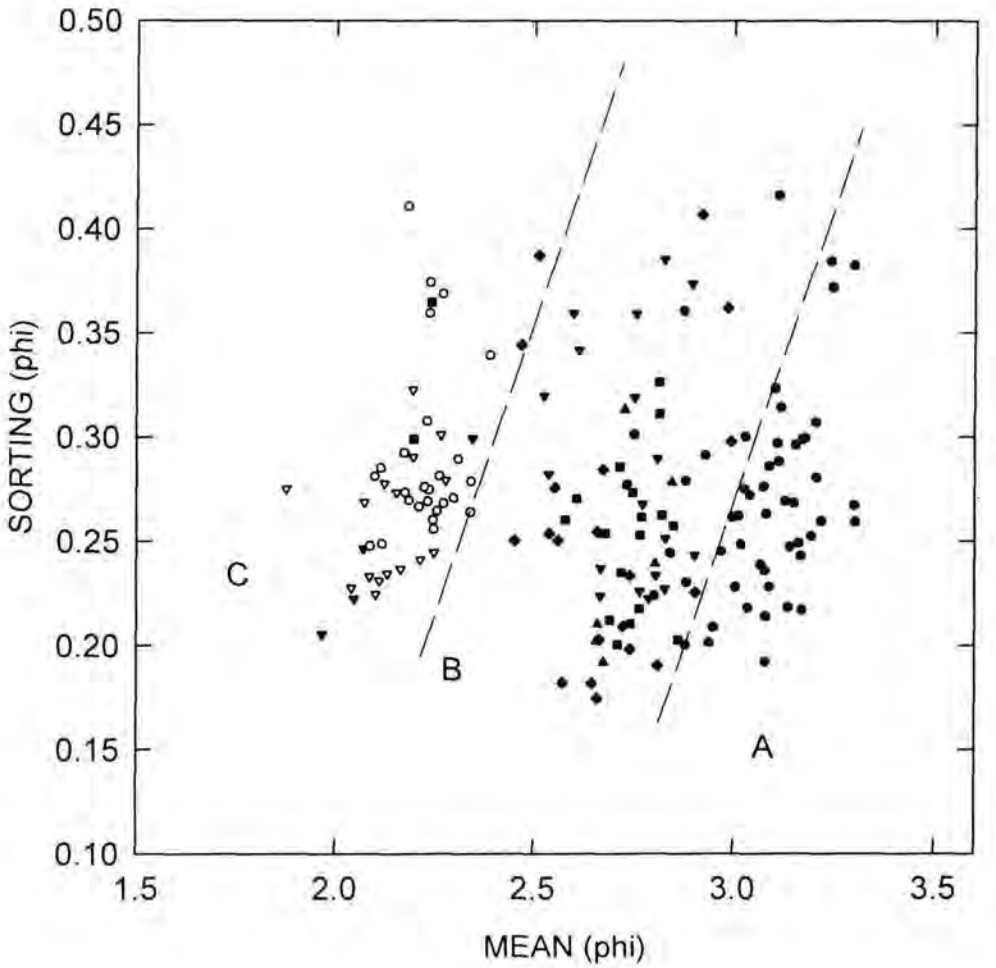

Fig. 5-7 Scatter plot of the degree of sorting against the mean grain size. The same facies as in Fig. 5-6 are identified.

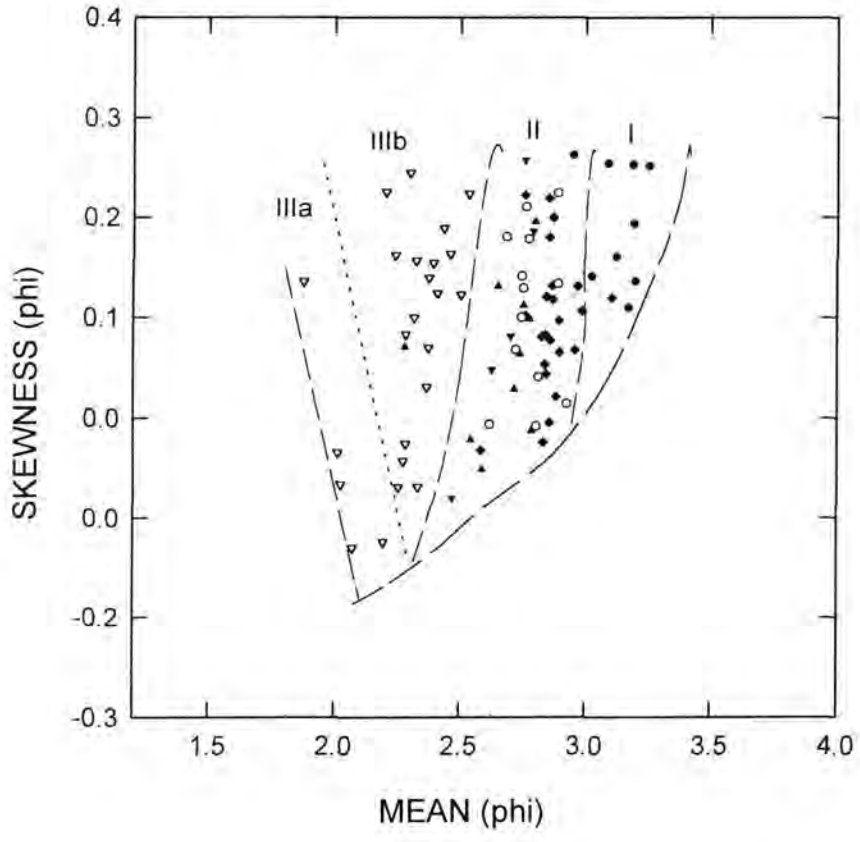

Fig. 5-8 Scatter plot of the sediment skewness against mean size. The three facies defined above are evident. In each of the groups the skewness increases towards more positive values as the sediment becomes finer landwards.

5.2.3 Implications of the energy gradient

If the inferred shore-normal energy gradient is interpreted to represent a shore-normal mean flow velocity gradient, then the farther away from the mainland coast an E-W oriented channel is situated the higher its flow velocity must become. A similar interpretation was made and confirmed by FLEMMING et al. (1992) for two tidal channels of the central area (Swinn- and Mittelbalje). Given that overbank flow velocities decrease away from the channel centre, then minimum flow velocities are

expected halfway between two adjacent channels (separated by an even topography), thus giving rise to two equal but opposite energy gradients. However, as already discussed, the mean flow velocity of a northern channel is higher than one situated south of it. The energy levels between such channels will therefore to a large extent be controlled by the northern channel, whereby a single energy gradient with or without subdivisions may result, as pointed out earlier. This fact is best demonstrated

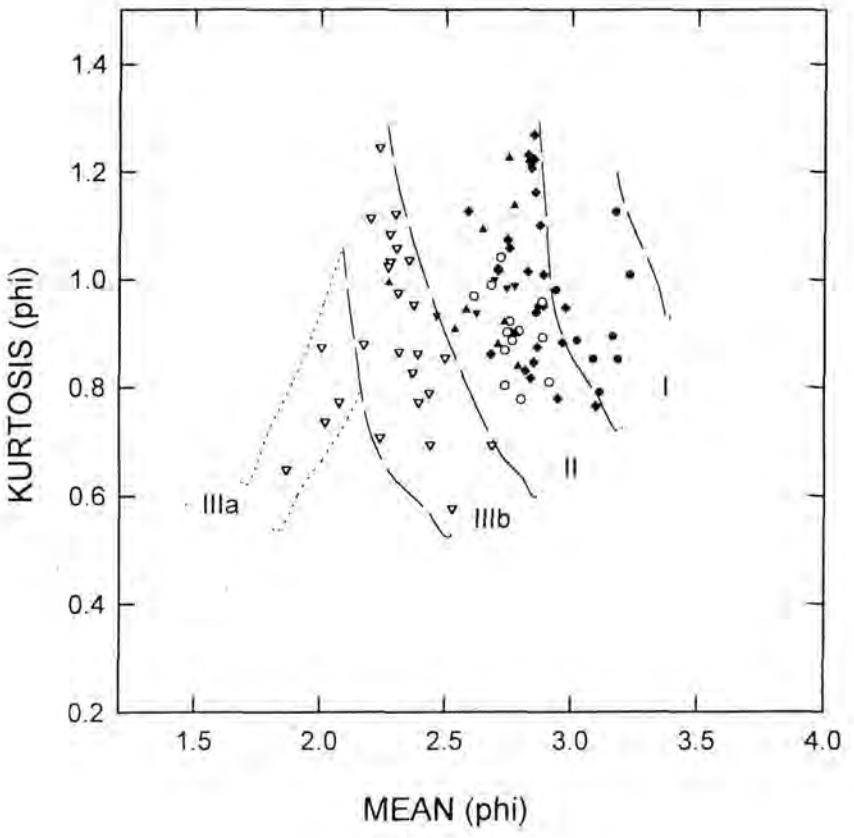

Fig. 5-9 Scatter plot of kurtosis against the mean grain size. The three groups are evident upon drawing physiographic boundaries. Generally, there is a group-wise decrease in kurtosis with the landward fining of the sediment.

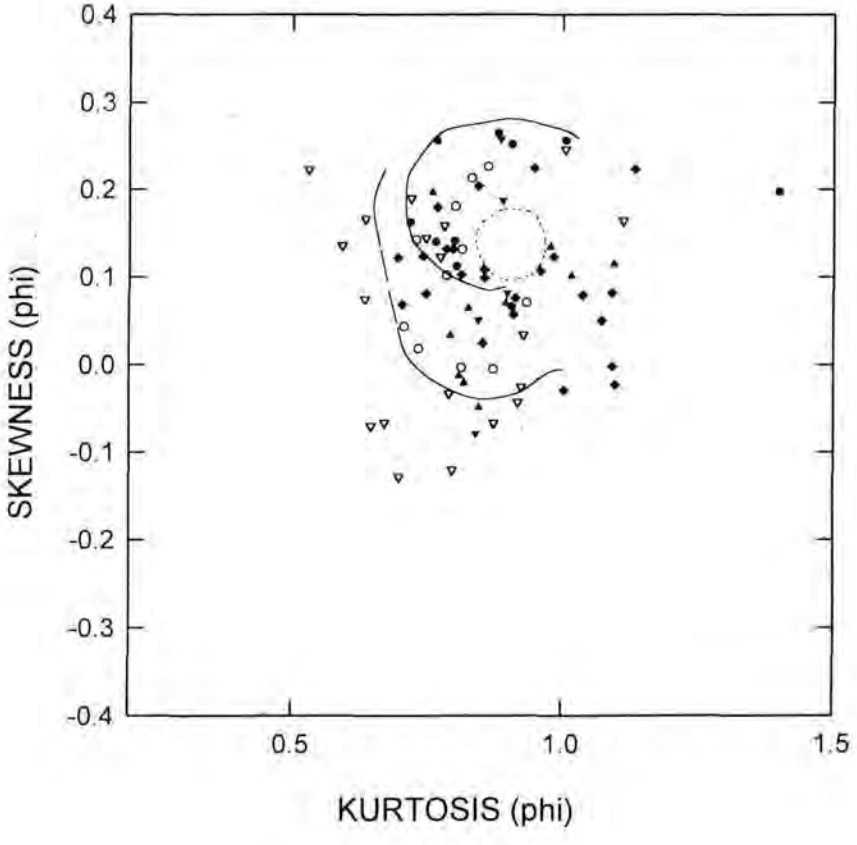

Fig. 5-10 Scatter plot of skewness against kurtosis. No separate clusters have been formed. The groups appear to plot in circular envelopes.

by the consideration of the flow kinetic energy. Since kinetic energy is proportional to the square of the flow velocity, which from the linear regression deduced earlier, is itself an exponential function of the distance to the base of two ($V = 2^{-kX}$), then the kinetic energy is still a stronger exponential function of the distance. This means that a channel with lower flow velocities than its neighbouring, more northerly situated channel will have a weaker influence due to the exponential energy loss than would have been the case if the loss was linear.

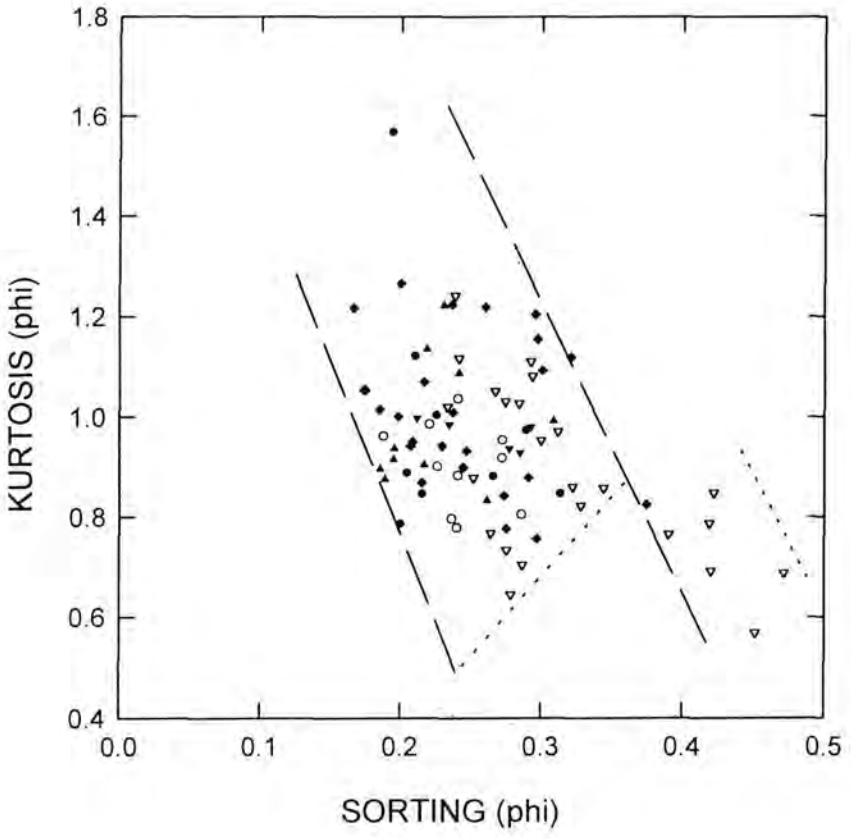

Fig. 5-11 Scatter plot of kurtosis against sorting. Kurtosis generally decreases with increasing poorer sorting of the sediment.

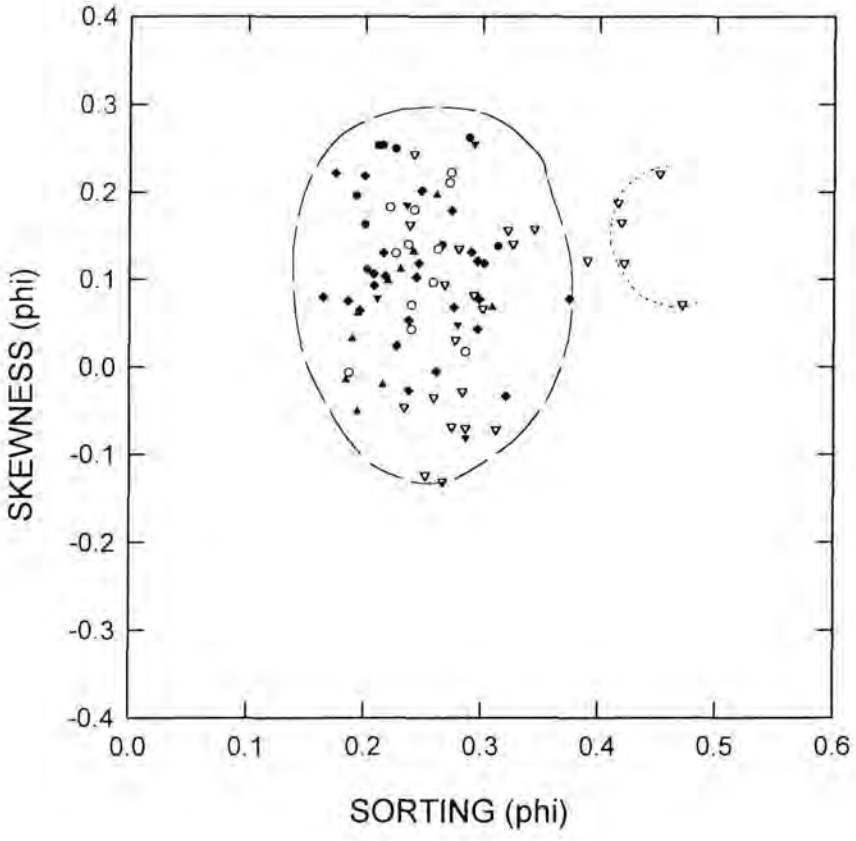

Fig. 5-12 Scatter plot of skewness against sorting.

5.3 Transport modes and depositional processes

5.3.1 Transport modes

In sections 5.2.1 and 5.2.2 three depositional environments have been suggested. When plotted on a modified C-M diagram (FLEMMING, 1977) the three sediment facies show two transport modes (Fig. 5-13). Facies A sediments which are deposited nearest to the coast (along the dyke) are very fine ($>$ 3.0 phi), very well sorted ($\sigma <$ 0.35Φ) and positively skewed (SK $>$ 3Φ). These are transported mainly in uniform suspension. This explains why the very fine sediments are distributed largely in

sheltered and high elevation areas. Facies B & C sediments are fine grained (2 - 3 phi), well to very well sorted and slightly positively skewed (SK < 3Φ). These sediments, which occupy the central interchannel and the northern flank (island margin of the tidal flats) regions, are transported in graded suspension, with the slightly coarser flank (facies C) sediments being transported closer to the bottom.

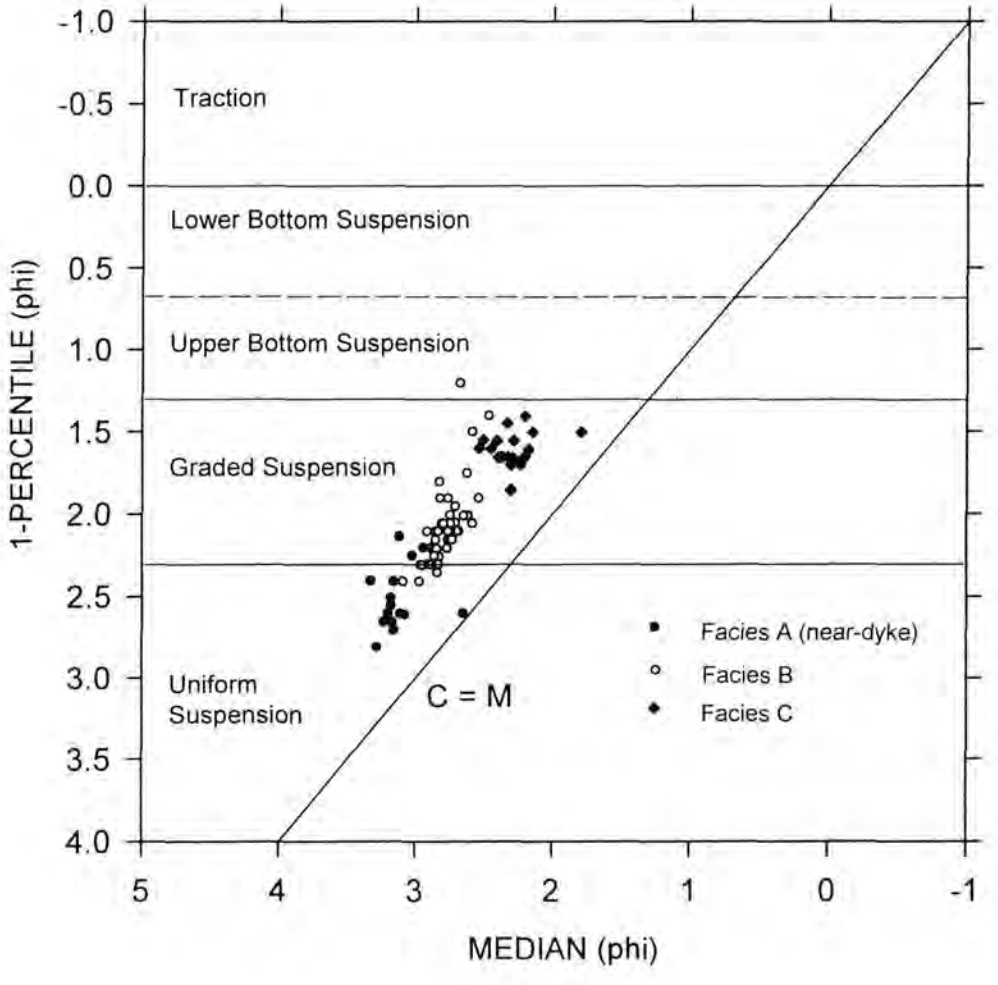

Fig. 5-13 Transport modes of the Spiekeroog bakbarrier sediments as defined by the modified C-M diagram (FLEMMING, 1977).

5.3.2 Transport sorting and mixing processes

Studies of the grain size trends are widely used to determine transport pathways (McLAREN, 1981; McLAREN & BOWLES, 1985; GAO & COLLINS, 1992; 1994). Empirical knowledge of how a given set of parameters change along a transport path is a precondition for the genetic interpretation of grain size trends. The shape of the frequency curve has been shown to be very useful in identifying sorting and mixing processes along a transport path (FLEMMING, 1977; 1988). This, in effect, amounts to the analysis of grain size modes. Progressive sorting is characterised by a progressive fining or coarsening in a unimodal sediment. The presence of more than one mode in a grain size distribution curve indicates mixing between two or more populations. In a classical mixing situation between two normally distributed hydraulic populations, one consisting of finer and the other of coarser material, e.g. fine sand and medium sand, the coarse population decreases in its proportion along the transport path while the finer population shows the reverse (FOLK & WARD, 1957; FOLK & ROBLES, 1964). In the absence of progressive size sorting processes there is no shift in the modes along the transport path. Having identified three spatially separate sediment facies in the study area, it is investigated in this section how these sediments might mix or become progressively sorted along their transport directions.

5.3.2.1 NW-SE along the main tidal channel

Along the main tidal channel (Schillbalje) connecting to the inlet both mixing and size sorting processes are depicted (Fig. 5-14). Starting with sample W_{10} representing the inlet throat region, which is marked by large depths and coarse sediments, its mode lies at about 1 phi. As the flow velocities (ebb jet) decrease seawards of this point the sediment becomes finer (Fig. 5-15 (a)). However, the small proportion of finer material (Mode about 2.7 phi) which was originally present in the source sediment is totally eliminated. This indicates that the energy level, though lower than in the throat area is still too high for the deposition of this secondary mode of finer material.

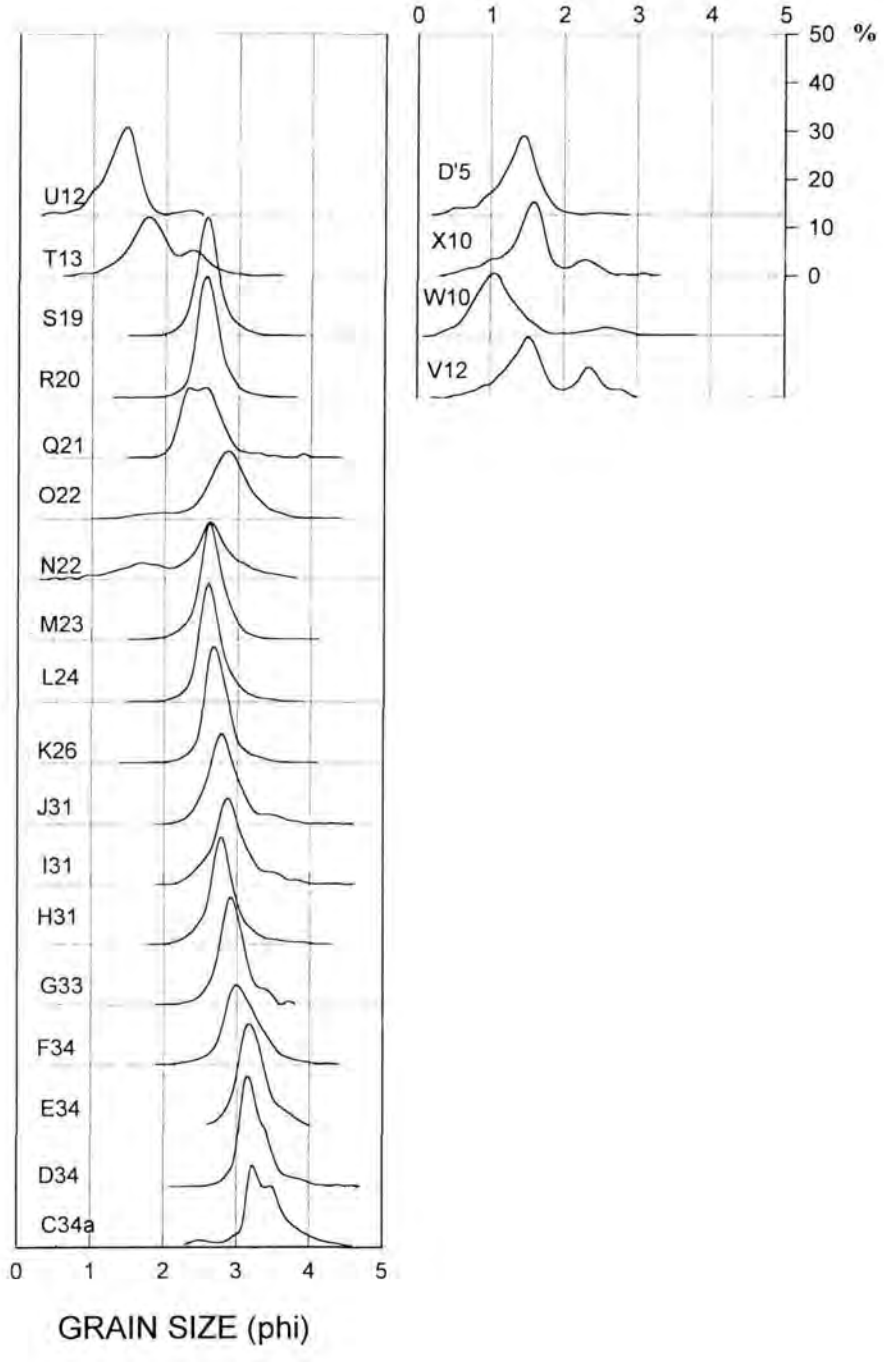

Fig. 5-14 Grain size curves along the main channel (Schillbalje) of the Otzum Balje. Both progressive size sorting (progressive shift of the mode) and mixing (more than one mode) processes are observable. See Fig. 5-24 for the profile position.

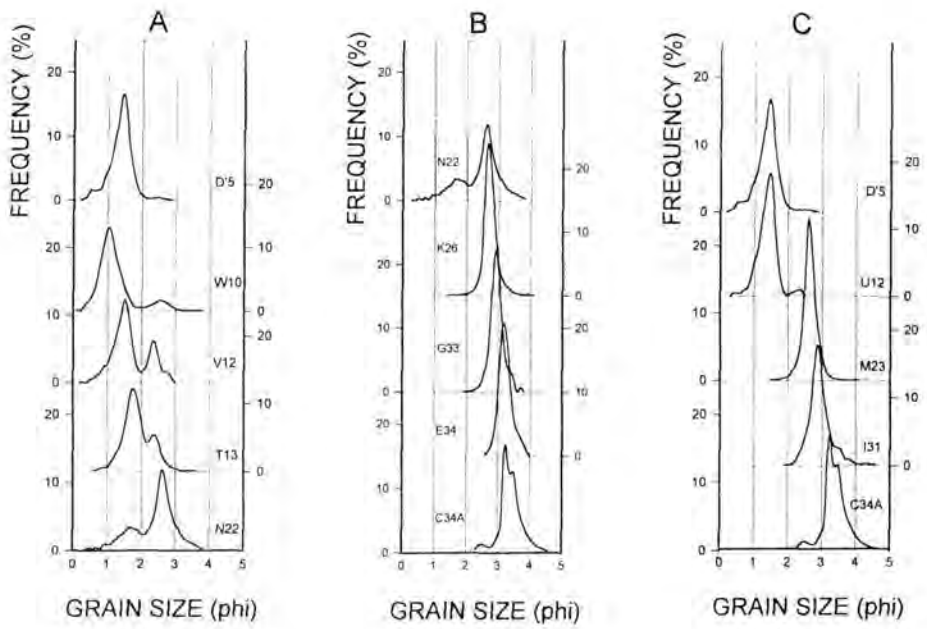

Fig. 5-15 Progressive sorting and mixing processes along Schillbalje (main tidal channel). A:- Progressive size sorting of the primary mode is observed landward and seaward of the throat area (W_{10}) whereas mixing with a secondary mode is observed between W_{10} and N_{22}; B:- Progressive size sorting of the secondary mode landward of N22; C:- How insufficient sampling density may affect the interpretation.

Landward of position W_{10} the primary mode of coarse sediments becomes progressively finer and less abundant and is almost non-existent at N22 (Fig. 5-15A). The secondary mode, on the other hand, initially increases in proportion landwards, but without any obvious size sorting (Fig. 5-15A). Progressive size sorting commences landward of N22 (Fig. 5-15B). This shows two things: firstly, the minor mode, which makes up the bulk of the main channel samples (samples N22 - S19), has undergone progressive mixing with the progressively sorted primary source sediment from the inlet gorge (inlet throat area). Secondly, after the secondary mode has become the only constituent of the sediment, it also undergoes progressive size sorting. This means that the decreasing energy from the source initially leads to the progressive fining of the coarse mode, while at the same time the proportion of the

finer mode increases. As the energy decreases further down-stream to a level where the primary mode can no longer be transported, progressive size sorting of the finer mode begins. These results clearly discriminate between miscible and immiscible facies. The near-dyke facies (facies A), which is essentially finer than 3 phi, does not mix with any of the other facies. These latter facies result from progressive size sorting of interchannel sediments (facies B) which have their modes typically between 2.5 and 3 phi. The interchannel sediments, on the other hand, are progressively mixed with sediments from the inlet gorge. Both progressive size sorting and mixing processes are thus responsible for the grain size distributions along the Schillbaje channel.

It is important to note, however, that in order to sufficiently resolve the mixing and size sorting trends along a transport direction a dense sampling grid is necessary. This is demonstrated in Fig. 5-15C in which a comparison of widely spaced samples entirely miss the mixing section along the profile.

5.3.2.2 N-S across the shore

This profile, running N-S through the central part of the backbarrier area clearly exhibits progressive size sorting from north to south (Fig. 5-16A). With the lack of a well established N-S transport mechanism this indicates the presence of a latitudinal energy differentiation related to an E-W channel network as established in the previous chapter. Along this transect mixing is very subordinate, being only observed along the backbarrier side of Spiekeroog island (Fig. 5-16B) where very fine sands mix in small quantities with the island (northern flank) sediments. Figure 5-17 further shows that the shift in the modes along this transect is not as intense as observed in the case of the Schillbalje. It also shows the existence of three energy zones with different energy gradients, as indicated by the different degrees of modal shifts, thereby confirming the energy compartments deduced in section 5.2.1. The mean, sorting and skewness trends along the transect are presented in Fig. 5-18. The mean shows a clear landward fining trend which corresponds to the landward decrease in the energy level. In correspondence with the decreasing energy level, the sorting also

becomes better with the landward fining of the sediment. The skewness variation reflects the spatially fluctuating nature of the energy level brought about by the energy contrast between channels and tidal flats or simply topographic variations. These trends are consistent with the transport sorting processes.

5.3.2.3 E-W along the tidal channels

It is by now clear that two strong energy gradients, one along the main tidal flow direction and another generally normal to the shore, exist in the study area. However, it is interesting to note that there is no marked energy gradient along the tidal channels feeding the main inlet channel. This trend is shown in Fig. 5-19 in which the frequency curves along a shore-normal transect are plotted alongside those along a tidal channel. If an E-W energy gradient exists at all, it is effectively masked by the much stronger N-S gradient.

5.3.2.4 Ebb and flood tidal channels

The energy level variations in the channels are not restricted to transport directions only. Instead, channel banks and central channel regions show marked energy differences. Flood- and ebb-dominated channel sections commonly observed in wide tidal channels may exhibit different characteristics from one another due to tidal asymmetry. In the Otzum tidal inlet the tides show both time and velocity asymmetries. The available sedimentological data has been assessed to find out whether there is an imprint of this velocity asymmetry.

By plotting the mean grain size at their geographic locations along several cross-channel transects, a definite trend (Fig. 5-20) was obtained. Profiles D' and Z from the narrow inlet throat region depict each a single grain size maximum occupying the channel centre. But along the widest region of the main channel (profiles U & T) two well defined zones of coarse grain sizes are observed. The grain size coarsens from

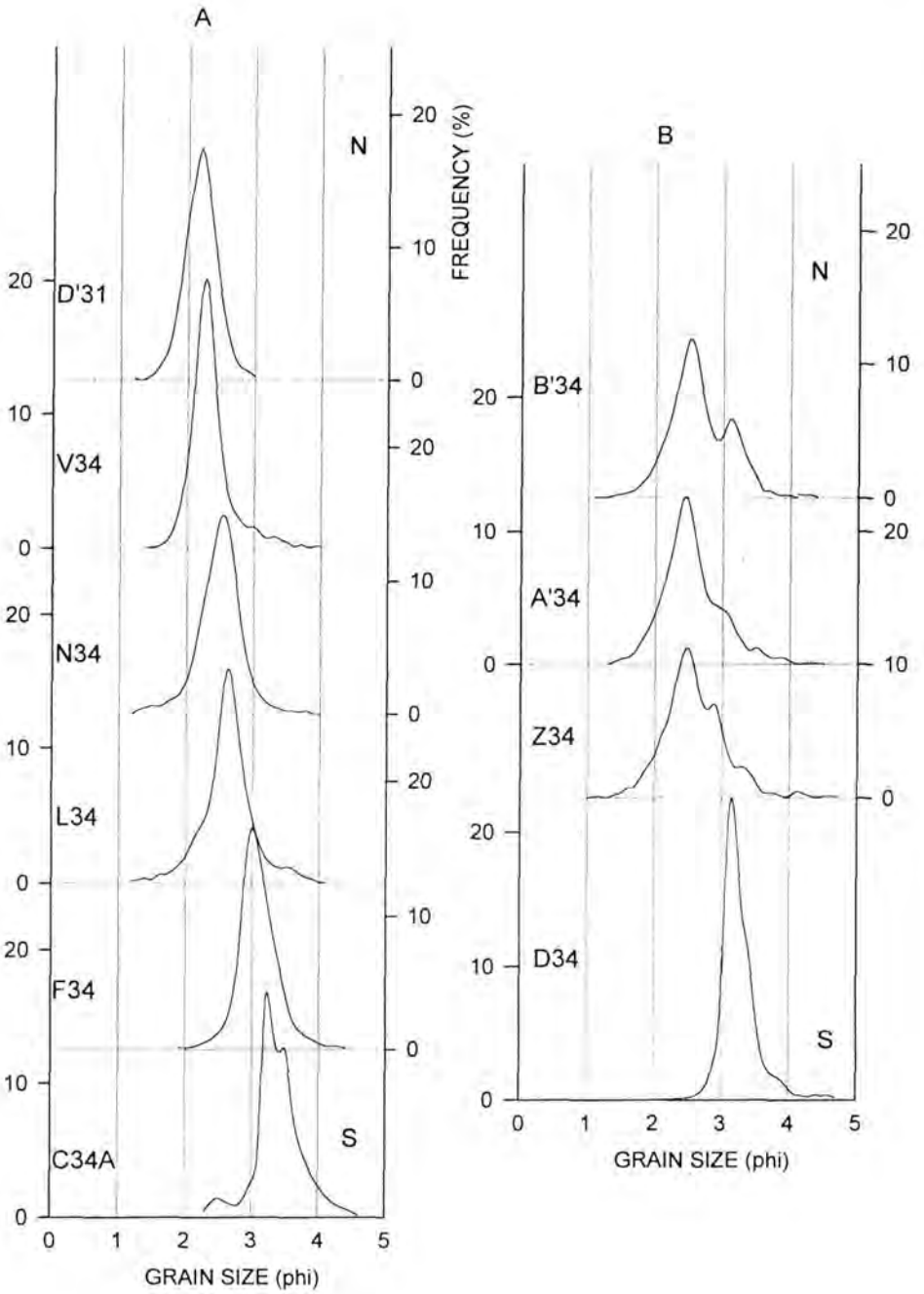

Fig. 5-16 Grain size curves along a N-S transect, P34 (ref. Fig. 5-24). The general trend indicates a clear progressive size sorting (A) with a subordinate mixing along the backbarrier beach of Spiekeroog (B).

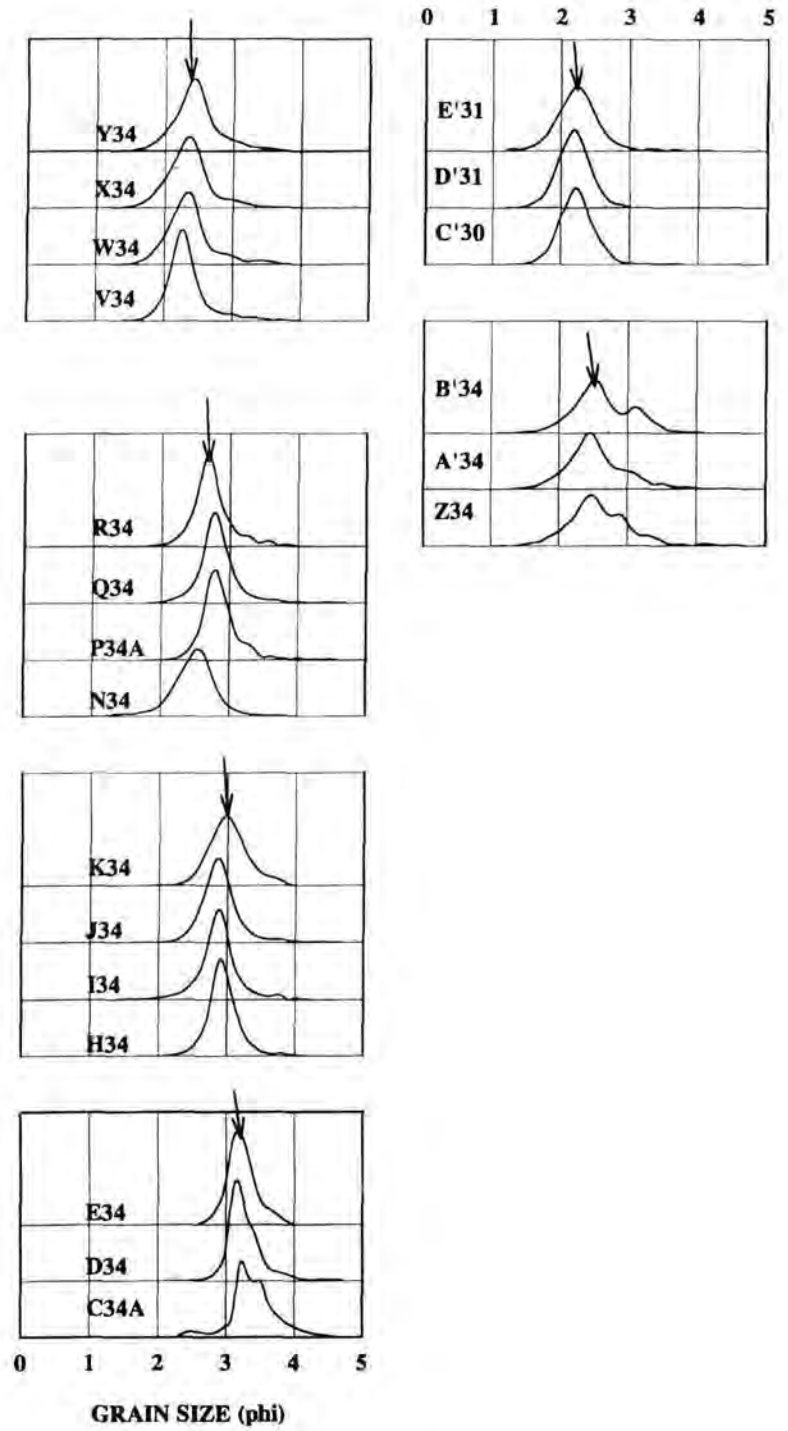

Fig. 5-17 N-S grain size curve groupings according to the varying degrees of modal shifts (along P34) reflecting the existing energy zones.

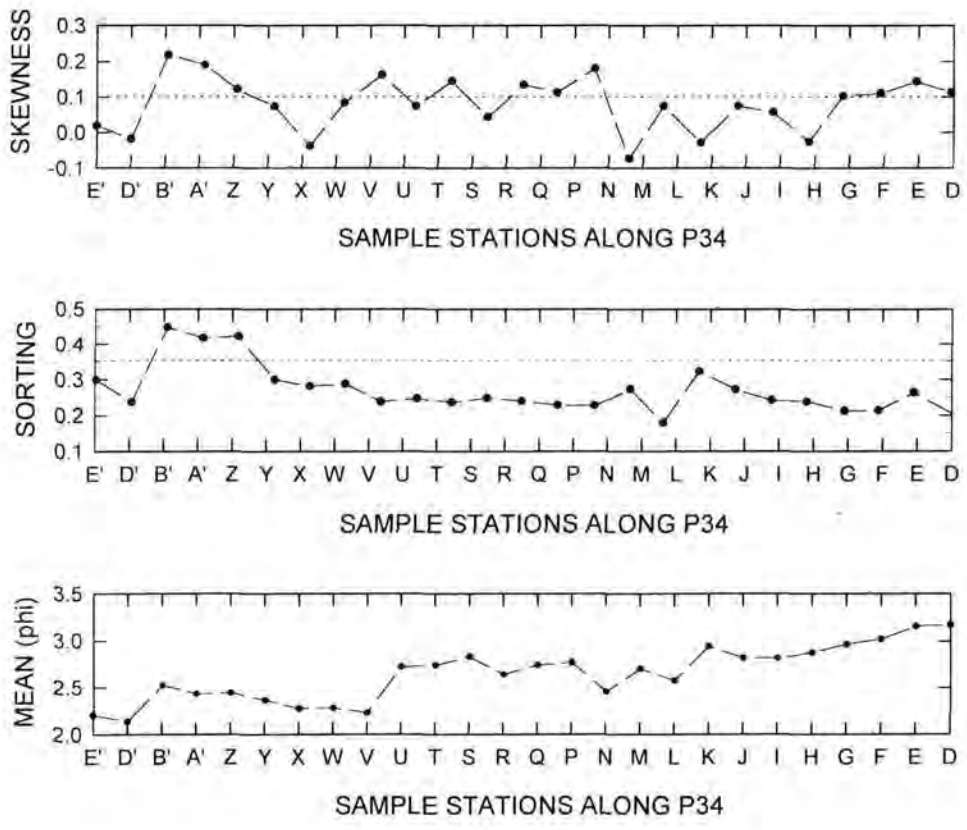

Fig. 5-18 Mean, sorting and skewness trends normal to the shore (profile P34 on Fig. 5-24) across the backbarrier area of Spiekeroog. The trends show consistency with the transport sorting processes.

the flanks towards the centre of the channel. The maximum values are separated by a zone of finer grain sizes occupying the channel's central axis. The zones of coarsest grain sizes correspond to zones of high energy which are interpreted as representing the zones of ebb and flood flow paths or channel sections. Despite the fact that there are no distinct flood and ebb channels evident on the bathymetric chart, the effect of coriolis force would generally result in the flood flows becoming intensified towards the western part of the channel and ebb flows to the east (coriolis force acts to the right of the flow direction in the northern hemisphere). This seems to be a plausible

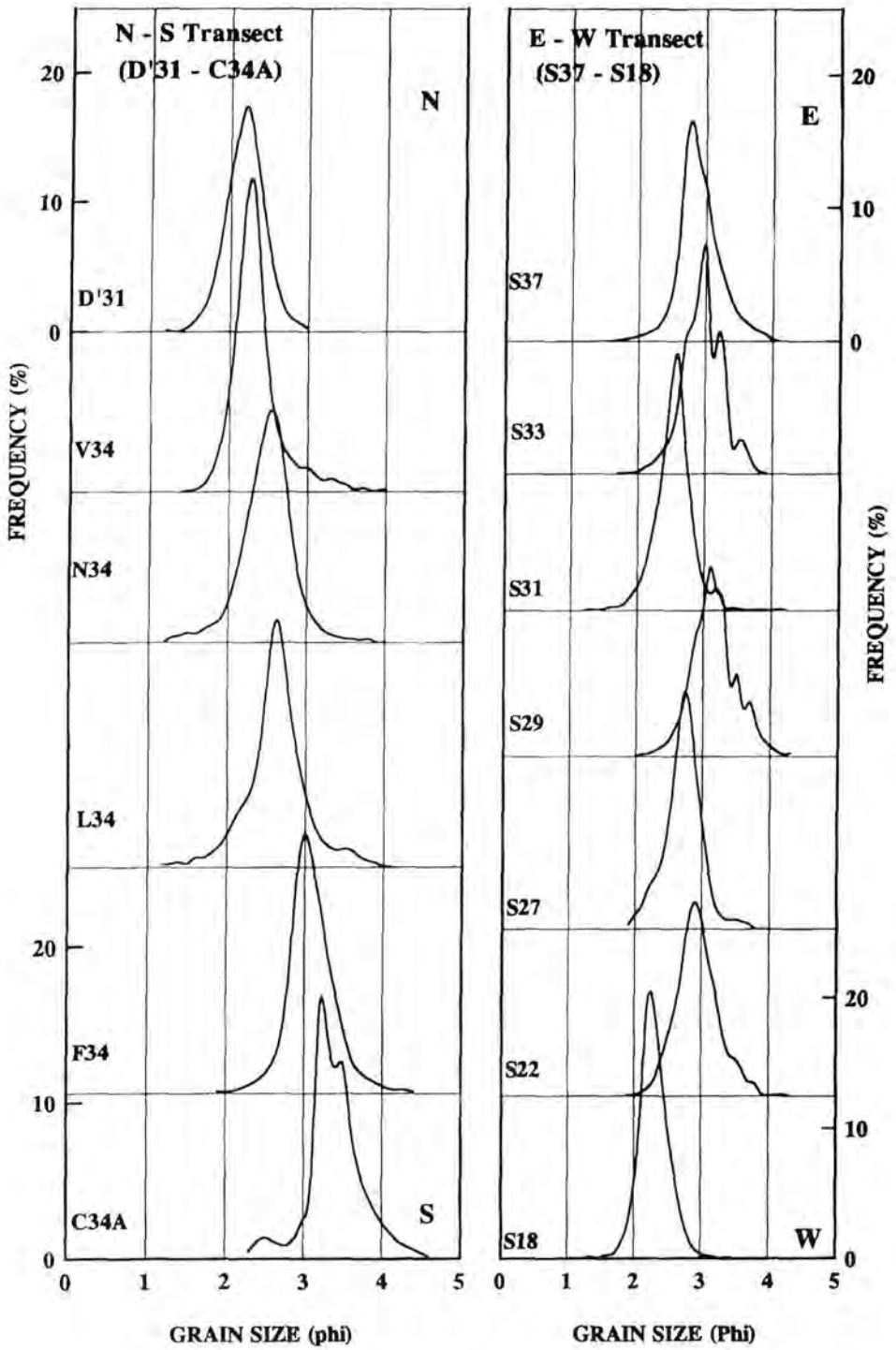

Fig. 5-19 Comparison of the grain size curves along a N-S, shore-normal transect with an E-W transect (ref. Fig. 5-24). The modal shift is clearly stronger normal to the shore, indicating a stronger energy gradient in this direction.

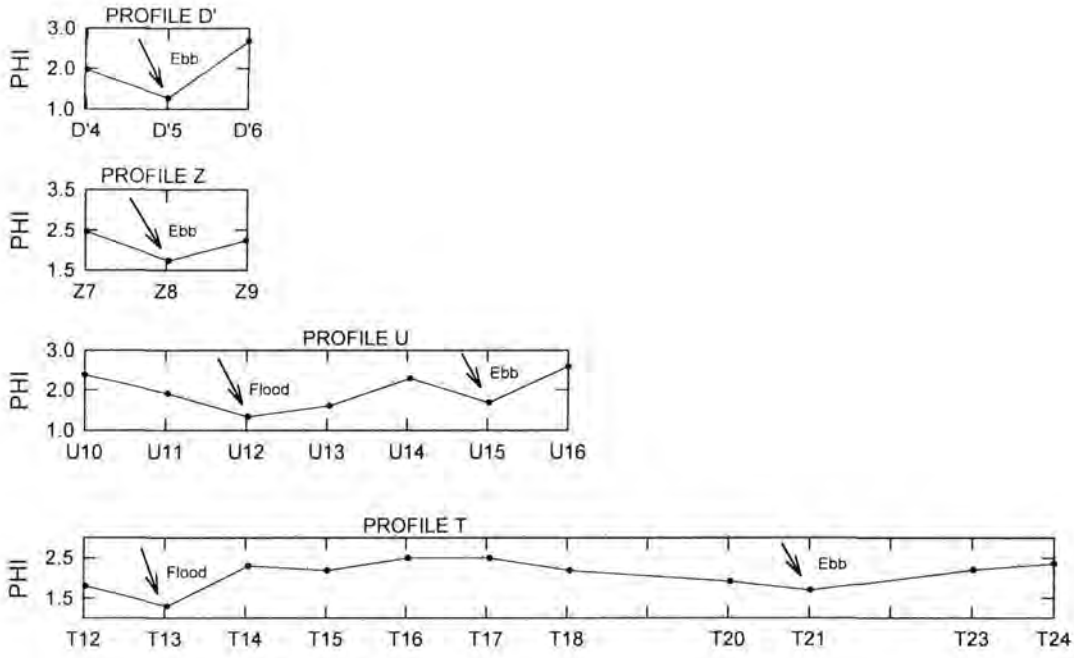

Fig. 5-20 Mean grain size trends across the main channel (Schillbalje). Coarser sediment zones represent ebb- and flood-dominated channel sections, located to the east and west sides of the inlet, respectively. The profile positions are shown on Fig. 5-24.

explanation of the grain size trends across the widest section of the main channel (inlet).

Most of the flow measurements made at various stations in the main channel (Schillbalje) reveal the velocity asymmetry with dominant flood currents (faster) (Fig. 5-21). This feature is reflected in the sediment distribution by the occurrence of coarse sediments in the flood channels (western flank) and relatively finer in the ebb channels (eastern flank). There is thus clear evidence for the imprint of tidal asymmetry in the channel sediments.

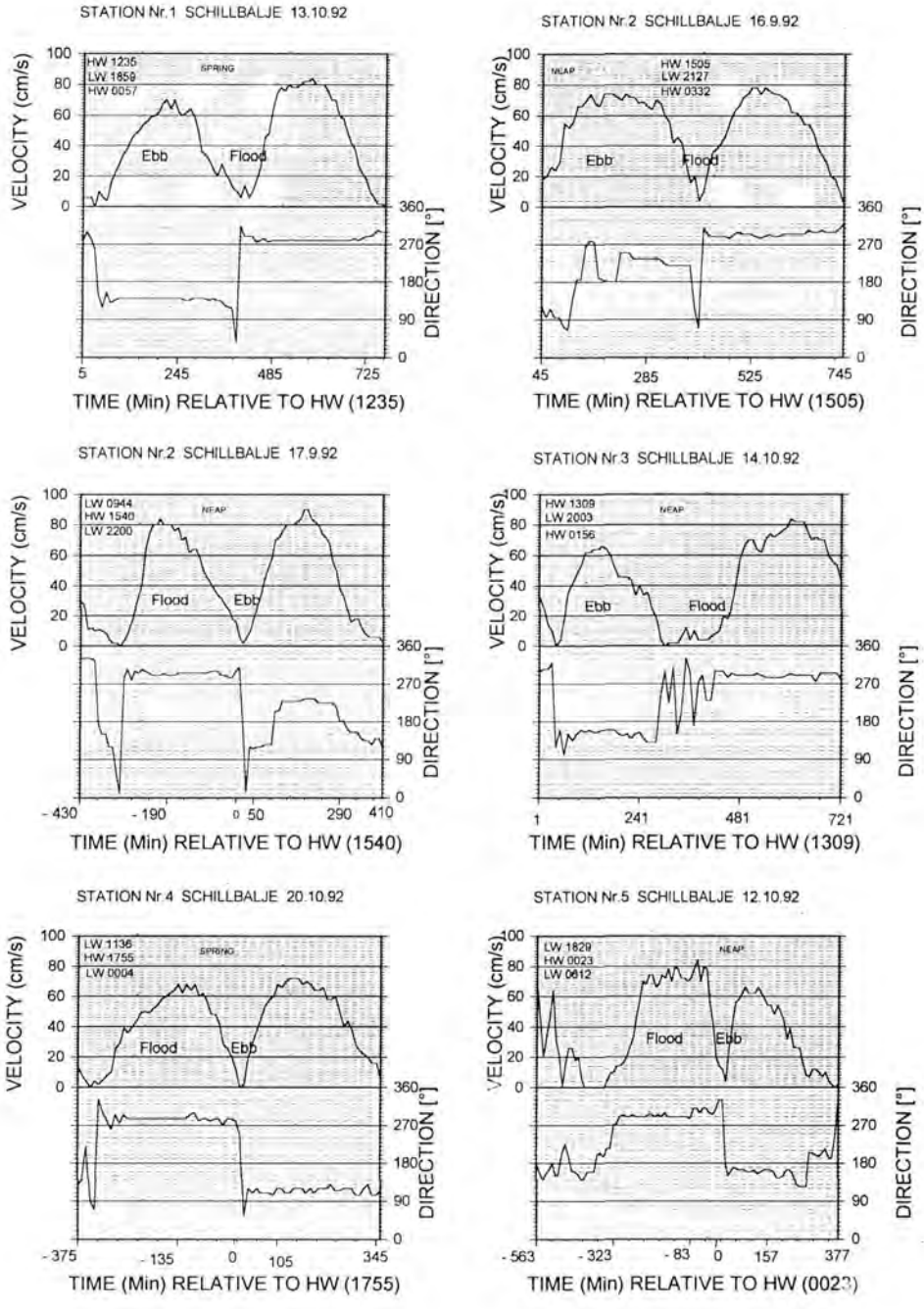

Fig. 5-21 Tidal flow strengths at various locations along the Schillbalje channel (ref. Fig. 5-24). Velocity asymmetry is clearly evident at all stations. In wider channels, where flood and ebb channels are separate, such velocity asymmetry would result in different sediment textures between the channels and the intervening region.

5.3.2.5 Mixing of hydraulic energy levels

The physical motor for progressive size sorting and mixing processes lies in the hydrodynamics. The hydraulic process leading to the commonly observed progressive size sorting from source to deposit or simply along any section of the transport path has, amongst others, been explained by the summary model of McLAREN (1981). The major requirement is a change in hydraulic energy along the flow path. As the energy decreases down-stream, the capacity of the flow medium to carry coarse (correspondingly heavier) material decreases and, as a result, the material in transport becomes progressively finer (lighter). Sediments successively deposited in the course of this process show the progressive size sorting trend. This is exemplified by many fluvial systems.

Reversing currents in tidal environments are accompanied by large variations in the turbulent energy over short periods of time, say over half a tidal cycle. At high flow velocities (high energy levels) only the coarse sediment is deposited, whereas relatively finer sediment is deposited at lower flow velocities. Where two different energy levels occur, each of which favouring deposition of sediment of a different modal size class, sediment mixing is expected. The following situations are typical of the backbarrier region:

a) Velocity asymmetry of the tides.
b) Differences in strength between spring and neap tidal phases.
c) Differences in flow strengths during strong and calm weather conditions
d) Separation of food and ebb flow paths.
e) Physiographic influences such as embayments and around newly erected structures inducing different set of hydrodynamic conditions.

5.4 Longshore energy gradient

It is well known that variations in longshore currents, rip currents and wave intensity produce variations in sediment dynamics along a shore (e.g. KOMAR, 1976). The

grain size patterns should, therefore, reflect the energy conditions prevailing at various sites. To assess the energy conditions along the Spiekeroog backbarrier shore the grain size trends along the shore were analysed. Figure 5-22 shows a summary grain size trend along the backbarrier shore of Spiekeroog. Regions with differing grain size trends are clearly identifiable with distance along any given longshore direction. Their boundaries correspond with the zones of erosion and accretion (deposition) established through the mass balance analysis (chapter 3). Whereas the zones of deposition are characterised by mean grain sizes which are essentially finer than their surrounding areas (backbarrier source), erosion zones are marked by coarser grain sizes (overwash source). The sorting deteriorates from the zones of erosion towards deposition zones. The skewness changes in such a way that zones of deposition are made up of exclusively positively skewed sediments while erosion zones are negatively skewed.

An examination of the grain size frequency curves along the transect (Fig. 5-23) simplifies the interpretation of these patterns. Firstly, there is a very weak shift in the primary mode, indicating that progressive size sorting is not very pronounced (weak energy gradient). Secondly, the curves show that deposition zones are characterised by population mixing between the primary mode of the beach-derived overwash sands (mode coarser than 2.5 phi) and a finer mode of backbarrier-derived sands (mode finer than 3.5 phi). Whereas the primary mode experiences a westward progressive fining from 2.25 phi at the eastern margin of the island (western bank of Harle inlet) to 2.5 phi in the embayment to the western reaches of the Ostplate, the secondary mode of finer sediments shows a progressive increase in proportion. The evolution of the mean grain size pattern from west to east is thus produced by a combination of both progressive size sorting (westward fining of the primary mode) and mixing with a finer mode. Where mixing occurs, the mean grain size becomes excessively fine, the sorting poorer and the skewness more positive, thus accounting for the trends illustrated in Fig. 5-22. The negative skewness of the erosion zones, on the other hand, is a result of winnowing of fines in the course of overwash.

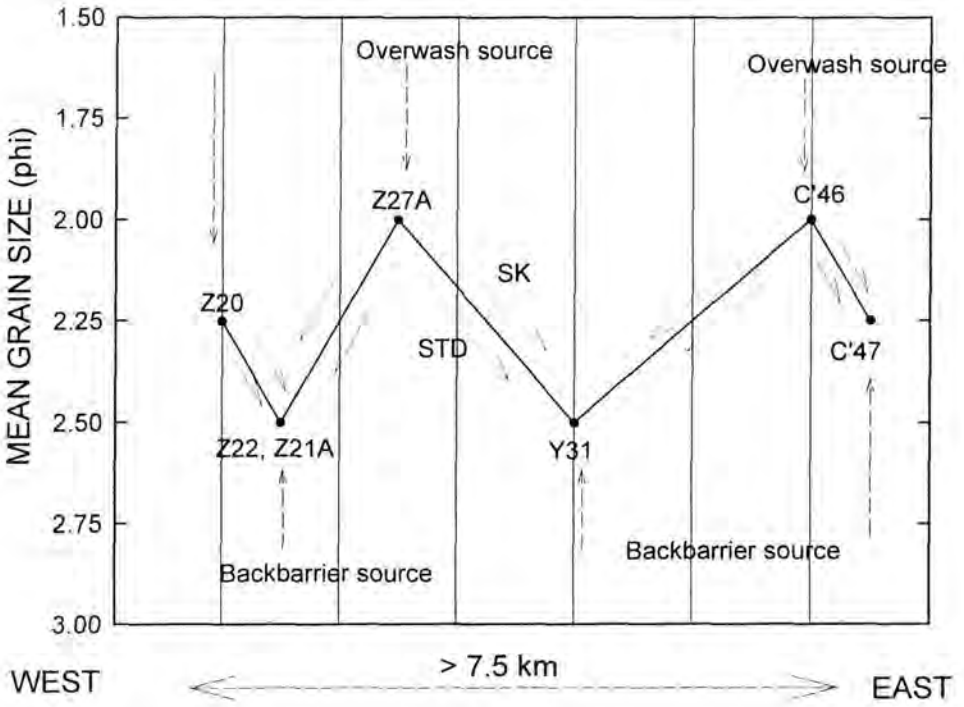

Fig. 5-22 Grain size trends along Spiekeroog backbarrier shore (ref. Fig. 5-24). Sediments from overwash and backbarrier sources are represented by the peaks and troughs, respectively. They also correspond to the erosion and deposition zones identified by mass balance analysis (chapter 3).

The skewness evolution from negative values in the zones of erosion towards positive values in the deposition zones reflects the source-deposit relationship between the two zones. This however, does not reveal the source of the fine mode (finer than 3.5 phi) which must be located some distance away. These finer sediments are typical of the tidal flats close to the mainland coast. Since they comprise very fine sands, they are transported in suspension and are thus easily moved around. Their deposition can therefore only take place at locations where favourable low energy conditions exist (less turbulent). Given the fact that coarse sediments along the backbarrier shore of the island are derived from the island beach by episodic overwash processes, the finer

sediments are deposited in the course of intervening low energy periods, when the upper backbarrier shore has a similar energy gradient as the mainland shore.

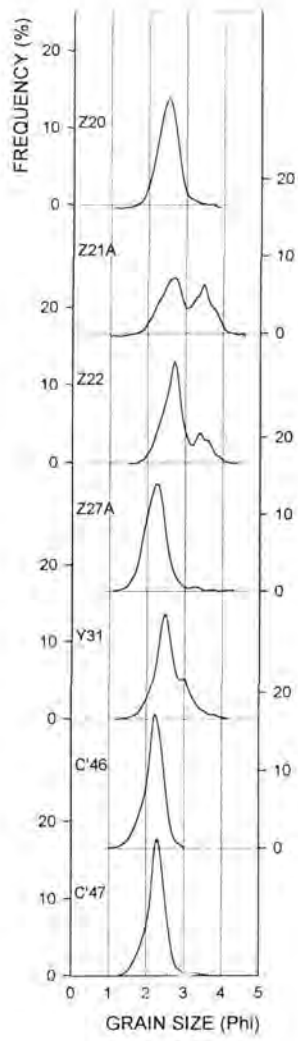

Fig. 5-23 Grain size curves along the Spiekeroog backbarrier shore (ref. Fig. 5-24). Regions of deposition are characterised by mixing between coarser, overwash-derived beach sands and finer, backbarrier-derived sediments. Progressive size sorting is not significant.

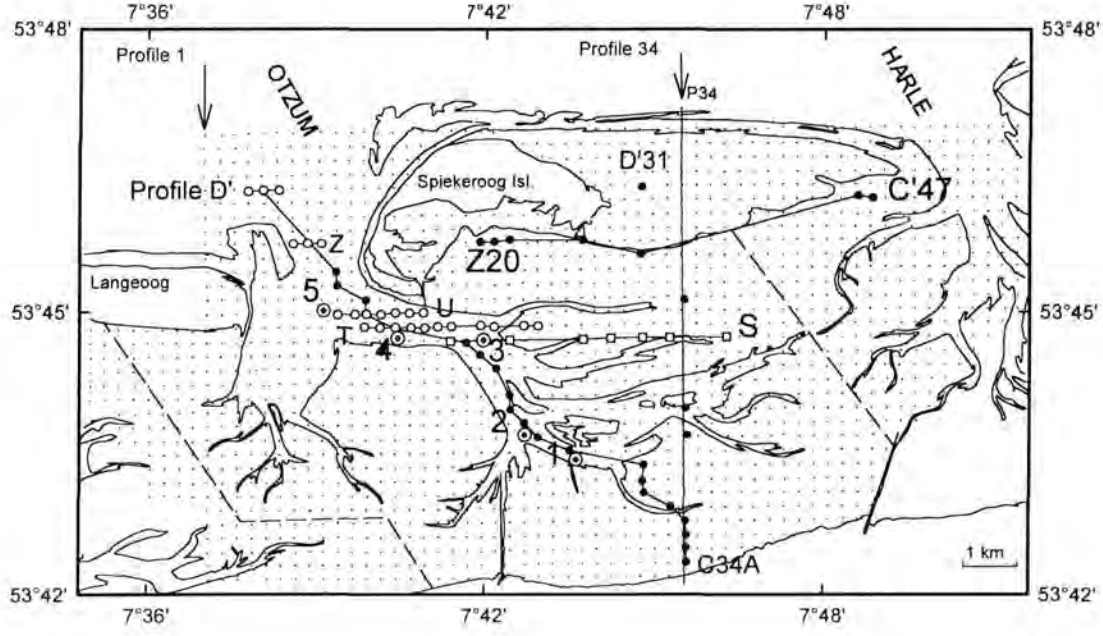

Fig. 5-24 Summary map of the positions of the profiles referred to in figures 5-14 to 5-23.

5.5 Rising sea level and the influence of man

Backbarrier systems commonly comprise depositional sequences that progress landwards from sand flats, followed by mixed flats, mud flats and finally culminating in extensive salt marshes (e.g. REINECK & SINGH, 1973; OERTEL, 1985). In contrast to natural backbarrier environments, the cross-shore depositional sequences along the southern North Sea coast has been interrupted by artificial sea dykes, construction of which commenced some 1000 yr. B.P. The continuing slow sea-level rise over the last 5000 years would normally have resulted in a progressive shift of the depositional sequence onto the coastal plain (Fig. 5-25). Along the southern North Sea, this shift has been curtailed by the dykes. As a result, the energy gradient has

been substantially steepened. This has led to the progressive elimination of the finest, most landward situated sediment facies (Fig. 5-26).

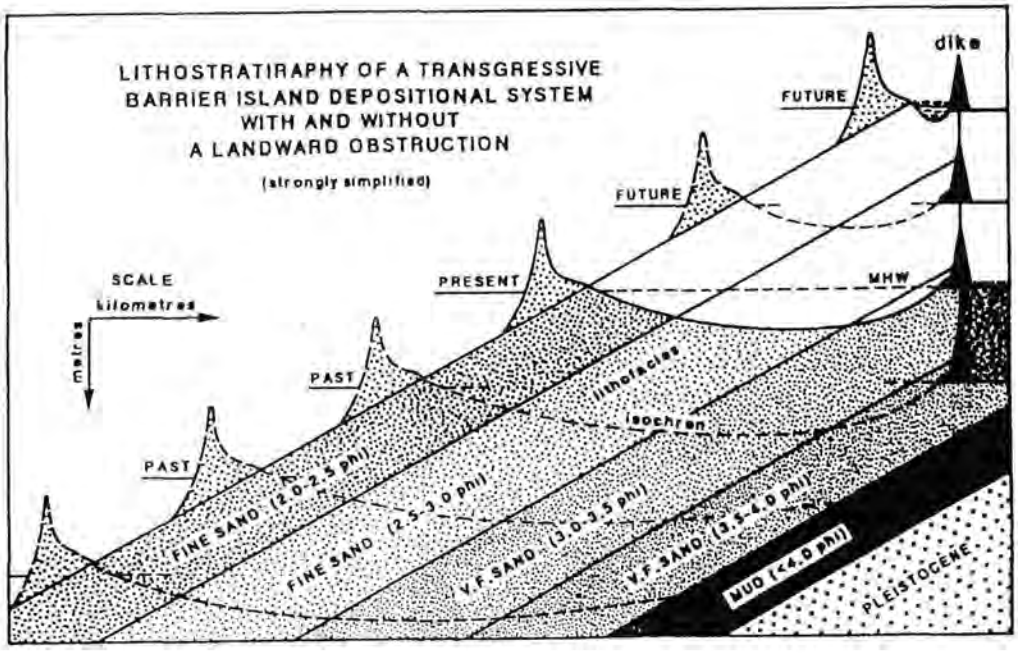

Fig. 5-25 The effect of dyking (schematised) on the lithostratigraphy of a transgressive barrier island depositional system (after FLEMMING & NYANDWI, 1994).

To test the proposed sediment elimination process, a comparison was made between the cross-shore percentage composition of various size fractions in the very narrow backbarrier tidal flats behind the island of Baltrum and the wide tidal flats behind Spiekeroog island (FLEMMING & NYANDWI, 1994). The difference is indeed striking (Fig. 5-27). In the Baltrum area the coarser very fine sand belt (3 - 3.5 phi) shows a much shorter seaward extension than the equivalent belt in the Spiekeroog area. More significant, however, is the fact that the sediments finer than 3.5 phi are almost completely lacking in the Baltrum near-dyke area. This means that the near-dyke energy level is higher behind Baltrum than in the Spiekeroog area, thus attesting to the observation that fine sediment elimination from the backbarrier area is the result of a steepening energy gradient in the wake of a rising sea transgressing against a dyked coast, associated with a narrowing of the island-coast distance.

The present facies distribution in the Spiekeroog backbarrier area (Fig. 5-26B) therefore represents an intermediate situation between a non-dyked coast (Fig. 5-27A) and the more advanced stage along the Baltrum coast.

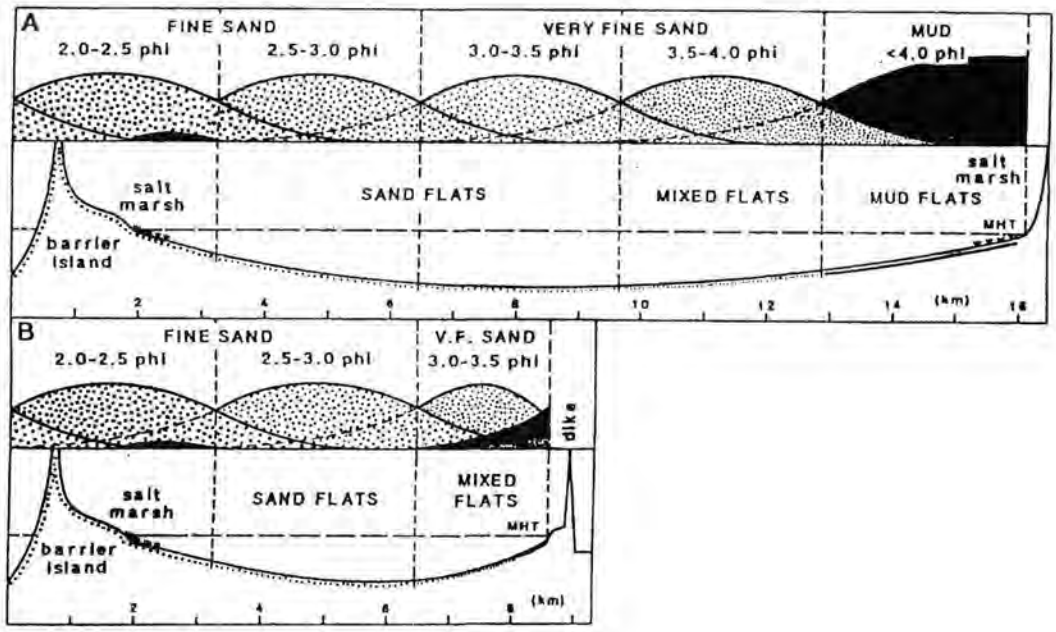

Fig. 5-26 Lateral facies sequence in the Spiekeroog backbarrier area. A) Schematic situation had the coast remained undyked. B) Present situation (after FLEMMING & NYANDWI, 1994).

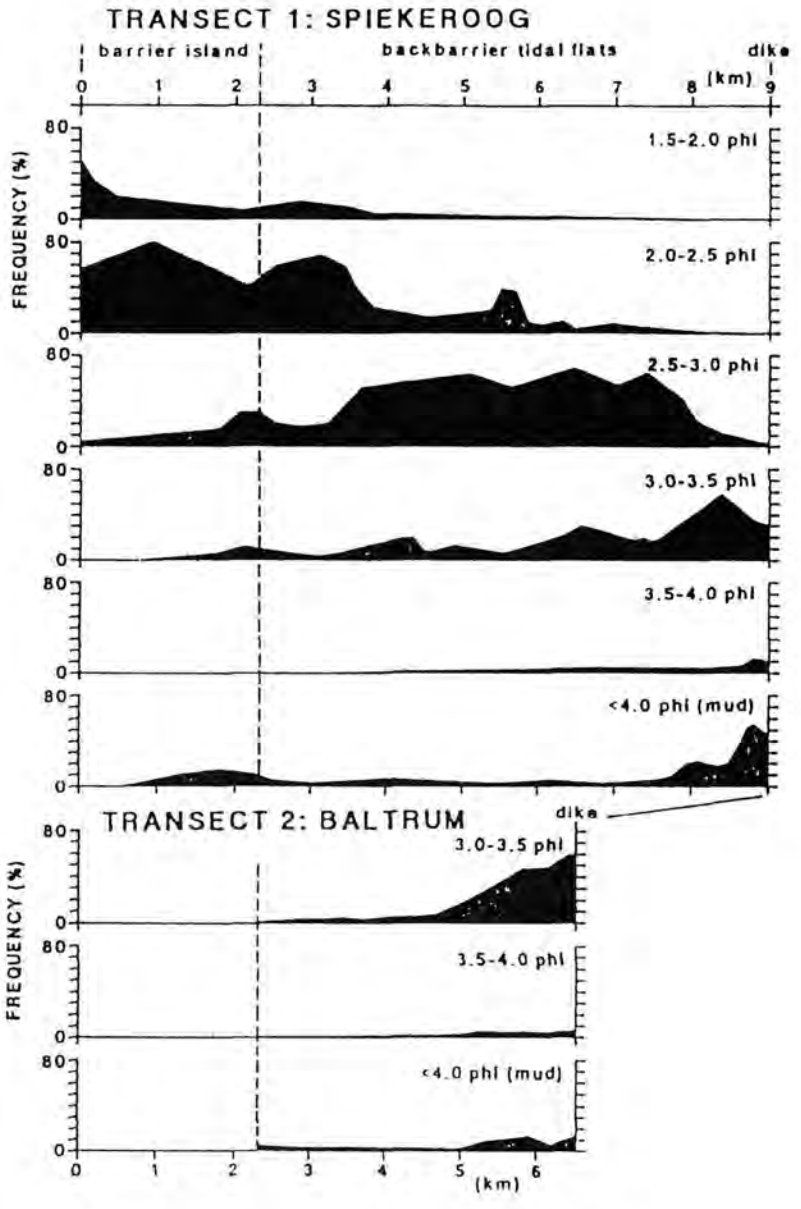

Fig. 5-27 Comparison of the island-coast distribution of the dominant fractions between narrow (Baltrum) and wider (Spiekeroog) tidal flats (after FLEMMING & NYANDWI, 1994).

CHAPTER 6

A PHYSICAL MODEL FOR THE SHORE-NORMAL ENERGY GRADIENT

6.1 Introduction

Based on the main tidal flow directions, which follow the main orientations of the tidal channels and the inlet, a primary energy gradient is expected along the inlet axis (NW-SE). Similarly, a nearly E-W gradient should be expected along the generally E-W oriented tidal channels draining the tidal flats between consecutive tidal watersheds. However, as already noted in the previous chapter, whereas an E-W gradient is virtually undetectable on the basis of the sediment textural parameters, a N-S (shore-normal) gradient forms a pronounced secondary trend to the primary NE-SW gradient. The energy gradient along the inlet axis (NE-SW) is clearly understood as corresponding to the general decrease in the strengths of the tidal currents away from the inlet throat area. The expected E-W gradient, on the other hand, may be masked by the strong shore-normal gradient. But since the shore-normal gradient (N-S direction) is not consistent with any established tidal flow direction, it remains of primary interest to establish its origin, applicable to the whole East Frisian backbarrier environment.

6.2 Model background

Tidal currents constitute the major hydraulic force in tidal environments. Whatever the nature of this hydraulic force in the study area, it must be changing in character across the tidal flats in a manner corresponding with the resulting energy gradient (VAN STRAATEN & KUENEN, 1958). Given the E-W orientation of the tidal channels, the energy gradient is considered to imply larger discharges the farther away from the coast a channel is situated. The magnitudes of the flow discharges, however, are not only controlled by the volumes involved but also by the channel form and basin structure.

6.2.1 Tidal currents in channels

The tidal filling of the backbarrier basin can be considered as a tidal pumping through the inlet into the tidal channels. Assuming the channels to be basins with rectangular plan, then the following can be deduced to build up a model for the evolution of the tidal currents in a channel:

The horizontal discharge, $Q_{Horizontal} = A_C.V$ (i)

and

The vertical discharge, $Q_{Vertical} = A_H.dH/dT$ (ii)

Where, V is the flow velocity; A_c is the channel cross-sectional area; A_H is the channel surface area; and dH/dT is the rate of rise of the tidal stage.

Applying the law of continuity, $Q_{Horizontal} = Q_{Vertical}$

Thus, $A_c.V = A_H.dH/dT$

and the velocity, $V = (A_H/A_c).dH/dT$ (iii)

6.2.2 Rate of rise of tidal stage in natural channels

Since the tidal channel-forms are in fact different from a rectangular basin and their banks do not rise up to the high water mark, some of the flow is actually overbank and the rate of water level rise (dH/dT) and the surface area (A_H) are controlled by the basin structure (topography). The channel cross-sectional area is the only variable remaining constant at bankfull level. The tidal water demand which is brought about by the increasing tidal stage above the channel banks will have to be satisfied by an increased discharge and thus, velocity surges at the channel entrance (PETHICK, 1980).

In this case, equation (iii) above will have to be evaluated at time intervals by summation of the contributions to the tidal prism by different elevations. Now taking A_{H0} to represent the surface area of the channel at chart datum, A_{H_i} the surface area of any other level, dH/dT the rate of rise of the tide between the chart datum and the high water mark, with dH_i/dT being the rate of rise of the tide between any other level and the high water mark;

$$V = 1/A_c\{A_{H0}(dH_0/dT) + \Sigma(A_{H_i}.dH_i/dT)\}$$

or simply,

$$V = 1/A_c\{\Sigma(A_{H_i}.dH_i/dT)\} \qquad \text{(iv)}$$

6.2.3 Predicted maximum flow velocity

In order to evaluate the flow velocities using equation (iv) a large scale (1:25,000) topographic map of the study area, the Otzum tidal catchment area was used. The tidal channels numbered I - IV (Fig. 6-1), occupying different grain size zones and having clearly delimitable catchment areas were selected and their surface areas at chart datum measured. Additionally surface areas between selected contour intervals, NN + 0, 0.25 and 1.0 m and the high water mark, NN + 1.3 m were evaluated. If each contour from the lowest upwards is considered as forming the base of a basin with vertical walls rising to the high water mark, then in filling up of such a basin the actual volume is represented by the area difference between the contour and the one below it. Equation (iv) above is therefore modified as follows:

$$V = 1/A_c\{\Sigma(A_{H*}.dH_i/dT)\} \qquad \text{(v)}$$

where, $A_{H*} = A_{H_i} - A_{H_{i-1}}$

It follows from this formulation that the basins are filled up during the same time interval. Assuming the tides to have a time symmetry, a time interval (dT) of 6 hours

was used. It should be mentioned, however, that the use of the fixed time interval is in a strict sense not correct. The actual duration times of the water level rise between successive elevations above the chart datum and the high water level may be shorter and hence the actual velocity estimates higher. The underestimation factor of the expected velocities, however, remains the same for corresponding elevations in the whole basin. As such, use of field measurements of the tidal rises would have quantitative but no qualitative effect on the model. Tables 6-1 & 6-2 summarise the computational details and the results.

It can be seen that the predicted flow velocities are highest in channel I followed by channel II, III and IV (Fig. 6-1). The flow velocities and hence, the energy level increase northwards i.e perpendicular to the coast.

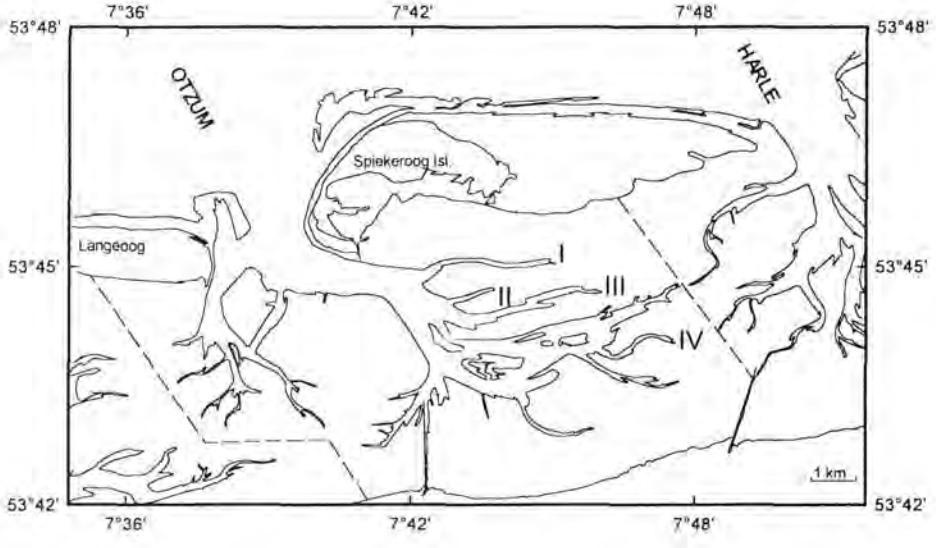

Fig. 6-1 Location map showing the tidal channels used in the estimation of the flow velocity corresponding to the mean settling velocity of the sediment.

Table 6-1 Distribution of the ground elevations in selected catchments.

Channel Nr	I	II	III	IV	
H_i (m)	A_{H_i} (Km^2)	A_{H_i} (Km^2)	A_H (Km^2)	A_{H_i} (Km^2)	dH_i/dT (mm/sec)
-1.5	0.477	0.105	0.919	0.228	0.13
0	4.734	0.923	4.110	1.044	0.06
0.25	4.837	1.071	4.186	-	0.05
1.0	7.465	-	-	-	0.01

Table 6-2 Estimated peak velocities at the mouths of selected channels.

Channel Nr	X-Sectional area	$V = 1/A\ (\Sigma A_{H*}.dH_i/dT)$
	(m^2)	(m/s)
I	305.879	1.18
II	90.27	0.78
III	451.407	0.70
IV	125.504	0.69
$A_{H*} = A_{H_i} - A_{H_{i-1}}$		

6.3 Implications of the model

The agreement between the gradients of the estimated velocity and the mean grain settling velocity (Fig. 6-2) validates the hypothetical causal relationship between the tidal flow velocity and surficial sediment distribution. The current velocity relationship is represented by the equation,

$$V_{cm/s} = -75.83psi + 24.87 \qquad (8)$$

where, $psi = -\log_2 W$ and W is the grain settling velocity in centimetres per second.

The velocity gradient implies that, overbank flow velocities between any two adjacent channels will be influenced largely by velocities in the northern channel. The effect of the southern channel therefore, will be to modify that influence, a fact which is thought to explain the scatter in the data points in the interchannel region of the energy gradient (Fig. 5-3).

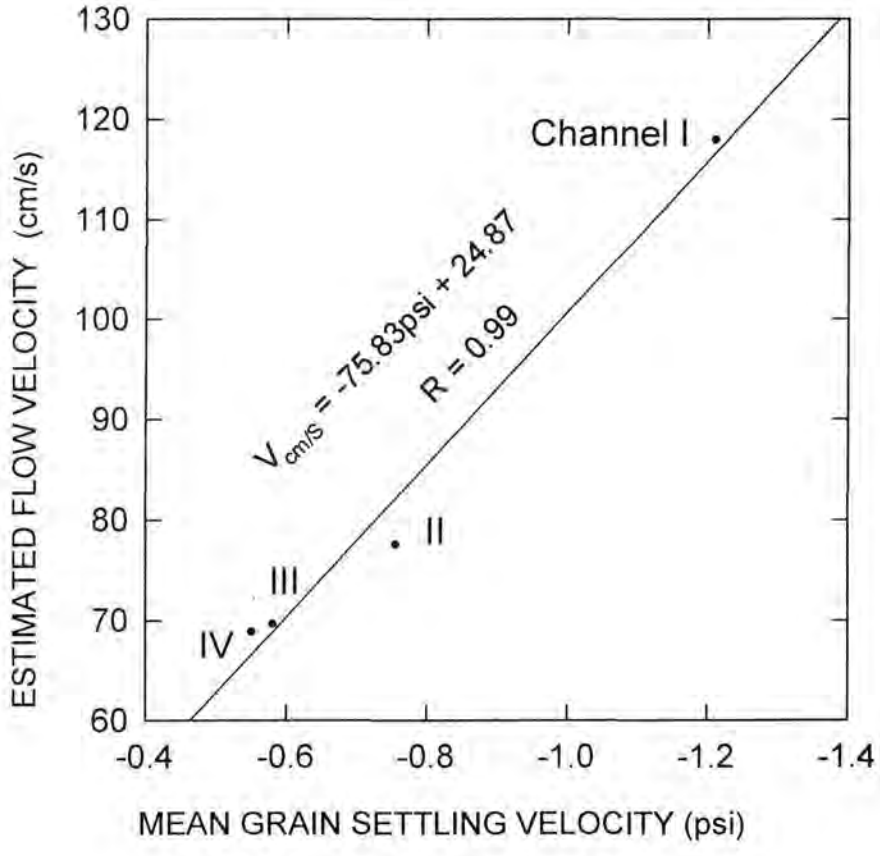

Fig. 6-2 The relationship between estimated current velocity in the channel and the mean grain settling velocity of the bottom sediment.

In the light of the model the energy gradient would in the absence of the E-W tidal channels follow the inlet's course (NW-SE). But the presence of the E-W channels feeding the inlet has led to the development of a N-S gradient in addition to the NW-SE one. Occurrence of pockets of finer sediment at some locations as opposed to a

smooth linear gradient (Fig. 5-4) implies in turn the presence of pockets of low energy level. As shown by the model such areas are expected in the interchannel regions, particularly the high elevation tidal water divides. The supply of finer sand fractions including mud is thus directed more towards these areas. A look at the distribution of the mud pockets other than those found close to the dyke and in the lee of the island shows clearly that they are concentrated along the major drainage divides of the inlets as well as along some minor divides between tidal channels (Fig. 4-22). This means that the mud pockets are controlled by both the low energy levels and high elevation at a place.

The dependence of the mud distribution on the topography has also been pointed out by e.g. VAN STRAATEN & KUENEN (1958) and REINECK et al. (1986). Shorter water columns enhances deposition over shorter quiet periods. Following the fact that the mud is deposited along with finer sand fractions to which its settling velocity differs the mud must have been aggregated so that its effective settling velocity became comparable to that of the hydraulically equivalent sand fraction (FLEMMING & NYANDWI, 1994).

The biological enrichment of mud has also been frequently suggested to be solely responsible for the mud pockets. Bottom filter feeders extracting very fine particles out of suspension as well as the sea bed excrete small lumps of mud or faecal pellets. FLEMMING (1991) observes that the mud deposits occurring away from the dyke exist as surface coatings in and around shell beds (mussel beds), a fact which points to biological enrichment. Other observations have shown however, that the faecal pellets produced by the bottom filter feeders rarely settles long on the bottom before they are recycled (SMETACEK, 1980; PEINERT et al, 1982; TEN BRINKE & DRONKERS, 1993). The distribution of the mussel beds and other important suspension feeders on the other hand is generally limited to the mud flats especially at elevations (high) above mean low tide (FLEMMING et al, 1992). These findings support the notion that not only does the topography control the mud deposition along high elevation drainage divides but also controls the concentration of the mud enriching organisms in the areas.

CHAPTER 7

CONCLUSIONS

This study was carried out with the primary objective to establish the nature and cause of the energy gradient across backbarrier areas which is generally shown by sediment distribution patterns. The other inherent objective was to establish the geomorphological and hydrological control on the sediment distribution i.e. the interrelationship between geomorphology, hydrology and sedimentation. In the course of the study therefore, some characteristic geomorphological, hydrological and sedimentological parameters were established and their interrelationships examined.

7.1 Morphology and morphodynamics of tidal catchment systems

The inlet catchment systems in the East Frisian region of the Wadden Sea are mainly characterised by NW-SE oriented tidal inlets which separate adjacent islands. Between the islands and the mainland coast the inlets branch into networks of E-W oriented tidal channels which dissect the tidal flats. Each tidal channel constitute its own catchment area such that the total inlet catchment area is divided into numerous sub-catchments according to the number of existing tidal channels. The tidal flats and the channels are highly dynamic. By using empirical relationships between different dimensional parameters it is possible to predict the course of change in different parameters.

It has been shown in this study that the size of a tidal channels is proportional to the volume of tidal water it discharges. On the average, a given volume of discharge through a particular channel fills a catchment basin of a given surface area. That is, the size of the channel is also proportional to the size of the area it drains. The size of a channel may be represented by volume, cross-sectional area or length. These parameters have all shown a strict proportionality to the size of the cathment area. In this respect tidal drainage systems appear to resemble closely fluvial systems of similar proportions. In both tidal and fluvial systems channels draining large areas are

correspondingly longer than those with smaller catchments. As the channels become very long they tend to meander. Nevertheless, this feature which is commonly well developed in the lower reaches of large rivers appears to be less developed in tidal systems. The analysis of the sinuosity index in the Otzum catchment area, for instance, gives values typically less than 1.5, the lowest value for defining a meander. As to the other size parameters namely, width, depth and cross-sectional area, they too provide useful relationships. Large channels are usually both wide and deep. Since the cross-sectional area grows proportionally to the volume of discharge, the width-depth relationship is primarily determined by the equilibrium conditions of the channel size. Therefore, in the inlet throat areas where the islands provide resistance to channel expansion the required large cross-section is maintained through increases in depth. As such, most of the inlets are considerably deeper and narrow in their throat regions.

As exemplified by channels in the Otzum catchment area, changes in channel sizes are not necessarily accompanied by changes in the size of the backbarrier basin. Increases in channel volumes deduced over the past 30 years were not accompanied by any appreciable change in the size of the Otzum catchment area but rather, deepening and widening of the channels at the expense of the tidal flats. Since the growth of individual channels requires expansion of their catchment areas, this has been maintained through the closure of smaller channels. This phenomenon can be followed from one map series to the other.

7.2 Sediment dynamics

The morphodynamics of the tidal flat areas is reflected also by sediment budget. Although the increase in channel sizes as mentioned above has been shown to reflect erosion of the channel bed and low-lying tidal flats, mass balance estimates gives a positive sediment budget. This is an indication that besides sediment influx into the backbarriers, sediment eroded from the channels and low-lying tidal flats does not leave the system but instead finds its way on the higher flats. On a mass balance map channels were found to represent negative balance (erosion) while the biggest part of the flats showed positive balance (accretion). The calculated mass balance of the

Otzum catchment (Spiekeroog backbarrier area) over the period 1962-75 corresponds to an average bottom rise of the basin of 16 cm/100 yr. If this value was to be compared with reported average sea level rise of 24 cm/100 yr. it would appear that the Wadden Sea as exemplified by the Spiekeroog backbarrier area is deepening. This is a clear sign that sediment influx from the North Sea is not at pace with the sea level rise at present. Assuming this to imply increasing water volumes, it is thus not suprising that increases in tidal channel volumes over the past 30 years have been deduced.

7.3 Sediment distribution patterns

Sediment distribution in the Spiekeroog backbarrier area is characterised mainly by landward fining trend. However, in the sand size class, the trend shows two distinct patterns:

1) Along the inlets, the sediment becomes finer landwards from as coarse as 1.0 phi in the throat region to 3.5 phi on the landward reaches. This pattern, coinciding with the main tidal flow direction through the inlets and the main channels, is not unexpected.

2) For the rest of the basin including tidal flats and channels, the pattern shows a distinct shore-normal character. The sediment becomes finer from 2.0 phi on the island to 3.0 phi on the tidal flats and down to 3.5 phi along the mainland coast (dyke). This pattern is the most conspicuous on the sediment distribution map but given the inlet NW-SE orientation and an E-W orientation of the tidal channels draining the flats, the pattern is rather unexpected.

7.4 The shore-normal energy gradient

Despite lack of a dominant North-South, shore-normal flow across the tidal flats, existence of a shore-normal energy gradient as implied by the sediment distribution patterns can not be challenged. Through a mathematical modelling of permissible flow velocities in the E-W oriented channels, it was possible to show that for any two

channels, tidal flows are stronger in the northern than in the southern channel. A weak peak velocity of only 69 cm/s was estimated in the landwardmost channel as compared to velocities as high as 1.18 m/s in the seawardmost (northern) channel. Thus, the hydraulic energy along the channels decreases southwards.

An account on how the sediment responds to the energy conditions arising from neighbouring channels is as follows:

- From a northern channel towards the next southerly situated channel, the overbank flow velocity, to which the sediment immediate to the channel banks responds, decreases southwards at all locations parallel to the channel.

- At some distance beyond the centre line overbank velocities from the two channels are equal and at their minimum. This process repeats itself between successive pairs of channels, ultimately resulting in a pronounced energy gradient.

REFERENCE

Antia, E. E. (1993). Sedimentology, Morphodynamics and facies association of a mesotidal barrier island shoreface (Spiekeroog, southern North sea). Berichte, Fachbereich Geowissenschaften, Universität Bremen, Nr. 32, 370 p.

Bagnold, R. A. (1968). Deposition in the process of hydraulic transport. Sedimentology, 10: 45-56.

Behre, K.-E., (1987). Meeresspiegelbewegungen und siedlungsgeschichte in den Nordseemarschen. Vortr. der Oldenburg. Landschaft, 17: 1-47.

Behre, K.-E., Menke, B. and Streif, H. (1979). The Quaternary development of the German part of the North sea. In: Oelele, E., Shüttenhelm, R. T. E. and Wiggers A. J. (eds.).The Quaternary history of the North sea. Acta Universitatis Upsaliensis Symposium, Annum Quingentesimum Celebrantis, 2: 85-113.

Berryhill, H. L. Jr., Dickinson, K. A. and Holmes, C. W. (1969). Criteria for recognising ancient barrier coastlines. Amer. Assoc. Petroleum Geologists Bull., 53: 706-707.

Beukema, J. J. (1976). Biomass and spicies richness of macrobenthic animals living on the tidal flats of the Dutch Wadden sea. Neth. J. Sea Res., 10: 236-261.

Brezina, J. (1979). Particle size and settling rate distributions of sand-sized material. Proc. 2nd Europ. Symp. Particle characterisation. Nürnberg, 1-44.

Bundesanstalt für Bodenforschung (1973). Geologische Übersichtskarte 1 : 200,000 CC 2310 Helgoland.

Carver, R. E. (1971). Procedures in sedimentary petrology. Wiley-Interscience, New York.

Caston, V. N. (1979). The Quaternary sediments of the North sea. In: Banner, F. T., Collins, M. B. and Massie, K. S. (eds.). The North-West European shelf seas: the sea bed and the sea in motion I. Geology and sedimentation. Elsevier, Amsterdam, 195-270.

Clark, M. W. (1981). More skewed against than skewing. In: Nio, S.-D., Shüttenhelm, R. T. E. and Van Weering, Tj. C. E. (eds.). Holocene marine sedimentation in the North sea basin. Spec. Publs. Int. Ass. Sediment., 5. Backwell Scientific Publications, Oxford, 111-121.

Davis, R. A. & Hayes, M. O. (1984). What is a wave dominated coast? Mar. Geol., 60: 313-329.

Dette, H. H. (1977). Ein Vorschlag zur Analyse eines Wellenklimas. Die Küste, 31: 166-180.

Deutsches Hydrographisches Institut (1981). Sedimentverteilung in der Deutschen Bucht (1:250 000).

Dieckmann, R. (1985). Geomorphologie, Stabilitäts- und Langzeitverhalten von Watteinzugsgebieten der deutschen Bucht. Mitteilungen des Franzius-Instituts für Wasserbau und Küsteningenieurwesen der Universität Hannover, 60: 133-361.

Dury, G. H. (1969). Hydraulic geometry. In: Chorley, R. J. (ed.). Introduction to fluvial processes. Methuen & Co Ltd, London, 146-156; 177-188.

Ehlers,J. (1988). The morphodynamics of the Wadden sea. A. A. Balkema, Rotterdam, 397p.

Elliot, T. (1978). Clastic shorelines. In: Reading, H. G. (ed.). Sedimentary environments and facies. Oxford, Blackwell, 143-177.

Etkins, B. & Epstein, E. (1982). The rise of global mean sea level as an indication of climate changes. Science, 215: 287-298.

Evans, G. (1965). Intertidal flat sediments and their depositional environments in the Wash. Quart. J. Geol. Soc. London, 121(482): 209-241.

Fitzgerald, D. M. & Penland, S. (1987). Backbarrier dynamics of the East Frisian islands. J. Sediment. Petrol., 54 (4): 746-754.

Fitzgerald, D. M., Penland, S. and Nummedal, D. (1984a). Changes in tidal inlet geometry due to backbarrier filling: East Frisian islands, West Germany. Shore and Beach, 52(4): 2-8.

Fitzgerald, D. M., Penland, S. and Nummedal, D. (1984b). Control of barrier island shape by inlet sediment passing: East Frisian islands, West Germany. Mar. Geol., 60: 355-376.

Flemming, B. W. (1977). Depositional processes in Saldanha Bay and Langebaan Lagoon. Professional Research Series No. 2, National Research Institute of Oceanology, CSIR, South Africa, 215pp.

Flemming, B. W. (1988). Process and pattern of sediment mixing in a microtidal coastal lagoon along the west coast of South Africa. In: de Boer et al (eds.). Tide-influenced sedimentary environments and facies, 275-288. D. Reidel Publishing Company.

Flemming, B. W. (1990). Zur holozänen Entwicklung, Morphodynamik und faziellen Gliederung der Ostfriesischen Insel Spiekeroog (südliche Nordsee). In: Willems et al (eds.). Beiträge zur Geologie und Paläontologie Norddeutschlands. Berichte, Fachbereich Geowissenschaften, Universität Bremen, Nr. 32: 13-73.

Flemming, B.W. (1991). Zur holozänen Entwicklung, Morphodynamik und faziellen Gliederung der Ostfriesischen Insel Spiekeroog (südliche Nordsee), Bericht Senckenberg-am-Meer, 91/3: 1-51

Flemming, B. W. & Davis, R. A. Jr. (1990). Sohlformentwicklung in einer hochdynamischen Rinne des Spiekerooger Watts in Abhängigkeit von der Tidephase, Wassertiefe und Strömungsgeschwindigkeit. SEDIMENT 90 (Bonn), Posterband 3 S.

Flemming, B. W. & Davis, R. A. Jr. (1994). Holocene evolution, morphodynamics and sedimentology of the Spiekeroog barrier island system (southern North sea). Senckenbergiana marit., 24(1/6): 117-155.

Flemming, B. W. & Nyandwi, N. (1994). Land reclamation as a cause of fine-grained sediment depletion in backbarrier tidal flats (Southern North sea). Netherlands J. Aquat. Ecol., 28(3-4): 299-307.

Flemming, B. W. & Thum, A. B. (1978). The settling tube - a hydraulic method for grain size analysis of sands. Kieler Meeresforschung, Sonderband, 4: 82-95.

Flemming, B.W., Schubert, H., Hertweck, G. and Müller, K. (1992). Bioclastic tidal channel lag deposits: a genetic model. Senckenbergiana marit., 22(3/6): 109-129.

Folk, R. L. (1966). A review of grain-size parameters. Sedimentology, 6:73-93.

Folk, R. L. & Robles, R. (1964). Carbonate sediments of Isla Perez, Alacran Reef Complex, Yucatan. J. Geol., 72: 255-292.

Folk, R. L. & Ward, W. C., (1957). Brazos river bar. A study in the significance of grain size parameters. J. Sediment. Petrol., 27: 3-26.

Fox, D. L. & Coe, W. R. (1943). Biology of the California sea mussel (Mytilus Californius) II. Nutrition, metabolism, growth and calcium deposition. J. Exp. Zool., 93: 205-249

Führböter, A. (1979). Wascheinlichkeiten und Häufigkeiten von Extremsturmfluten. Die Küste, 34: 40-52.

Gadow, S. & Reineck, H.-E. (1969). Abländiger Sandtransport bei Sturmfluten. Senckenbergiana marit., 50: 63-78.

Gao, S. & Collins, M. (1991). A critique of the "McLaren method" for defining sediment transport paths. J. Sediment. Petrol., 61: 143-146.

Gao, S. & Collins, M. (1992). Net sediment transport patterns inferred from grain-size trends, based upon definition of "transport vectors". Sediment. Geol., 81: 47-60.

Gao, S. & Collins, M. B. (1994). Analysis of grain size trends, for defining sediment transport pathways in marine environments. J. Coast. Res., 10(1): 70-78.

Gierloff-Emden, H. G. (1961). Nehrungen und Lagunen. Pettermans geographische Mitteilungen, 105 (2): 81-92; 105 (3): 161-176.

Gregory, K. J. & Walling, D. E. 1973. Drainage basin form and process. A geomorphological approach. Edward Arnold, London, 456p.

Gripp, K. (1956). Das Watt; Begriff, Begrenzung und fossile Vorkommen. Senckenbergiana. Leth., 37 (3/4): 149-181.

Groen, P. (1967). On the residual transport of suspended matter by an alternating tidal current. Neth. J. Sea Res., 3: 564-574.

Grotjahn, M. (1990). Sedimente und Mikrofauna der Watten bei der Insel Spiekeroog. Untersuchungen im Rahmen des "Sensitivitätesrasters Deutsche Nordsee Küste". Forschungsstelle für Insel- und Küstenschutz, Norderney, Jahresbericht, 39: 97-119.

Häntzschel, W. (1955). Tidal flat deposits (Wattenschlick). In: Trask, P. D. (ed.). Recent marine sediments. Soc. Econ. Palaeontologists and Mineralogists, Spec. Publ. 1, 1939, 195-206.

Hayes, M. O. (1975). Morphology of sand accumulations in estuaries: an introduction to the symposium. In: Cronin, L. E. (ed.). Estuarine research, vol. 2. Academic Press, New York, 3-22.

Hayes, M. O. (1979). Barrier island morphology as a function of tidal and wave regime. In: Leatherman, S. P. (ed.). Barrier islands. Academic Press, New York, 1-27.

Homeir, H. (1979). Die Verlandung der Harlebucht bis 1600 auf der Grundlage neuer Befunde. Forschungsstelle für Insel- und Küstenschutz, Norderney, Jahresbericht, 30: 105-115.

Homeir, H. & Luck, G. (1969). Das historische Kartenwerk 1:50,000 der Niedersächsischen Wasserwirtschaftsverwaltung als Ergebnis historisch-topographischer Untersuchungen und Grundlage zur kausalen Deutung der Hydrovorgänge im Küstengebiet. Göttingen.

Huntley, D. A. (1980). Tides on the north-west European continental shelf. In: Banner, F. T., Collins, M. B. and Massie, K. S. (eds.). The North-West European shelf seas: the sea bed and the sea in motion II. Physical and chemical oceanography, and physical resources. Elsevier, Amsterdam, 301-351.

Inman, D. L. (1949). Sorting of sediments in the light of fluid mechanics. J. Sed. Petrol., 19: 51-70.

Inman, D. L. (1952). Measures for describing the size distribution of sediments. J. Sediment. Petrol., 22: 125-145.

Kellerhals, P. & Murray, J. W. (1969). Tidal flats at Boundary Bay, Fraser river delta, British Columbia. Bull. Can. Petroleum Geologists, 17(1): 67-91.

Kirchner, J. W. (1993). Statistical inevitability of Horton's Laws and the apparent randomness of stream channel networks. J. Geology, 21: 591-594.

Kirchner, J. W. (1994). Statistical inevitability of Horton's Laws and the apparent randomness of stream channel networks, Reply. J. Geology, 22: 380-381.

Knop, F. (1963). Küsten- und Wattveränderungen Nordfrieslands - Methoden und Ergebnisse ihrer Überwachung. Die Küste, 11: 1-33.

Koch, M. & Luck, G. (1975). Untersuchung zu den Stromungsverhaltnissen auf dem westlichen Juister Watt. Forschungsstelle für Insel- und Küstenschutz, Norderney, Jahresbericht, 13: 29-33.

Koch, M. & Niemeyer, H. D. (1978). Sturmtiden-Strommessungen im Berreich des Norderneyer Seegats. Forschungsstelle für Insel- und Küstenschutz, Norderney, Jahresbericht, 29: 91-108

Komar, P. D. (1976). Beach processes and sedimentation. Prentice-Hill, New Jersey, 429p.

Lancaster, N. (1986). Grain size characteristics of linear dunes in the southwestern Kalahari. J. Sediment. Petrol., 56(3): 395-400.

Lassen, H. (1989). Örtliche und zeitliche Variationen des Meeresspigels in der südöstlichen Nordsee. Die Küste, 50: 65-95.

Luck, G. (1976a). Inlet changes of the East Frisian islands. Proc. 15th Conf. Coastal Engr., Amer. Soc. Civ. Engr., New York, Vol.2: 1938-1957.

Luck, G. (1976b). Protection of the litoral and seabed against erosion. Forschungsstelle für Insel- und Küstenschutz, Norderney, Fallstudie Norderney, Jahresbericht, 27: 9-78.

Loring, D. H. & Nota, D. J. G. (1973). Morphology and sediments of the Gulf of St. Lawrence. Bull. Fisheries Resear. Board Canada, Bull. 182: 147p.

McCave, I. N. (1978). Grain size trends and transport along beaches: an example from England. Mar. Geol., 28: M43-M51.

McLaren, P. (1981). An interpretation of trends in grain size measures. J. Sediment. Petrol., 51 (2): 611-624.

McLaren, P. & Bowles, D. (1985). The effects of sediment transport on grain-size distributions. J. Sediment. Petrol., 55 (4): 457-470.

Menard , H. W. (1950). Sediment movement in relation to current velocity. J. Sediment. Petrol., 20: 148-160.

Niedersächsisches Landesamt für Bodenforschung (1970). Geologische Karte von Niedersachsen 1:25 000 Nr. 2212 Spiekeroog, 2. Auflage, Hannoner.

Niemeyer, G. (1972). Ostfriesische Inseln, Sammlung geographischer Führer, 8, Berlin, Stuttgart, Bornträger, 189p.

Niemeyer, H. D. (1979). Untersuchungen zum Seegangsklima im Bereich der ostfriesischen Inseln. Die Küste, 34:53-70.

Nota, D. J. G. (1958). Sediments of the western Guiana shelf. Rep. Orinoco Shelf Exped. 2 Meded. Landbouwhogschool Wageningen, 58: 98p.

Nota, D. J. G. (1968). Geomorphology and sedimentary petrology in southern Gulf of St. Lawrence. Geol. Mijnbouw, 47: 59-52.

Nummedal, D. & Penland, S. (1981). Sediment dispersal in Norderneyer Seegat, West Germany. In: Nio, S.-D., Shüttenhelm, R. T. E. and Van Weering, Tj. C. E. (eds.). Holocene marine sedimentation in the North sea basin. Spec. Publ. Int. Ass. Sediment., 5: 187-210. Blackwell Scientific Publishers, Oxford, 524p.

Oertel, G. F. (1985). The barrier island system. Mar. Geol., 63: 1-18.

Partenscky, H.-W. (1980). Neue Erkentnisse über das Stabilitätsverhalten und den Sedimenttransport in Watt-Prielsystemen. Mitteilungen des Franzius-Instituts für Wasserbau und Küsteningenieurwesen der Universität Hannover, 50: 59-74.

Passega, R. (1957). Texture as characteristic of clastic deposits. Bull. Amer. Assoc. Petroleum Geologists, 41: 1952-1984.

Passega, R. (1964). Grain size representation by CM patterns as a geological tool. J. Sediment. Petrol., 34: 830-874.

Peinert, L., Saure, A., Stegmann, P., Stienen, C. & Haardt, H. (1982). Dynamics of primary production and sedimentation in a coastal ecosystem, Neth. J. Sea Res., 16: 276-289.

Peltier, W. R. & Tushingham, A. M. (1989). Global sea level rise and the greenhouse effect: May they be connected? Science, 244: 806-810.

Pethick, J. S. (1980). Velocity surges and Asymmetry in Tidal Channels. Est. Coast. Mar. Sci., 11: 331-345.

Pettijohn, F. G., Potter, P. D. and Siever, R. (1972). Sand and sandstone. Springer Verlag, New York, 618p.

Postma, H. (1961). Transport and accumulation of suspended matter in the Dutch Wadden sea. Neth. J. Sea Res., 1(1,2): 148-190.

Ragutzki, G. (1982). Verteilung der Oberfläschensedimente auf den Niedersächsischen Watten. Forschungsstelle für Insel- und Küstenschutz, Norderney, Jahresbericht, 32: 55-67.

Reineck, H.-E. (1958). Longtudinalle Schrägschicht im Watt. Geologische Rundschau, 47: 73-82.

Reineck, H.-E. (1967). Layered sediments of tidal flats, beaches and shelf bottoms of the North sea. In: Lauff, G. H. (ed.). Estuaries. Amer. Assoc. Adv. Sci., Spec. Publ. 83: 191-206.

Reineck, H.-E. (1972). Tidal flats. In: Rigby, J. K. & Hamblen, W. K. (eds.). Recognition of ancient sedimentary environments. Soc. Econ. Palaeontologists and Mineralogists. Spec. Publ., 16: 146-159.

Reineck, H.-E. (1975). German North sea tidal flats, In: Ginsburg, R. N. (ed.) Tidal deposits: A casebook of recent examples and fossil counterparts. Springer Verlag, 5-12.

Reineck, H.-E. & Siefert, W. (1980). Factoren der Schlickbildung im Sahlenburger und Neuwerker Watt. Die Küste, 35: 26-51.

Reineck, H.-E. & Singh, I. B. (1973). Depositional sedimentary environments. Springer Verlag Berlin, Heidelberg, 439pp.

Reineck, H.-E., Chen, C. M. and Wang, S. S. (1986). Die Rückseitenwatten zwischen Wangerooge und Festland, Nordsee. Senckenbergiana Marit., 17, 241-252.

Reineck, H.-E., Dörjes, J. Gadow, S. and Hertweck, G. (1968). Sedimentologie, Faunazonierung und Faziesabfolge vor der Ostküste der inneren Deutschen Bucht. Senckenbergiana lath., 49: 261-309.

Reineck, H.-E., Gutman, W. F. and Hertweck, G. (1967). Das Schlickgebiet südlich von Helgoland als Beispiel rezenter Schelfablagerungen. Senckenbergiana lath., 48: 219-275.

Renger, E. & Partenscky, H.-W. (1974). Stabilitätsverhalten von Watteinzugsgebieten. Die Küste, 25: 73-86.

Renger, E. (1976). Quantitative Analyse der Morphologie von Watteinzugsgebieten und Tidebecken. Mitteilungen des Franzius-Instituts für Wasserbau und Küsteningenieurwesen der technischen Universität Hannover, 43: 161-355.

Rodloff, W. (1970). Über Wattwasserläufe. Mitteilungen des Franzius-Instituts für Wasserbau und Küsteningenieurwesen der technischen Universität Hannover, 34: 1-88.

Sahu, B. K. (1964). Depositional mechanisms from the size analysis of clastic sediments. J. Sediment. Petrol., 34 (1): 73-83.

Self, R. P. (1977). Longshore variation in beach sands, Nautla area, Veracruz, Mexico. J. Sediment. Petrol., 47: 1437-1443.

Shi, Z. (1992). Application of the "Pejrup Approach" for the classification of the sediments in the microtidal Dyfi estuary, West Wales, U.K. J. Coast. Res., 8(2): 482-491.

Smetacek, V. S. (1980). Zooplankton standing stock, copepod faecal pellets and particulate detritus in Kiel Bight. Est. Coast. Mar. Sci., 11: 477-490.

Spencer, D. W. (1963). The interpretation of grain size distribution curves of clastic sediments. J. Sediment. Petrol., 33(1), 180-190.

Stephan, H.-J. (1982). Seegangsleistung und Verweilzeit im Bereich der ostfriesischen Inseln zur Deutung morphologischer Vorgänge. Forschungsstelle für Insel- und Küstenschutz, Norderney, Jahresbericht 1980, 32: 27-39.

Steward, H. B. (1958). Sedimentary reflections of depositional environment in San Miguel Lagoon, Baja California, Mexico. Bull. Americ. Assoc. Petroleum Geologists, 42(11): 2567-2618.

Strahler, A. N. (1971). The earth sciences. Harper & Row, New York, 824p.

Ten Brinke, W. B. M. & Dronkers, J. (1993). Physical and biotic aspect of fine sediment import in the Oosterschelde tidal basin (The Netherlands). Neth. J. Sea Res., 31(1): 19-36.

Van Andel, T. J. & Veevers, J. J. (1967): Morphology and sediments of the Timor Sea. Dept. Nation. Development, Bureau Miner. Resour., Geology & Geophysics. Bull. 83: 172p.

Van Leussen, W. (1988). Aggregation of particles, settling velocity of mud flocs: A riview. In: Dronkers, J. and van Leussen, W. (eds.). Physical processes in estuaries. Springer Verlag, 437-403.

Van Straaten, L. M. J. U. (1961). Sedimentation in tidal flat areas. J. Alberta Soc. Petroleum Geologists, 9(7): 203-226.

Van Straaten, L. M. J. U., & Kuenen, Ph. H. (1957). Accumulation of fine grained sediment in the Dutch Wadden Sea. Geol. en Minjnbouw, 19: 329-354.

Van Straaten, L. M. J. U. & Kuenen, Ph. H. (1958). Tidal action as a cause of clay accumulation. J. Sediment. Petrol., 28 (4): 406-413.

Verwey, J. (1952). On the ecology of distribution of cockle and mussel in the Dutch Wadden sea, their role in sedimentation and the source of their food, with a short review of the feeding behaviour of bivalve molluscs. Arch. Neerl. Zool. 10: 172-239.

Walther, F. (1972). Zusammenhänge zwischen der Grösse der Ostfriesischen Seegaten mit ihren Wattgebieten sowie den Gezeiten und Strömungen. Forschungsstelle für Insel- und Küstenschutz, Norderney, Jahresbericht, 23: 7-32, 4 Tables, 8 Figures.